

EGE UNIVERSITY
GRADUATE SCHOOL OF NATURAL AND APPLIED SCIENCES

(Ph.D. THESIS)

**DEVELOPMENT OF MOLECULAR IMPRINTED
POLYMER BASED OPTICAL SENSOR FOR
DETERMINATION OF PESTICIDES**



Raif İLKTAÇ

Supervisor: Prof. Dr. Emür HENDEN

Co-Supervisor: Assoc. Prof. Dr. Nur AKSUNER

Department of Chemistry

Date of Presentation: 14.08.2017

Bornova-İZMİR

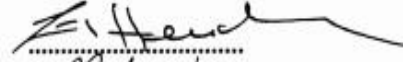
2017

Raif İLKTAÇ tarafından doktora tezi olarak sunulan “**Development Of Molecular Imprinted Polymer Based Optical Sensor For Determination Of Pesticides**” başlıklı bu çalışma E.Ü. Lisansüstü Eğitim ve Öğretim Yönetmeliği ile E.Ü. Fen Bilimleri Enstitüsü Eğitim ve Öğretim Yönergesi'nin ilgili hükümleri uyarınca tarafımızdan değerlendirilerek savunmaya değer bulunmuş ve **14.08.2017** tarihinde yapılan tez savunma sınavında aday oybirliği/oyçokluğu ile başarılı bulunmuştur.

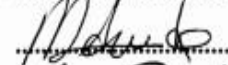
Jüri Üyeleri:

İmza

Jüri Başkanı : Prof. Dr. Emür HENDEN



Raportör Üye : Prof. Dr. Müşerref ARDA



Üye : Prof. Dr. Kenan DOST



Üye : Prof. Dr. Ahmet EROĞLU



Üye : Prof. Dr. Kadriye ERTEKİN



Üye : Doç. Dr. Nur AKSUNER



EGE ÜNİVERSİTESİ FEN BİLİMLERİ ENSTİTÜSÜ

ETİK KURALLARA UYGUNLUK BEYANI

E.Ü. Lisansüstü Eğitim ve Öğretim Yönetmeliğinin ilgili hükümleri uyarınca Doktora Tezi olarak sunduğum “**Development Of Molecular Imprinted Polymer Based Optical Sensor For Determination Of Pesticides**” başlıklı bu tezin kendi çalışmam olduğunu, sunduğum tüm sonuç, doküman, bilgi ve belgeleri bizzat ve bu tez çalışması kapsamında elde ettiğimi, bu tez çalışmasıyla elde edilmeyen bütün bilgi ve yorumlara atıf yaptığımı ve bunları kaynaklar listesinde usulüne uygun olarak verdiğimi, tez çalışması ve yazımı sırasında patent ve telif haklarını ihlal edici bir davranışımın olmadığını, bu tezin herhangi bir bölümünü bu üniversite veya diğer bir üniversitede başka bir tez çalışması içinde sunmadığımı, bu tezin planlanmasından yazımına kadar bütün safhalarda bilimsel etik kurallarına uygun olarak davrandığımı ve aksinin ortaya çıkması durumunda her türlü yasal sonucu kabul edeceğimi beyan ederim.

14/08/2017

Raif İLKTAÇ





ÖZET

PESTİSİT TAYİNİ İÇİN MOLEKÜLER BASKILI POLİMER ESASLI OPTİK SENSÖR GELİŞTİRİLMESİ

İLKTAÇ, Raif

Doktora Tezi, Kimya Anabilim Dalı

Tez Danışmanı: Prof. Dr. Emür HENDEN

İkinci Danışman: Doç. Dr. Nur AKSUNER

Ağustos 2017, 115 sayfa

Bu tezde, moleküler baskılanmış polimerler kullanılarak eser düzeydeki 1-naftol ve carbendazim pestisitlerinin tayinlerinin yapılması incelenmiştir.

Tezin ilk bölümünde, eser düzeydeki 1-naftol tayinini gerçekleştirmek üzere dört farklı moleküler baskılanmış polimer sentezlenmiş ve baskılama faktörü en yüksek olan polimer belirlenmiştir. 1-naftol tayini için optimum çalışma pH'ı 9, polimerin kapasitesi ise 70.86 ± 7.22 mg/g ($n=3$) olarak bulunmuştur. Yöntem, 1-naftol tayini için çeşitli su örneklerine uygulanmış ve nicel geri kazanım değerleri elde edilmiştir.

Tezin ikinci bölümünde ise, florimetrik carbendazim tayini öncesi manyetit-moleküler baskılanmış polimer literatürde ilk defa seçimli adsorban olarak kullanılmıştır. Hazırlanan polimerle carbendazim tayini için optimum çalışma pH'ı 8, polimerin kapasitesi ise 2.31 ± 0.63 mg/g olarak bulunmuştur. Geliştirilen yöntem, elma ve portakaldaki carbendazimi belirlemekte kullanılmıştır.

Anahtar sözcükler: 1-naftol, Carbendazim, Moleküler Baskılanmış Polimer (MIP), Spektroflorometre, Önderiştirme



ABSTRACT
**DEVELOPMENT OF MOLECULAR IMPRINTED POLYMER
BASED OPTICAL SENSOR FOR DETERMINATION OF
PESTICIDES**

İLKTAÇ, Raif

PhD thesis in Chemistry

Supervisor: Prof. Dr. Emür HENDEN

Co-Supervisor: Assoc. Prof. Dr. Nur AKSUNER

August 2017, 115 pages

In this thesis, molecularly imprinted polymers were used in order to investigate the determination of trace levels of 1-naphthol and carbendazim pesticides.

In the first chapter of the thesis, four different imprinted polymers were synthesized for the determination of trace levels of 1-naphthol and the polymer with the highest imprinting factor was determined. Optimum pH for 1-naphthol determination was found to be 9 and the polymer capacity was found to be 70.86 ± 7.22 mg/g (n=3). The method was applied to various types of water and quantitative recovery values were obtained.

In the second chapter of the thesis, magnetite-molecularly imprinted polymer has been used for the first time in the literature as selective adsorbent before the fluorimetric determination of carbendazim. Optimum working pH for determination of carbendazim with the synthesized polymer was found to be 8 and the capacity of the polymer was found to be 2.31 ± 0.63 mg/g. The proposed method was applied to apple and orange for the determination of carbendazim.

Keywords: 1-naphthol, Carbendazim, Molecular Imprinted Polymer (MIP), Spectrofluorometer, Preconcentration

ACKNOWLEDGEMENTS

I would like to express my gratitude to Prof. Dr. Emür HENDEN and Assoc. Prof. Dr. Nur AKSUNER, for their kind supervision, valuable suggestion and discussions through the whole study, and also for his patience during this long study. I am very thankful to Prof. Dr. Berrin YENİGÜL for her valuable contribution during the preparation of this thesis.

I would like to thank to Prof. Dr. Kenan DOST, member of Ph. D. thesis committee, for his suggestions during my study. I present my gratitude to Prof. Dr. Müşerref ARDA, member of Ph. D. thesis committee, for her suggestions during my study. I also would like to Prof. Dr. Kadriye ERTEKİN and Prof. Dr. Ahmet EROĞLU, members of Ph. D. thesis committee, for their suggestions and valuable advices.

I also would like to thank to Dr. Onur YAYAYÜRÜK, Dr. Özgür ARAR and Dr. Tülin DENİZ ÇİFTÇİ, for their support and valuable guidance, advice.

I would like to thank to my friends, Ezgi Elif ÖLÇER, Duygu YAPICI, Özgür TAĞ, Aslı TOPTAŞ TAĞ, Fehmi SALTAN, Yasemin İŞLEK COŞKUN, Aygün YAVUZ and Beyza BAŞARAN who assisted me during my study.

I am grateful to Ege University Research Fund for financial support during my study.

I would like to thank my family for their encouragement, understanding and attitude throughout my study.



CONTENTS

	<u>Page</u>
ÖZET	vii
ABSTRACT	ix
ACKNOWLEDGEMENTS	xi
LIST OF FIGURES	xix
LIST OF TABLES	xxiii
SYMBOLS AND ABBREVIATION	xxv
CHAPTER ONE - MOLECULARLY IMPRINTED POLYMER BASED FLUORIMETRIC SENSOR FOR THE PRECONCENTRATION AND DETERMINATION OF 1-NAPHTHOL	1
1. Introduction.....	1
1.1. 1-naphthol	1
1.2. Uses of 1-naphthol	2
1.3. Occurrence	3
1.4. Toxicity of 1-naphthol	5
1.5. Analytical methods used for determination of 1-naphthol	6
1.6. Molecularly Imprinted Polymers	9
1.7. Components of MIP.....	10
1.7.1. Template	10

CONTENTS (Continue)

	<u>Page</u>
1.7.2. Functional Monomer.....	11
1.7.3. Cross-linker.....	12
1.7.4. Porogen (Solvent)	13
1.7.5. Initiator.....	14
1.8. Molecular Imprinting Approaches	15
1.8.1. Covalent Imprinting	15
1.8.2. Non-covalent Imprinting	16
1.8.3. Semi-covalent Imprinting	18
1.9. Methods of Polymerization.....	18
1.9.1. Bulk Polymerization	18
1.9.2. Suspension Polymerization	19
1.9.3. Precipitation Polymerization.....	20
1.9.4. Multi-step Swelling Polymerization	20
1.9.5. Core-shell Emulsion Polymerization	21
1.10. Applications of MIPs	21
1.11. The aim of study	23
2. Experimental	24

CONTENTS (Continue)

	<u>Page</u>
2.1. Reagents.....	24
2.2. Apparatus and Operating Conditions.....	24
2.3. Synthesis of Molecular Imprinted Polymer for 1-naphthol.....	25
2.4. Extraction of 1-naphthol from MIPs	27
2.5. Re-binding studies of 1-naphthol to MIPs.....	27
3. Results and Discussion	28
3.1. Optic properties of 1-naphthol.....	28
3.1.1. Spectrophotometric properties.....	28
3.1.2. Fluorescence properties	28
3.2. Calibration graphs for 1-naphthol.....	30
3.3. The effect of monomer on 1-naphthol imprinting	32
3.4. FTIR analysis of the polymers.....	34
3.5. Re-binding studies for 1-naphthol	37
3.6. The effect of initial pH on 1-naphthol re-binding	38
3.7. Effect of re-binding time	39
3.8. Recovery studies of 1-naphthol	40
3.9. Effect of recovery time	40

CONTENTS (Continue)

	<u>Page</u>
3.10. Effect of adsorbent dose.....	41
3.11. Capacities of MIP and NIP	42
3.12. Reusability of imprinted polymer	44
3.13. Interference effects on determination of 1-naphthol.....	45
3.14. Analytical application	45
4. Conclusion	48
 CHAPTER TWO - SELECTIVE AND SENSITIVE FLUORIMETRIC DETERMINATION OF CARBENDAZIM IN APPLE AND ORANGE AFTER PRECONCENTRATION WITH MAGNETITE-MOLECULARLY IMPRINTED POLYMER.....	 51
1. Introduction.....	51
1.1. Carbendazim	51
1.2. Uses of carbendazim	51
1.3. Occurrence	53
1.4. Toxicity of carbendazim	56
1.5. Analytical methods used for determination of carbendazim	58
1.6. Magnetite-Molecularly Imprinted Polymers.....	61
1.7. Applications of MMIPs.....	63

CONTENTS (Continue)

	<u>Page</u>
1.8. The aim of the study	65
2. Experimental.....	66
2.1. Reagents.....	66
2.2. Apparatus and operating conditions	66
2.3. Synthesis of Magnetite Particles.....	67
2.4. Synthesis of Magnetite-Molecular Imprinted Polymer (MMIP) for Carbendazim.....	67
2.5. Extraction of carbendazim from MMIPs.....	68
2.6. Re-binding studies of carbendazim to MMIPs	69
3. Results and Discussion	70
3.1. Fluorescence properties	70
3.2. Calibration graphs for carbendazim.....	72
3.3. FTIR analysis of synthesized polymers.....	73
3.4. Re-binding studies for carbendazim	77
3.5. The effect of initial pH on re-binding of carbendazim	78
3.6. Effect of re-binding time	79
3.7. Recovery studies of carbendazim	80

CONTENTS (Continue)

	<u>Page</u>
3.8. Effect of recovery time	80
3.9. Effect of adsorbent dose.....	81
3.10. Capacities of MMIP and MNIP	82
3.11. Reusability of imprinted polymer	85
3.12. Interference effects on determination of carbendazim.....	85
3.13. SEM images and VSM analysis of the synthesized particles	86
3.14. Analytical application	88
4. Conclusion	91
REFERENCES.....	93
CURRICULUM VITAE.....	115

LIST OF FIGURES

<u>Figure</u>	<u>Page</u>
 CHAPTER ONE	
1.1. Structure of 1-naphthol.....	1
1.2. Molecular imprinting process.....	10
1.3. Functional monomers used in molecular imprinting process.....	12
1.4. Cross-linkers used in the MIP synthesis	13
1.5. Initiators used in the molecular imprinting technology	15
1.6. Schematic representation of covalent and non-covalent approaches in molecular imprinting process	17
1.7. Schematic illustration of synthesis of MIP and re-binding of template by semi-covalent approach.....	18
1.8. Schematic illustration of bulk polymerization	19
1.9. Schematic representation of suspension polymerization	20
1.10. Principle of MISPE	22
3.1. Fluorescence spectrum of 1-naphthol in water (1; blank, 2; 0.05 mg/L, 3; 0.1 mg/L, 4; 0.2 mg/L, 5; 0.4 mg/L and slit width: 5nm)	30
3.2. Fluorescence spectrum of 1-naphthol in methanol (1; blank, 2; 0.01 mg/L, 3; 0.02 mg/L, 4; 0.03 mg/L, 5; 0.05 mg/L, 6; 0.075 mg/L and slit width: 5nm)....	30
3.3. Calibration graph of 1-naphthol in water	31

LIST OF FIGURES (Continue)

<u>Figure</u>	<u>Page</u>
3.4. Calibration graph of 1-naphthol.....	32
3.5. Structures of functional monomer used in MIP synthesis	32
3.6. FTIR spectra of MIP, NIP and non-extracted MIP synthesized by methacrylic acid.....	34
3.7. FTIR spectra of MIP and NIP synthesized by using 2-(dimethylamino)ethyl methacrylate.....	34
3.8. FTIR spectra of MIP, NIP and non-extracted MIP synthesized by using acrylamide	35
3.9. FTIR spectra of MIP, NIP and extracted MIP synthesized by using 4-vinylpyridine.....	35
3.10. FTIR spectra of a) NIP b) non-extracted MIP c) MIP and d) 4-vinylpyridine	36
3.11. The effect of initial pH on re-binding efficiency of 1-naphthol (initial concentration: 1 mg/L, MIP amount: 20 mg, sample volume: 25 mL, contact time: 30minutes).....	39
3.12. The effect of contact time on 1-naphthol sorption efficiency (MIP amount: 30 mg, initial concentration: 2 mg/L (in water, pH~9), sample volume: 25mL)	39
3.13. Effect of time on recovery (MIP amount: 30 mg, initial concentration: 0.1 mg/L (in water, pH ~9), solvent volume: 25mL)	41

LIST OF FIGURES (Continue)

<u>Figure</u>	<u>Page</u>
3.14. Adsorbent dose for the imprinted polymer (initial 1-naphthol concentration: 2.000 mg/L, sample volume: 25 mL, sorption time: 30 minutes, MIP amount: 5-50 mg)	41
3.15. Scatchard plots of NIP (NIP amount: 15 mg, sample volume: 25 mL, initial concentration of 1-naphthol: 1-50 mg/L in water (pH ~9), contact time: 2 hours	43
3.16. Scatchard plots of MIP (MIP amount: 15 mg, sample volume: 25 mL, initial concentration of 1-naphthol: 1-50 mg/L in water (pH ~9), contact time: 2 hours	43
3.17. Reasability of the polymer.....	44
 CHAPTER TWO	
1.1. Structure of carbendazim.....	51
1.2. Preparation of MMIP particles	62
1.3. Schematic experimental procedure for MMIP	62
3.1. The fluorescence spectrum of carbendazim in water (1; blank, 2; 0.05 mg/L, 3; 0.1 mg/L, 4; 0.2 mg/L, 5; 0.3 mg/L and slit width: 5nm)	71
3.2. The fluorescence spectrum of carbendazim in methanol (1; blank, 2; 0.01 mg/L, 3; 0.025 mg/L, 4; 0.05 mg/L, 5; 0.1 mg/L, 6; 0.2 mg/L, 7; 0.3 mg/L, 8; 0.5 mg/L and slit width: 5nm)	71
3.3. Calibration graph of carbendazim in water	72
3.4. Calibration graph of carbendazim in methanol	73
3.5. FTIR spectrum of synhtesized MMIP	74

LIST OF FIGURES (Continue)

<u>Figure</u>	<u>Page</u>
3.6. FTIR spectra of MMIP (red line) and magnetite particles (blue line)	75
3.7. FTIR spectrum of extracted MMIP	75
3.8. FTIR spectra of extracted MMIP and MNIP	76
3.9. The effect of initial pH on re-binding efficiency of carbendazim (initial concentration: 0.2 mg/L, MMIP amount: 80 mg, sample volume: 10 mL, contact time: 30minutes	79
3.10. Effect of re-binding time (initial concentration: 0.05 mg/L (pH~8), sample volume: 15 mL, MMIP amount: 100 mg).....	79
3.11. Effect of time on recovery of carbendazim (MMIP amount: 100 mg, initial carbendazim concentration: 0.05 mg/L (in water, pH ~8), sample volume: 10 mL, solvent volume: 10 mL)	81
3.12. Adsorbent dose for quantitative sorption of carbendazim (initial carbendazim concentration: 0.1 mg/L (in water pH~8), sample volume: 15 mL, sorption time: 60 minutes, MMIP amount: 5-150 mg)	82
3.13. Scatchard plots of MNIP (MNIP amount: 30 mg, sample volume: 15 mL, initial concentration of carbendazim: 0.15-5 mg/L in water (pH ~8) contact time:4 hours)	83
3.14. Scatchard plots of MMIP (MMIP amount: 30 mg, sample volume: 15 mL, initial concentration of carbendazim: 0.15-5 mg/L in water (pH ~8) contact time:4 hours)	84
3.15. Reusability of the polymer	85
3.16. SEM images of a) magnetite b) MMIP	87
3.17. The magnetization curves of magnetite and MMIP	88

LIST OF TABLES

<u>Table</u>	<u>Page</u>
CHAPTER ONE	
1.1. Environmental fate of 1-naphthol.....	5
1.2. Toxic effects of 1-naphthol on different species	6
1.3. Advantages and disadvantages of covalent and non-covalent approaches....	17
2.1. Composition of the synthesized polymers	26
3.1. Maximum absorption wavelength of 1-naphthol in different solvents	28
3.2. Excitation (λ_{ex}) and emission wavelengths (λ_{em}) of 1-naphthol in different solvents	29
3.3. Imprinting factors of the synthesized polymers.....	33
3.4. Re-binding efficiency of 1-naphthol.	38
3.5. Recovery of 1-naphthol with different solvents	40
3.6. Q_{max} and K_d values calculated from the Scatchard plot	44
3.7. Interference effects on the determination of 1-naphthol (1-naphthol = 0.1 mg/L)	45
3.8. Determination of 1-naphthol in real water samples.....	46
3.9. Determination of 1-naphthol after photooxidation of naphthalene	47

LIST OF TABLES (Continue)

<u>Table</u>	<u>Page</u>
CHAPTER TWO	
1.1. General uses of carbendazim	52
1.2. Maximum Residue Levels of carbendazim in different types of crops in Turkey	53
1.3. Degradation half-lives of carbendazim in different conditions	55
3.1. Excitation (λ_{ex}) and emission wavelengths (λ_{em}) of carbendazim in different solvents	70
3.2. Re-binding efficiencies of carbendazim in different solvents	78
3.3. Recovery of carbendazim with different solvents.....	80
3.4. Q_{max} and K_d values calculated from the Scatchard plot	84
3.5. Interference effects on the determination of carbendazim (carbendazim = 0.050 mg/L).....	86
3.6. Determination of carbendazim in apple and orange	89
3.7. Analytical application of the proposed method	90

SYMBOLS and ABBREVIATIONS

<u>Abbreviations</u>	<u>Explanations</u>
DAD	Diode Array Detector
DNA	Deoxyribonucleic Acid
EC ₅₀	Effective Concentration
EFSA	European Food Safety Authority
FTIR	Fourier Transform Infrared Spectroscopy
HPLC	High Performance Liquid Chromatography
HPLC-DAD	High Performance Liquid Chromatography-Diode Array Detector
HPLC-UV	High Performance Liquid Chromatography-Ultraviolet
IUPAC	International Union of Pure and Applied Chemistry
JMPR	Joint Meeting on Pesticide Residues
K _d	Dissociation constants
LC ₅₀	Lethal Concentration
LOD	Limit of Detection
LOQ	Limit of Quantification
MAE	Microwave Assisted Extraction
MBC	Methylbenzimidazole-2-ylcarbamate
MIP	Molecularly Imprinted Polymer
MISPE	Molecular Imprinted Solid Phase Extraction
MMIP	Magnetite-Molecularly Imprinted Polymer
MNIP	Magnetite-Non Imprinted Polymer
MRL	Maximum Residue Level
mRNA	messenger Ribonucleic Acid
MS	Mass Spectrometry

SYMBOLS and ABBREVIATIONS (Continue)

<u>Abbreviations</u>	<u>Explanations</u>
NIP	Non Imprinted Polymer
NMR	Nuclear Magnetic Resonance
NOAEL	No Observed Adverse Effect Level
PVA	Polyvynil Alcohol
QCM	Quartz Crystal Microbalance
Q _{max}	Maximum Binding Capacity
RNA	Ribonucleic Acid
SEM	Scanning Electron Microscope
SCCS	Scientic Committee On Consumer Safety
UV	Ultraviolet
VSM	Vibrating Sample Magnetometer
WHO	World Health Organization
WFD-UKTAG	Water Framework Directive - United Kingdom Technical Advisory Group



CHAPTER ONE - MOLECULARLY IMPRINTED POLYMER BASED FLUORIMETRIC SENSOR FOR THE PRECONCENTRATION AND DETERMINATION OF 1- NAPHTHOL

1. Introduction

1.1 1-naphthol

1-naphthol, 1-Hydroxynaphthalene or α -naphthol is an organic compound with the formula of $C_{10}H_8O$. 1-naphthol has molecular weight of 144.17 g/mol, density 1.10 g/cm³, flash point 125 °C, melting point 94-96 °C, boiling point 278-280 °C and vapour pressure 2.3 hPa at 100 °C. Acid dissociation constant (pK_a) of 1-naphthol is 9.34.

1-naphthol has light brown-yellow colour and it was derived from naphthalene and belongs to phenol family. Since it derives from an organic skeleton, 1-naphthol is soluble in organic solvents but slightly soluble in water. Structure of 1-naphthol is shown in Figure 1.1.

1-naphthol has an isomer which is called as 2-naphthol or β -naphthol. Naphthols can differ from each other by the location of the hydroxyl group. Different position of the hydroxyl group brings different values in physical properties like solubility, melting and boiling points. Despite they have different physical properties, naphthols exhibit fluorescence.

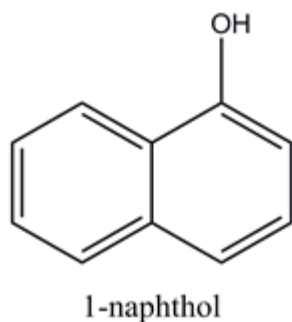


Figure 1.1. Structure of 1-naphthol.

1.2 Uses of 1-naphthol

Naphthols are one of the most important naphthalene derivatives because they act as an intermediate in the production of many chemicals. 1-naphthol can be used as precursor in the production of pesticides and active pharmaceutical ingredients. It can also be used in the production of azo compounds.

In the production of pesticides like 1-naphthoxyacetic acid, carbaryl and devrinol, 1-naphthol was used as precursor in all reactions.

In the synthesis of 1-naphthoxyacetic acid, which is used as growth regulator, the product is prepared by aqueous alkylation of chloroacetic acid by 1-naphthol. Devrinol herbicide is produced by the reaction of 1-naphthol and N,N-diethyl- α -bromopropionamide in methanol and sodium methoxide reflux. N-methylcarbamate pesticide carbaryl is synthesized by the reaction of 1-naphthol with methyl isocyanate (Booth, 2000).

In the pharmaceutical industry, 1-naphthol has been used for the production of some important chemicals. Alphenol, as antiseptic and antirheumatic, inderal, as adrenergic β -blockers and nadolol as antiarrhythmics are produced by using 1-naphthol (Booth, 2000).

1-naphthol can be used in the synthesis of the azo compounds. Synthesis of 1-naphthol-azo-dyes under solvent free conditions was obtained by Bamoniri et al. (2013). The diazo coupling of 1-naphthol with diazotized sulfanilic acid was investigated to produce monoazo dyes (Bourne et al., 1990).

1-naphthol is used as a raw material in the production of rubber antioxidants (Sulekha, 2002). 1-naphthol is also used as oxidative hair dye substance (SCCS, 2008). 1-naphthol, is used as a pigment in inks and coatings and used as additive in polymers (Bayer, 2003).

1-naphthol can also be used as reagent in some tests to determine organic and biological compounds. 1-naphthol is known as Molisch's reagent to detect the presence of carbohydrates (Foulger, 1931). Molisch's test was based on the dehydration of the carbohydrate by sulfuric acid to produce an aldehyde, which condenses with 1-naphthol resulting in a violet colour.

Sakaguchi test was used for detection of arginine aminoacid in proteins. In Sakaguchi test, arginide in arginine can be detected by the production of a pink or red colour when certain guanidine derivatives are treated with 1-naphthol and sodium hypochlorite in an alkaline solution (Baker, 1947).

Wilson et al. (1985) suggest that 1-naphthol can be possibly used as an antitumor agent and 1-naphthol also has been classified as a plant growth regulator (Gambino et al., 2008).

1.3 Occurrence

In the environment, 1-naphthol is mainly formed by the breakdown of carbaryl and naphthalene.

Carbaryl, N-methylcarbamate insecticide, is one of the most frequently used insecticides and widely used for the control of a variety of pests on fruit, vegetables, and many other crops (Mathew et al., 1995).

Carbaryl can be degraded to 1-naphthol in the environment mainly by hydrolysis. 1-naphthol is the major degradation product. In water, as pH increases carbaryl degrades faster. Carbaryl degrades at pH 7 and 9 at 25°C, with the half-lives of 10-17 days and 3 hours, respectively (Kanan, 2002). The other degradation products of hydrolysis are methylamine and carbondioxide. (Larkin and Day, 1986). In seawater, Armbrust and Crosby (1991) reported that hydrolysis half-lives of carbaryl pH 7.9 and 8.2 at 24°C were 24 and 23 hours, respectively. When exposed to artificial sunlight, carbaryl had a half-life of 5 hours.

In soil, the photodegradation of carbaryl was investigated and under artificial sunlight, it was found to be 30 days. In aerobic soil, carbaryl was quickly degraded with an approximate half-life of 4 days and it degrades more slowly in anaerobic aquatic soil with an estimated half-life of 72 days (Xu, 2000).

Naphthalene is used as a precursor in production of many pigments, dyes and pharmaceuticals. It is also used as pesticide to control moths.

Decomposition of naphthalene is also an important pathway to produce 1-naphthol in the environment. Naphthalene can be degraded to 1-naphthol under aerobic conditions by different microorganisms (Montgomery, 2007). In water,

naphthalene was metabolized to 1-naphthol by microorganisms as stated by Cerniglia et al. (1980). In the atmosphere, hydroxyl radicals and nitric oxides react with naphthalene to form 1-naphthol (Atkinson et al., 1987). By photolytic irradiation of naphthalene, 1-naphthol was found as one of the metabolites (Montgomery, 2007). McConkey et al. (2002) also studied the photodecomposition of naphthalene.

Naphthalene is metabolically transformed into 1-naphthol in human body (Preuss et al., 2003). Yang et al. (1999) showed that the amount of 1-naphthol found in body among smokers were significantly higher than non-smokers. In animals, exposed to naphthalene, 1-naphthol was detected as a metabolite (Turkall et al., 1994).

Table 1.1 shows the general environmental fate of 1-naphthol. In water, studies show that in the absence of dissolved oxygen, 1-naphthol is stable in all pHs and as concentration of dissolved oxygen increases, rate of oxidative transformation of 1-naphthol increases. In seawater, half-life of 1-naphthol under sunlight was 7 days, whereas in the absence of light it was 15 days. 1-naphthol was stable in dark in sterile seawater over a three-day period, but was degraded to undetectable levels in 96 hours in seawater. Under artificial sunlight, 1-naphthol was completely degraded after 2 hours. The degradation half-life of 1-naphthol in soil was found to be 0.9 days (Bayer, 2003).

Table 1.1. Environmental fate of 1-naphthol (Bayer, 2003).

Photodegradation	$t_{1/2} = 1.9$ hours
Fugacity	Air = 0.07 % Water = 39.8 % Soil = 59.8 % Sediment = 0.3 %
Biodegradability	96% after 14 days

1.4 Toxicity of 1-naphthol

Several studies have been made for investigating the toxicity of 1-naphthol and papers have been published for the toxic effects of 1-naphthol. Especially, the studies have been focused on toxic effects of 1-naphthol on human and animal life.

As stated in literatures (Meeker et al., 2004; Meeker et al., 2006), 1-naphthol has negative effects on semen quality and testosterone level and it causes significant changes on the functions of enzymes and immunological system and gives damage to DNA. Kapuci et al. (2014) suggest that 1-naphthol may cause DNA damage on human lymphocytes.

Acute toxicity of 1-naphthol to some marine organisms were studied by Stewart et al. (1967). Rao et al. (1984) showed that 1-naphthol has toxic effects to fish. Bruner and Fisher (1993) stated that toxicity of 1-naphthol to midge larvae increases as temperature increases.

Effective concentration (EC_{50}), lethal concentration (LC_{50}) and (No Observed Adverse Effect Level) NOAEL values of 1-naphthol are shown in Table 1.2.

Table 1.2. Toxic effects of 1-naphthol on different species (Bayer, 2003).

Acute Fish Toxicity (96 hours)	LC ₅₀ = 0.75 mg/L (L. Macrochirus) LC ₅₀ = 4.24 mg/L (P. Promelas)
Acute Invertebrate Toxicity (48 hours)	EC ₅₀ = 3.53 mg/L (Daphnia magna)
Algal Toxicity (20 days)	EC ₅₀ = 20-50 mg/L (Chlorella vulgaris)
Acute Mammal Toxicity	1000-3000 mg/kg bw (Oral, rat) >97 mg/m ³ (Inhalation, rat) > 10000 mg/kg (Dermal, rabbit)
Mammal Mutagenicity	Negative
Chromosome Aberration	Negative
Repeated Dose Toxicity	NOAEL= 130 mg/kg/d (13 week, oral, rat)
Reproductive toxicity	NOAEL= 0.5 % (two generation study, dermal, rat)

1.5 Analytical methods used for determination of 1-naphthol

In analytical chemistry, it is very important to develop sensitive, selective and robust methodologies for the determination of pesticides especially in food, environmental and biological samples since they can be toxic and persistent in the matrix.

Different spectroscopic and electrochemical techniques can be used for the quantitative determination of 1-naphthol. High-pressure liquid chromatography (HPLC), Fourier transform infrared spectroscopy (FTIR), fluorescence spectrometry, phosphorimetry, spectrophotometry and quartz crystal microbalance (QCM) are the most widely used techniques used for the determination of 1-naphthol.

Zhou et al. (2014) has been used a high performance liquid chromatography system, which consisted of two pumps and an ultraviolet detector to preconcentrate and determine the phenolic compounds. They have suggested a new method using conventional dispersive liquid–liquid microextraction system for preconcentration and determination of bisphenol A, 1-naphthol, 2-naphthol and 2,4-dinitrophenol in water samples.

Asensio-Ramos et al. (2012) have developed a system which is consist of a hollow-fiber liquid-phase microextraction integrated with HPLC and fluorescence detection to determine a group of pesticides including 1-naphthol.

Preuss and Angerer (2004) have also developed a HPLC system that can be determine 1-naphthol and 2-naphthol simultaneously with the detection limits in the lower ppb range.

Daghbouche et al. (1995) preconcentrate and determine carbaryl and its main metabolite 1-naphthol by using FTIR while Jia et al. (2007) determine both chemicals by using fluorescence spectrophotometer. Lopez et al. (1999) has been used another sensitive spectroscopic technique, phosphorimetry to determine 1-naphthol and 2-naphthol.

Spectrophotometric determination of 1-naphthol was also performed. Pearse Jr. (1963) developed a method which was based on the formation of the colored product obtained by the reaction of 1-naphthol, iodine and sodium hydroxide in a water immiscible solvent. The absorbance of the non-aqueous system was measured at 528 nm. In an other study, two methods based on charge-transfer formation for spectrophotometric determination of 1-naphthol was performed by Mohammed (2010). In first method, reaction was occurred between 1-naphthol and chloranil whereas in the second method, reaction was occurred between 1-naphthol and 2,3-dichloro-5,6-dicyano-1,4-benzoquinone which absorb light maximally at 349 nm and 423 nm, respectively.

Chemometric strategies were applied in new studies for simultaneous and sensitive determinations of naphthols. Four-way kinetic-excitation-emission fluorescence data processed by multi-way algorithms was used for determination of carbaryl and 1-naphthol in water samples by Maggio et al. (2010) and Yuan et al. (2010) used QCM with the combination of chemometry to determine 1-naphthol and 2-naphthol simultaneously. Santa-Cruz and Garcia-Reiriz (2014) applied multivariate calibration algorithms for determination of carbaryl, naphthol and propoxur by using spectroscopic data.

Electrochemical studies were also investigated for determination of 1-naphthol. Zhu et al. (2012), prepared gold nanoparticles/hollow nitrogen-doped

carbon microsphere hybrids functionalized with thiolated- β -cyclodextrin and applied for sensitive and simultaneous electrochemical detection of naphthols and when compared with other electrochemical sensors, the proposed electrode results in improved detection limits of about four times for 1-naphthol. Simultaneous determination of naphthols by using poly(3-methylthiophene)-nano-Au modified electrode was performed by Li et al. (2015). Zhong et al. (2011) studied the determination of naphthols and bisphenol A by capillary zone electrophoresis after preconcentrated by cloud point extraction.

SnO₂ nanooctahedron with (2 2 1) high-index facet was synthesized and employed for determination of 1-naphthol by Huang et al. (2012) and the results showed that the system demonstrated higher electrochemical activity and lower limit of detection toward 1-naphthol when compared to glassy carbon electrode. Sensitive detection of 1-naphthol based on G-DNA modified gold electrode by using electrochemical impedance spectroscopy was reported by Liang et al. (2013). Voltammetric studies have been carried out for 1-naphthol determination. Zhang and Zhuang (2009) studied the voltammetric behavior of 1-naphthol was studied with a poly (acridine orange) film modified glass carbon electrode.

Over the last decade, nanoparticles can be used for sample treatment, separation of analytes and detection of the pollutants. The most widely used nanoparticles in analytical chemistry includes silica nanoparticles, carbon based nanoparticles, mainly fullerenes and carbon nanotubes, and metallic nanoparticles (Kaur and Gupta, 2009). Among these nanoparticles, carbon nanotubes have been widely used as efficient adsorbents to remove organic pollutants. Sequestration mechanism of 1-naphthol on discharged multi-walled carbon nanotubes was investigated by Yang et al. (2012). Wu et al. (2012) investigated pH effect on the transformation and sorption of 1-naphthol on multiwalled carbon nanotubes. Wu et al. (2015) investigated the adsorption of 1-naphthol onto carbon nanoparticles pillared multi-walled carbon nanotubes. The maximum adsorption capacity of the adsorbent was found to be 37.74 mg/g. Wang et al. (2015) studied the adsorption of 1-naphthol and phenanthrene on to colloidal graphene oxide nanoparticles. Kinetic and thermodynamic study of 1-naphthol adsorption from aqueous solution to sulfonated graphene nanoparticles was studied by Zhao et al. (2011). Removal of 1-naphthol by using magnetic nanoparticles was evaluated by Zhang et al. (2014).

In recent years, polymeric structures were studied as an alternative way to remove organic compounds especially in industrial wastewater due to their high adsorption capacities. Zhang et al. (2009) investigated the sorption of 1-naphthol onto a hydrophilic hyper-cross-linked polymer resin and the adsorbent was used to remove 1-naphthol from contaminated waters. Usage of diethyl aminoethyl cellulose adsorbed and crosslinked white radish peroxidase for the removal of 1-

naphthol was evaluated by Ashraf and Husain (2010) in batch and continuous process. Zhang et al. (2008) performed the removal of 1-naphthol and 1-naphthylamine by using polymeric adsorbents. Zhang et al. (2006) investigated the adsorption behaviours of 1-naphthol and 1-naphthylamine onto nonpolar macroreticular adsorbents at different temperatures.

1.6 Molecularly Imprinted Polymers

Molecularly imprinted polymers (MIPs) are one of the most widely used adsorbents for the sensitive and selective determination of organic and inorganic compounds, in recent years. Molecular imprinting technology depends on creating specific binding sites for a molecule inside of a polymer structure. The recognition mechanism is mainly based on weak non-covalent interactions, such as hydrogen bond, ion-pair, hydrophobic interactions and dipolar associations (da Silva and Casimiro, 2012).

In the molecular imprinting process, monomer interacts with the target molecule (analyte or template), by the aid of functional groups, in the presence of porogen (solvent) and a cross-linker that fixes the monomer-template complex within a porous polymer matrix (da Silva et al., 2010). This relationship between monomer and template and principle of creating the imprinted cavities for template is based on the idea of key-lock mechanism. Molecularly imprinted polymers act as an alternative adsorbents to provide tailor-made receptor binding sites via the rearrangement of the template and functional monomer. Because of their selectivity, MIPs have been used in different application areas such as food, biotechnological, pharmaceutical and environmental analysis over the last decade.

Briefly, the molecularly imprinted polymers are synthesized by mixing the template molecule with functional monomer, cross-linker and initiator in an appropriate solvent. This mixture is called to be pre-polymerization mixture. Solvent used in MIP synthesis preferred to be an aprotic and non polar solvent. The pre-polymerization mixture is irradiated with UV light or subjected to heat in order to initiate polymerization. After initiating the polymerization, the complex formed between the template molecule and the functional monomer. The complex will be stabilized within the rigid structure, which is highly cross-linked polymer. After polymerization completed, the template is extracted out of the polymer, resulting the formation of the imprinted polymer which possess recognition site for binding of the template (Yan and Row, 2006).

Figure 1.2 shows the schematic mechanism of molecular imprinting process. As shown in Figure 1.2, the imprinting process can be divided mainly in to three steps. In the first step, functional monomer-template conjugates are formed by covalent or non-covalent interactions. In second step, the monomer-template

complex are fixed in three-dimensional rigid structure of the cross-linked-polymer. In the third and the last step, the template molecules are removed from the polymer and the cavity of the template molecule is left inside the polymer structure.

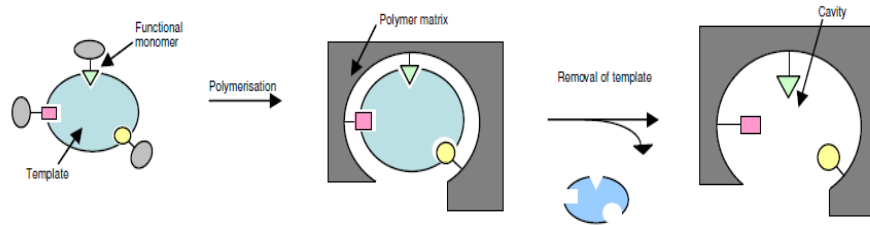


Figure 1.2. Molecular imprinting process (Walsh, 2010).

The interactions between template and a functional monomer can be proceeded via hydrogen bonding, reversible covalent bonds, electrostatic interactions and van der Waals forces. The interactions can be collected in three main categories; covalent, non-covalent and semi covalent interactions.

1.7 Components of MIP

The chemicals required to synthesize a MIP can be divided into five components. These components can be classified as; template, functional monomer, cross-linker, initiator and solvent (porogen).

1.7.1 Template

Analyte molecule can also be called as target molecule or template molecule in imprinting technology. Since its cavities are formed inside of the polymer structure, it is preferably to be called as template molecule rather than analyte or target molecule.

The template molecule chosen must be chemically inert and stable under polymerisation conditions since the polymerisation reactions are based on the free radical interactions. The template should also be stable under UV exposure or high polymerisation temperature. The other parameters that affect the selection of the template are its cost, availability and functional groups that define its ability for strong interactions with the functional monomers (Cormack and Elorza, 2004).

When the template is not suitable for the conditions mentioned above, a closely structural analogue to the analyte was chosen as template molecule and this molecule is called to be dummy molecule. The dummy approach is also used to prevent the risk of template leaking from the polymer (Pichon and Chapuis-Hugon,

2008). Bleeding of the template is the main problem in quantitative analysis at trace levels when the template molecules can not be able to successfully extracted out from the polymer structure (Lee, 2006). In recent years, Yu et al. (2015) and Xiao et al. (2015) used dummy imprinting technology for selective and sensitive determinations.

1.7.2 Functional Monomer

The functional monomer is an important component of the MIP since it interacts with the template, and therefore it is responsible for creating specific binding sites for the template inside the polymer structure. Functional monomers can interact with target molecules through covalent, non-covalent and semi covalent interactions.

The selection of the functional monomer can be determined by the structure of the template. Some spectroscopic techniques and studies can be useful for selecting the appropriate monomer in the synthesis by investigating the potential interactions between monomer and template (Turkewitsch et al., 2005). Interactions can be evaluated by using various spectroscopic techniques such as NMR (Courtois et al., 2006) and molecular modeling studies (Piletsky et al., 2001). According to Brüggeman (2003), for templates with amino groups, acidic monomers should be chosen for the best result in MIP synthesis and for templates with carboxylic acid groups, the best choice seems to be a basic functional monomer. Scorrano et al. (2011) investigated the effect of different functional monomers onto imprinting efficiency of amino acid derivatives. Figure 1.3. illustrates the most commonly functional monomers used in the molecular imprinting process.

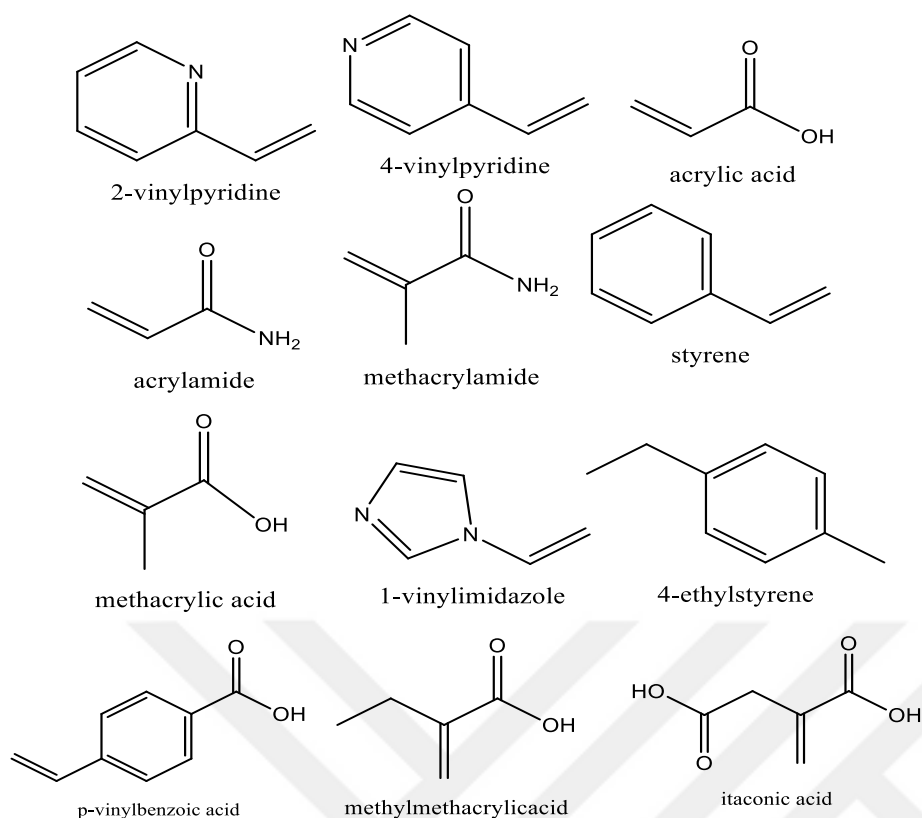


Figure 1.3. Functional monomers used in molecular imprinting process (Yan and Row, 2006).

1.7.3 Cross-linker

In the imprinting process, with the aid of suitable crosslinking agent, random polymerization occurs successfully and the functional residues derived from the functional monomers are uniformly distributed in the polymer network. Cross-linking agent has different and important functions in imprinting process. The main role of the cross-linker is to fix and control the morphology of the polymer matrix besides from stabilise the imprinted binding sites. Another function of the cross-linker in polymer structure is to make the imprinted polymer insoluble in solvents and supply the mechanical stability to the polymer matrix (Komiya et al., 2003).

The mole ratios of cross-linker to functional monomer are also important. High cross-link ratios are generally preferred in order to access permanently porous materials and to generate polymers with adequate mechanical stability. If the ratios are too small, the guest-binding sites are located so closely to each other that they can not work independently and this situation leads to inhibition of the template binding to the neighbour sites. When the ratios are too high, both the binding of the template to cavities proceeds too slow and the binding capacity of the polymer decreases. Generally, polymers with a high degree of cross-linking (70-90%) polymers are preferred to be used in the polymer synthesis for the optimum usage

in sorption studies (Komiya et al., 2003). Figure 1.4 illustrates the mostly used cross-linkers in the MIP synthesis.

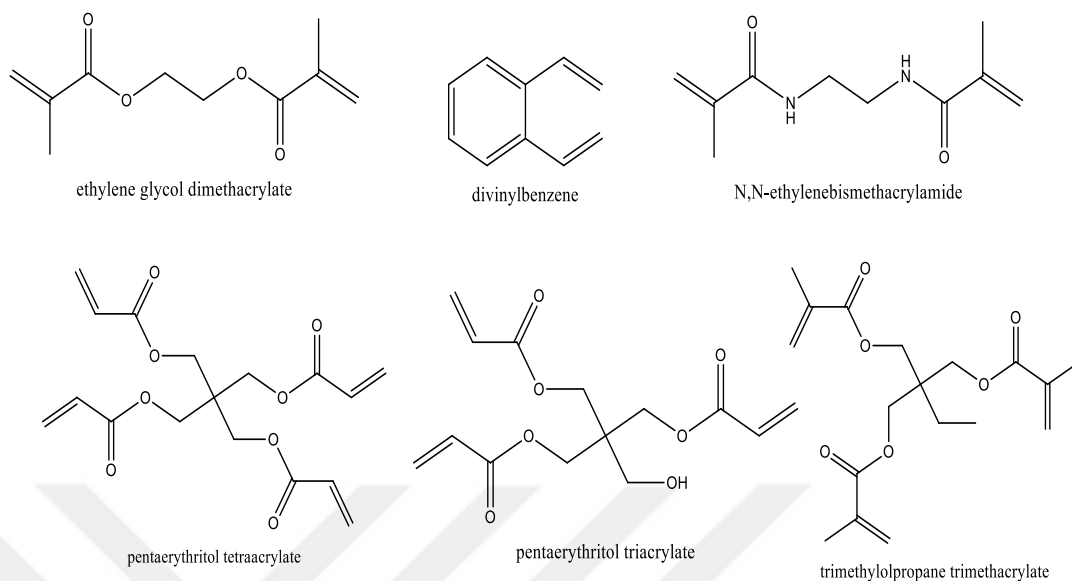


Figure 1.4. Cross-linkers used in the MIP synthesis (Walsh, 2010).

Since the cross-linkers also have the ability to interact other materials like monomer and template in the polymer structure, the nature of the cross-linker must also be considered.

1.7.4 Porogen (Solvent)

Solvents used in the MIP synthesis have vital roles. The main role of the solvent is to dissolve all components used in the MIP synthesis. During the synthesis solvent evaporates and creates pores inside the rigid polymer structure. Thus, solvent can also be called as porogen in molecular imprinting technology.

The porogen should be selected due to the type of imprinting. In covalent imprinting, many kinds of solvents can be used as long as they dissolve all the components but especially in the non-covalent imprinting, the properties of porogen affects the strength of the interactions occurred between monomer and template. Since the interactions are mainly based on the Hydrogen bonds and van der Waals interactions in non-covalent approach, a moderately polar and aprotic solvent, such as toluene, dichloromethane, chloroform and acetonitrile should be selected as porogen during the synthesis. When the polarity of the solvent increase, the interactions would be inhibited. Thus, porogen used in the MIP synthesis has a vital role on the selectivity and the capacity of the polymers synthesized (Pichon and Chapuis-Hugon, 2008).

Another role of solvents is to disperse the heat of reaction generated on polymerization. Otherwise, the temperature of reaction mixture is locally elevated, and undesired side-reactions will occur (Komiyama et al., 2003).

1.7.5 Initiator

The role of initiator in molecular imprinting process is to initiate the polymerization reaction. The initiator used in polymerization reactions may be triggered by different ways like heat, UV radiation or chemicals. After initiation, free radicals were formed and react with monomer or cross linking agent in order to propagate into longer chains. Polymerisation process stopped when two free radicals reacted with each other. The amount of initiator used in the synthesis is relatively at low level compared to the template and monomer (Lee, 2006).

Since oxygen can easily accept electrons from radicals, oxygen gas retards free radical polymerizations, thus in order to maximize the rates of monomer propagation, dissolved oxygen should be removed by ultrasonication or by sparging of the solution by an inert gas like nitrogen or argon (Yan and Row, 2006).

Photochemical initiation can be performed at low temperature, and therefore should be considered in cases where a thermally labile template is used. Photochemical initiation is also preferable in non-covalent imprinting approach since non-covalent interactions are stronger at lower temperatures. While, heat initiation might be preferred with light-sensitive or poorly soluble templates (Turkewitsch et al., 2005). The choice of initiator is also affect the morphology and binding capacity of MIPs. Therefore, initiators should be selected carefully. Figure 1.5 shows the initiators used in molecular imprinting technology.

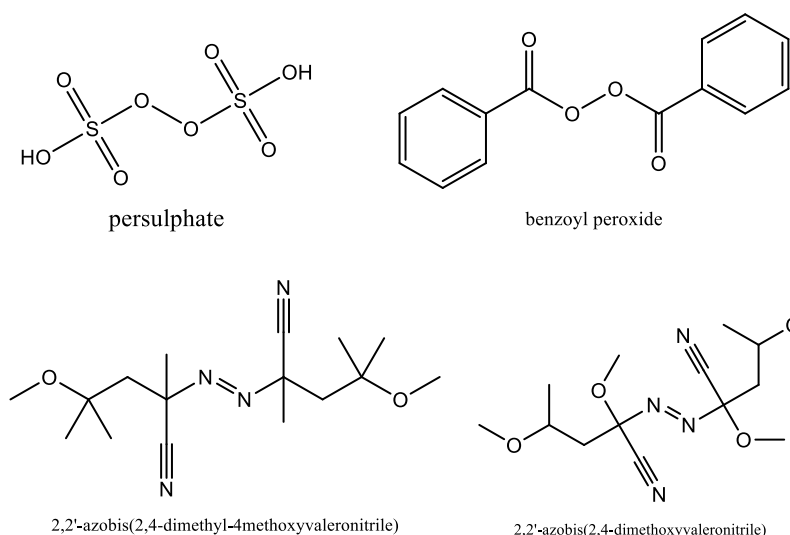


Figure 1.5. Initiators used in the molecular imprinting technology (Pakade, 2012).

1.8 Molecular Imprinting Approaches

Depending on the binding types between template and functional monomer, there are three main types of imprinting approaches in molecular imprinting technology. They can be classified as covalent, non-covalent and semi-covalent imprinting.

1.8.1 Covalent Imprinting

In the covalent approach, the interactions between the template and the functional monomer are proceeded via covalent bonds. The binding relies on the reversible covalent bonds. In this approach, monomer-template conjugates are stable and stoichiometric and a wide range of conditions like high temperatures, high or low pHs and highly polar solvents may be used (Komiyama et al., 2003), but since the binding and extraciton kinetics are slow, the covalent imprinting is not generally used in MIP synthesis (Beltran et al., 2010).

The other disadvantage of the approach is the limitation of the number of the covalent linkage. Covalent imprinting generally involves the ability of forming covalent bonds of limited range of functional groups. Reversible condensation reactions like boronate ester, ketal/acetal and Schiff's base formation can be used in covalent approach. Boronate ester reactions can be used in imprinting of carbohydrate derivatives and Schiff's base method can be used for imprinting of amino acid derivatives whereas ketal/acetal reaction can be take place in the presence of diol and a carbonyl group. Since the covalent bonding is stoichiometric, there is no need the usage of excess of functional monomer so non-specific binding may be greatly reduced (Mayes and Whitcombe, 2005).

1.8.2 Non-covalent Imprinting

For the preparation of MIPs, the non-covalent approach is the most frequently used method because of its simplicity and fastness. In the non-covalent approach, ionic interactions, hydrogen bonds, dipole-dipole interactions and van der Waals forces have taken place between the template and the monomers.

In non-covalent approach a broad range of template and functional monomers can be used. Since weak interactions has been occurred in the non-covalent imprinting approach, excess amount of functional monomer should be used to get more stable template-monomer conjugate. Excess amount of monomer provides equilibrium to shift towards the formation of template-monomer conjugate. Negative point of the excess amount of monomers is creating the non-specific binding sites. In non-covalent approach, the template-monomer complex is not necessary to be stoichiometric but the experimental conditions should be chosen carefully since the interactions may be collapsed especially in the polar medium.

It is generally assumed that in non-covalent imprinting a pre-polymerisation complex is formed between the template and functional monomers. This pre-polymerization complex is formed via the non-covalent interactions and the complex was polymerized with an appropriate cross-linker and initiator. Conversely to the covalent approach, different types of monomers may be used in non-covalent approach since the functional groups like amine, amino, carbonyl and hydroxyl has the ability for non-covalent interactions (Lee, 2006). The template can be removed and re-bound to the imprinted sites easily in non-covalent imprinting (Lok and Son, 2009). Generally, in non-covalent binding, excess amount of monomers are used but in some cases stoichiometric interactions may also be used.

Main advantages and disadvantages of covalent and non-covalent approaches mentioned above are summarized in Table 1.3.

Table 1.3. Advantages and disadvantages of covalent and non-covalent approaches (Lee, 2006).

	Covalent binding	Non-covalent binding
Re-binding and release of template	slow	fast
Polymerization conditions	wide range	restricted
Removal of template after polymerization	difficult	easy
Stoichiometry of binding	stoichiometric	non-stoichiometric

Figure 1.6 shows the schematic representation of covalent binding and non-covalent interaction in MIP synthesis.

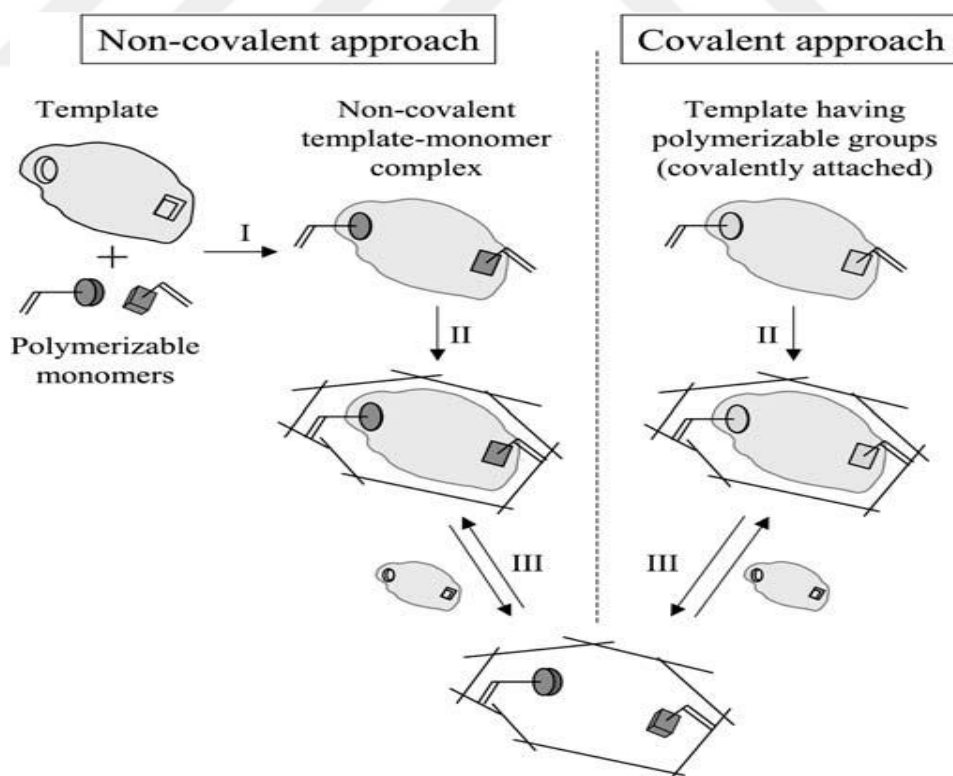


Figure 1.6. Schematic representation of covalent and non-covalent approaches in molecular imprinting process (Lee, 2006).

1.8.3 Semi-covalent Imprinting

The semi-covalent approach is the combination of the non-covalent and the covalent approaches mentioned above. In this approach, covalent bonds are formed between the template and the functional monomer before polymerization and when the template has been removed from the polymer, re-binding of template can be conducted via non-covalent interactions (Jiang et al., 2007).

In other terms, in semi covalent approach the formation of template-monomer complex is based on covalent bonds but the re-binding of template onto imprinted sites are based on the non-covalent interactions. So, the method aims to combine the advantages of both method. Figure 1.7 shows the schematic illustration of synthesis of MIP and re-binding of template by semi-covalent approach.

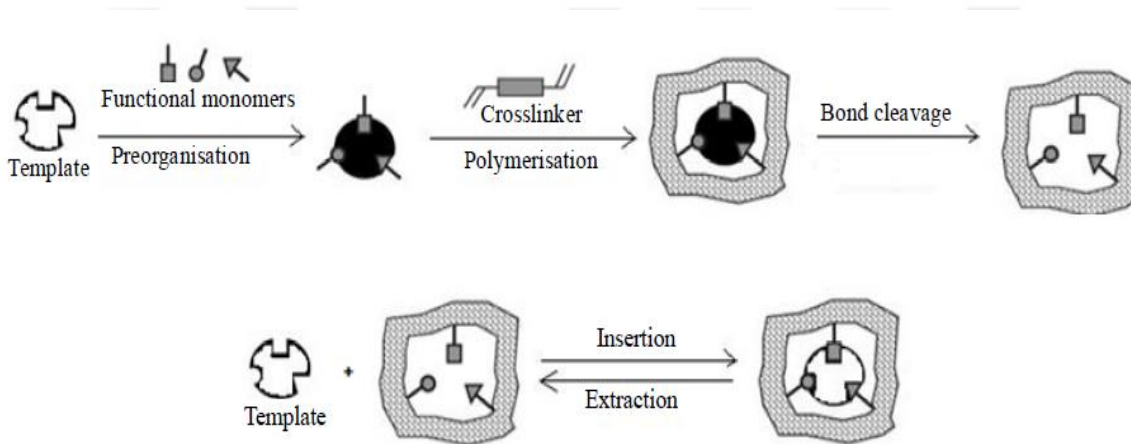


Figure 1.7. Schematic illustration of synthesis of MIP and re-binding of template by semi-covalent approach (Garcia et al. 2011).

1.9 Methods of Polymerization

Several methods can be used for the preparation of MIPs. Among these techniques, bulk polymerization is the most widely used technique because of its simplicity and rapidity.

1.9.1 Bulk Polymerization

Bulk polymerization is the most popular method used in the synthesis of the imprinted polymers. The technique is also called as traditional polymerization. In this method, template, monomer and cross-linker are mixed and dissolved in a porogen and polymerization take place by the aid of initiator in a reaction vessel or simply in a glass tube under UV light or in a water bath. Polymerization conditions can easily be controlled in this method. Generally, the minimum amount of porogen

is used in bulk method to let the growing polymer chains to precipitate in bulk forming a single monolith solid (Pakade, 2012).

It is generally preferred due to its rapidity, simplicity, and economic instrumentation. On the other side, the polymer should undergo a time-consuming process which includes the crushing, grinding and sieving of polymer particles into suitable size. This process also reduces the yield of polymer and irregular particles can be formed after grinding process. Polymers with heterogeneous binding sites are obtained with bulk method and this is the most important parameter that prevents the use of imprinted polymers as adsorbents in chromatographic studies (Chen et al. 2011). Schematic representation of bulk polymerization is shown in Figure 1.8.

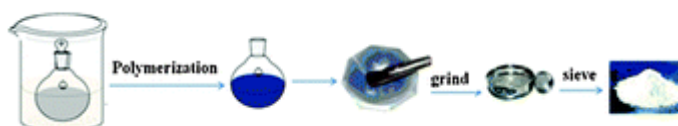


Figure 1.8. Schematic illustration of bulk polymerization (Chen et al., 2011).

1.9.2 Suspension Polymerization

Suspension polymerization is a heterogeneous type polymerization since it involves two immiscible phases; continuous phase and the dispersed phase. Dispersed phase is an organic phase and the continuous phase is generally an aqueous phase whereas paraffin and perfluorocarbon can also be used. Dispersed phase contains the monomer, initiator, porogen and the template. Dispersed phase is directly in contact with the continuous phase, generally stabilized by gelatin, polyvinylalcohol or hydroxyethyl cellulose. It can be said that, the polymerization mixture is suspended as droplets in a continuous phase. The polymerization reaction proceeds in the droplets. By using this technique, shape and size of the particles can be controlled (Branger et al., 2013).

In literatures it is also mentioned that the use of water as a continuous phase may be the main problem of this technique since water can interrupt template-monomer bonding if the non-covalent imprinting approach is used (Pakade, 2012).

Suspension polymerization technique produces high-yield-polymers and polymers have better chromatographic characteristics when compared with bulk method (Garcia et al., 2011). Schematic representation of the suspension polymerization system is shown in Figure 1.9.

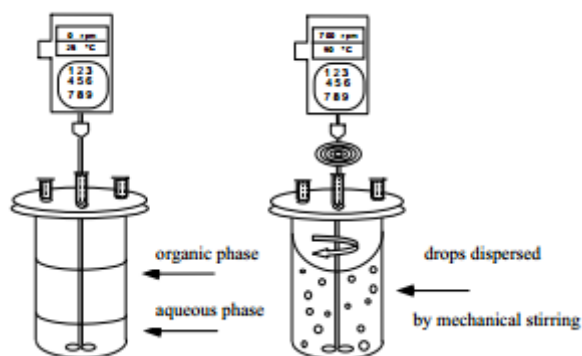


Figure 1.9. Schematic representation of suspension polymerization (Morejon et al., 2005).

1.9.3 Precipitation Polymerization

Precipitation polymerization brings the improved spherical properties of the imprinted polymers. This important property makes the polymers to be used in MISPE applications. The method was based on the growing of polymeric chains until reaching a certain critical mass and begin to precipitate. Generally the size of the particles do not exceed 10 μm . The most important parameter that affects the quality of the produced polymers, is the polymerization conditions. The polymerization conditions and the components such as template, porogen and functional monomers used in precipitation polymerization must be chosen carefully (Beltran et al., 2010).

Polymerization conditions in this method are generally similar to those in the bulk method except that the amount of solvent can be highly greater than the bulk method. More uniform size particles can be produced compared to the bulk method and the conditions affect the size of the particles produced at the end of the synthesis (Walsh, 2010).

1.9.4 Multi-step Swelling Polymerization

This technique involves several swelling steps before the polymerization reaction. Monodisperse particles can be produced by using multi-step swelling polymerization technique. Particles with the suitable size can be used in HPLC for chromatographic determinations (Lok and Son, 2009).

In this method, particles are suspended in water and after several additions of organic solvents, the initial particles begin to swell. Once the particle swelled up to desired size, components which are used for the polymerization reaction are added

to the reaction vessel and the polymerization reaction take place. The method is time consuming because of the multi-step swelling procedures. The presence of water is also another disadvantage of the method which may disrupt the non-covalent interactions between the template and the functional monomer (Pakade, 2012).

1.9.5 Core-shell Emulsion Polymerization

By the aid of this method, monodisperse core-shell particles are produced. These particles can be used for surface imprinting. Core-shell latex particles consist of solid or liquid cores surrounded by shells of either organic or inorganic materials (Chen et al., 2012).

Different methods can be used for the preparation of core-shell particles. Among them, emulsion polymerization, seed polymerization and phase separation methods are generally used for the synthesis of core-shell particles. These techniques aim the deposition of an imprinted polymer based layer on nanoparticles (Poma et al., 2010).

In seed polymerization, polymerization reaction take place on the surface of seed particles and a shell layer formed on the seed. In phase separation method, two phases which are rich in different polymer, are created during polymerization and the phases form the core and the shell structures. Core-shell particles are generally used in the adsorption and recovery studies in chromatography (Liu et al., 2015).

The complex procedures for the synthesis is the main disadvantage of the method whereas variety of the applications, high yield and improved kinetics of the mono-disperse materials are the main advantages of the method.

1.10 Applications of MIPs

MIPs can be used in many application areas in order to separation and sensitive determination of organic and inorganic materials. Imprinted polymers can be used especially in chemistry, biology, engineering and medicine.

Chromatography is an important application area of MIPs. MIPs can be used for the separation of organic materials. Huge number of studies are reported in the literature on MIP combined with chromatography. Luo et al. (2006) used MIPs for the chiral separation of C_2 -asymmetric bi-naphthyl compounds. Molecular imprinting technology was combined with HPLC for the separation of aspirin by Byun et al. (2010).

Mostly used method for imprinted polymers is Solid Phase Extraction (SPE) which is called to be Molecularly Imprinted Solid Phase Extraction (MISPE). MISPE is generally used with liquid chromatographic techniques with on-line and off-line modes for both preconcentration and separation of the organic materials. In recent years, MISPE is used for the studies of biological and environmental samples. Basic steps of MISPE is shown in Figure 1.10 (Vasapollo et al., 2011).

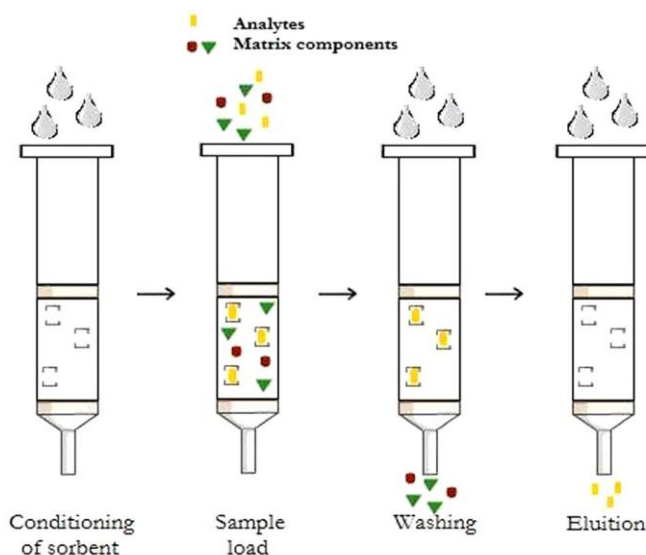


Figure 1.10. Principle of MISPE (Vasapollo et al., 2011).

Extensive usage of MISPE over last decade depends on its selectivity, stability and low cost of preparation of the imprinted materials. Different types of extraction and variety of polymerization methods used for preparation of polymers, make MISPE a well-rounded technique which can be used in different areas (Baggiani et al., 2007).

MISPE used by Anderson et al. (2008) for the detection of benzodiazepines in hair samples. Widstrand et al. (2004), used MISPE technique for the extraction of β -agonists from calves urine. Beside chromatography, MIPs can be used with the combination of spectroscopic techniques for the sensitive determination of organic and inorganic compounds.

Alvarez-Diaz et al. (2009) used brominated and iodinated imprinted polymers for the phosphorimetric determination of carbaryl in room temperature. Ge et al. (2012) developed a multi-branch chemiluminescence-molecular imprinting sensor for the determination of carbofuran and omethoate pesticides in food samples. Molecularly imprinted silica particles were used for selective adsorption of naphthalene by Guo et al. (2011) before fluorimetric determination. In an other study, Monte Carlo model was developed by Chen et al. (2004) to obtain the best design for fluorimetric MIP sensor.

Ebrahimzadeh et al. (2015) used magnetic ion-imprinted polymer as an adsorbent for preconcentration of Pb(II) and the method was applied to beverage samples and flame atomic absorption spectrometer was used for the analysis. Imprinted polymeric nanobeads were used for selective preconcentration and spectrophotometric determination of Ni(II) in water samples by Rajabi and Razmpour (2016).

Electrochemical methods are also used with MIPs in selective and sensitive determinations. Nasiri-Majd et al. (2015) used ionic imprinted polymer for the selective voltammetric determination of thallium. Magnetic molecularly imprinted polymer nanoparticles are used for selective absorption of N-acyl-homoserine-lactones with the measurement of differential pulse voltammetry (Jiang et al., 2016). Tan et al. (2015) used molecularly imprinted polymer reduced graphene oxide and gold nanoparticles modified electrode for detection of carbofuran.

1.11 The aim of study

As stated before, trace levels of 1-naphthol has negative effects on semen quality and testosterone level and it causes significant changes on the functions of enzymes and immunological system and gives damage to DNA. Therefore, preconcentration and quantitative determination of trace levels of 1-naphthol is very important. This study aims to develop a molecular imprinted polymer based optical sensor for the determination of 1-naphthol pesticide.

2. Experimental

2.1 Reagents

All reagents and chemicals were analytical grade. Glassware was cleaned by soaking them in dilute nitric acid (10%) and rinsed with distilled water prior to use.

1-naphthol (99%) was purchased from Alfa Aesar. Methacrylic acid (99%), ethylene glycol dimethacrylate (97%), chloroform (>99.5%), ethanol (>99.5%), methanol (>99.5%), acetonitrile (>99.5%), dichloromethane (>99.5%), 2,2'-azobis(isobutyronitrile) (98%), tetrahydrofuran (>99.5%), sodium hydroxide (98%), hydrochloric acid (37%), naphthalene (98%) and methylisobutylketone (98.5%) were purchased from Merck. 4-vinylpyridine (95%), 2-(dimethylamino)ethyl methacrylate (98%), carbendazim (97%), carbofuran (98%) and thiabendazole (98%) were purchased from Aldrich. Carbaryl pestanal (>99.5%) and acrylamide (98%) were purchased from Fluka. Benomyl (95%) was purchased from Santa Cruz.

Stock 1-naphthol solutions (100 mg/L) were prepared by dissolving appropriate amount of pesticide in methanol and diluting with methanol to 100 mL.

Stock 1-naphthol solutions (50 mg/L) were prepared by dissolving solid in the appropriate amount of the methanol and diluting with distilled water and stored at 4°C in the dark. Working standard solutions were prepared by diluting the stock standard solutions daily.

Carbaryl, thiabendazole, naphthalene, carbofuran and carbendazim solutions were prepared by dissolving the appropriate amount of pesticide in a minimum amount of methanol and diluting it by distilled water.

2.2 Apparatus and operating conditions

UV-160A Shimadzu type spectrophotometer was used for the spectrophotometric measurements. The cuvettes of quartz glass (1-1 cm) were used.

The spectrofluorometric measurements were carried out using a Shimadzu RF- 5301 PC spectrofluorophotometer.

Fourier transform infrared spectra (FTIR) were recorded on a Perkin-Elmer FTIR One B spectrometer.

Nüve BM 302 water bath shaker and Biosan Orbital OS-10 shaker were used.

25, 53, 75 and 125 μm Retsch ASTM E11 sieves were used for sieving polymer particles.

The pH measurements were performed by using a Orion 4 Star pH meter. pH meter was calibrated before every measurement.

Tacussel electronique model magnetic stirrer used for stirring during pH studies.

For centrifugation, Nüve NF 800 was used at 3000 rpm.

Chiltert model hot-plate was used.

All weight measurements were performed using a Precisa XB220A (readability: 0.0001 g)

2.3 Synthesis of Molecular Imprinted Polymer for 1-naphthol

Molecularly imprinted polymers (MIPs) and non-imprinted polymers (NIPs) for 1-naphthol were synthesized by using bulk method. For determination of the best imprinting factor, four different monomers were used in the synthesis.

As shown in Table 2.1, 1-naphthol was used as template molecule, methacrylic acid, 4-vinylpyridine, acrylamide and 2-(dimethylamino)ethyl methacrylate were used as functional monomers, ethylene glycol dimethacrylate was used as cross-linker and 2,2'-azobis(isobutyronitrile) was used as initiator, in the synthesis.

Table 2.1. Composition of the synthesized polymers.

	1-naphthol	Monomer	Cross-linker	Initiator	Solvent
MIP1	1 mmol	4 mmol 4-vinylpyridine	20 mmol	40 mg	10 mL Chloroform
MIP2	1 mmol	4 mmol 2-(Dimethylamino)ethyl methacrylate	20 mmol	40 mg	5 mL Chloroform
MIP3	1 mmol	4 mmol Acrylamide	20 mmol	40 mg	10 mL Chloroform
MIP4	1 mmol	4 mmol Methacrylic acid	20 mmol	40 mg	5 mL Chloroform
NIP1	-	4 mmol 4-vinylpyridine	20 mmol	40 mg	10 mL Chloroform
NIP2	-	4 mmol 2-(Dimethylamino)ethyl methacrylate	20 mmol	40 mg	5 mL Chloroform
NIP3	-	4 mmol Acrylamide	20 mmol	40 mg	10 mL Chloroform
NIP4	-	4 mmol Methacrylic acid	20 mmol	40 mg	5 mL Chloroform

1 mmol of template, 4 mmol of functional monomer, 20 mmol of cross-linker and 40 mg of initiator dissolved in chloroform were put into a glass tube (16 mm i.d. and 100 or 160 mm length). The mixture was degassed with N₂ for 10 minutes and then the tube was sealed and put into a water bath at 60°C for 24 hours. A control polymer (NIP) was prepared following the same procedure without the template (1-naphthol). The both glass tubes were smashed and MIP and NIP were crashed and dried at 50°C in oven.

2.4 Extraction of 1-naphthol from MIPs

Synthesized MIPs were crushed and ground in a agat mortar and pestle sieved to three suitable particle sizes between 25-53, 53-75 and 75-125 µm. Soxhlet extraction was applied for the extraction of 1-naphthol from MIPs. MIP (0.5 – 1 g) was tightly packed with filtration paper and placed in the soxhlet extractor. The removal of the template was conducted in methanol. 150-200 mL methanol was used for the extraction.

After 24 hours, fluorescence of the solution was measured at λ_{max} : 357 nm for the calculation of the percentage of extracted 1-naphthol and it was seen that 1-naphthol extraction efficiencies from MIP were below 100%. To prevent the potential blank signal in the re-binding studies, produced by the non-extracted 1-naphthol in the polymer, MIPs were cleaned with distilled water and methanol, respectively, until the template was not detected by spectrofluorimetry. Similar procedure was applied to NIPs. After the washing step, MIPs and NIPs were dried in oven.

2.5 Re-binding studies of 1-naphthol to MIPs

MIPs obtained from the soxhlet extraction were used to investigate the re-binding studies of 1-naphthol.

Re-binding procedure was performed as follow: 30 milligrams of polymer was added to a 50-mL falcon tube containing 25 mL of 1.000 mg/L 1-naphthol solution. After being shaken for 1 hour at room temperature, the samples were centrifuged. The free 1-naphthol concentration in the supernatant solution was detected by spectrofluorimetry and concentration of 1-naphthol was calculated by using a calibration curve. The adsorption of 1-naphthol to NIP was also measured in a similar manner.

3. Results and Discussion

3.1 Optic properties of 1-naphthol

3.1.1 Spectrophotometric properties

Spectrophotometric properties of 1-naphthol were investigated in different solvents. Maximum absorption wavelength (λ_{\max}) of 1-naphthol in different solvents are shown in Table 3.1.

Table 3.1. Maximum absorption wavelength of 1-naphthol in different solvents.

Solvent	Maximum absorption wavelength (λ_{\max}) (nm)
Dichloromethane	235
Methanol	213
Ethanol	211 and 234
Tetrahydrofuran	216 and 238
Chloroform	244 and 296
Water	210 and 292

3.1.2 Fluorescence properties

Fluorescence properties of 1-naphthol in different solvents were investigated. Excitation (λ_{ex}) and emission wavelengths (λ_{em}) are shown in Table 3.2.

Table 3.2. Excitation (λ_{ex}) and emission wavelengths (λ_{em}) of 1-naphthol in different solvents.

Solvent	Excitation wavelength (λ_{ex}) (nm)	Emission wavelength (λ_{em}) (nm)
Dichloromethane	293-295	326 and 341
Methanol	290-295	357
Ethanol	295-300	357
Tetrahydrofuran	300	343
Acetonitrile	300	357
Water	300	465
Chloroform	-	-
Methyl isobutyl ketone	-	-

As shown in Table 3.2, 1-naphthol gives fluorescence in different solvents and these solvents can be investigated in re-binding and recovery studies during this study except chloroform and methyl isobutyl ketone.

Fluorescence spectra of 1-naphthol in water and methanol are shown in Figures 3.1 and 3.2, respectively. The spectra of 1-naphthol in these solvents were given since 1-naphthol can be re-bound to the imprinted polymer in water and re-bound 1-naphthol can be recovered in methanol.

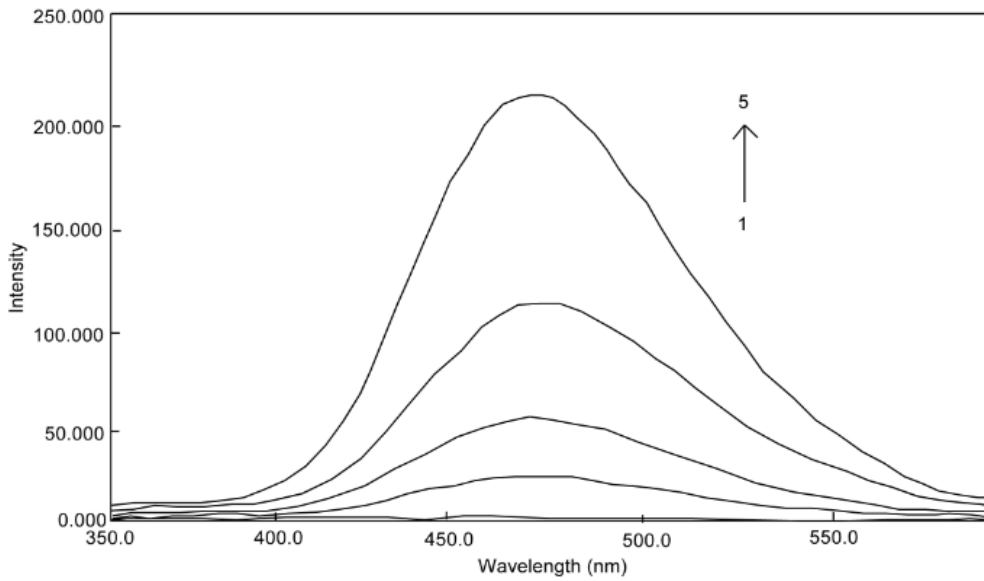


Figure 3.1. Fluorescence spectrum of 1-naphthol in water (1; blank, 2; 0.05 mg/L, 3; 0.1 mg/L, 4; 0.2 mg/L, 5; 0.4 mg/L and slit width: 5nm).

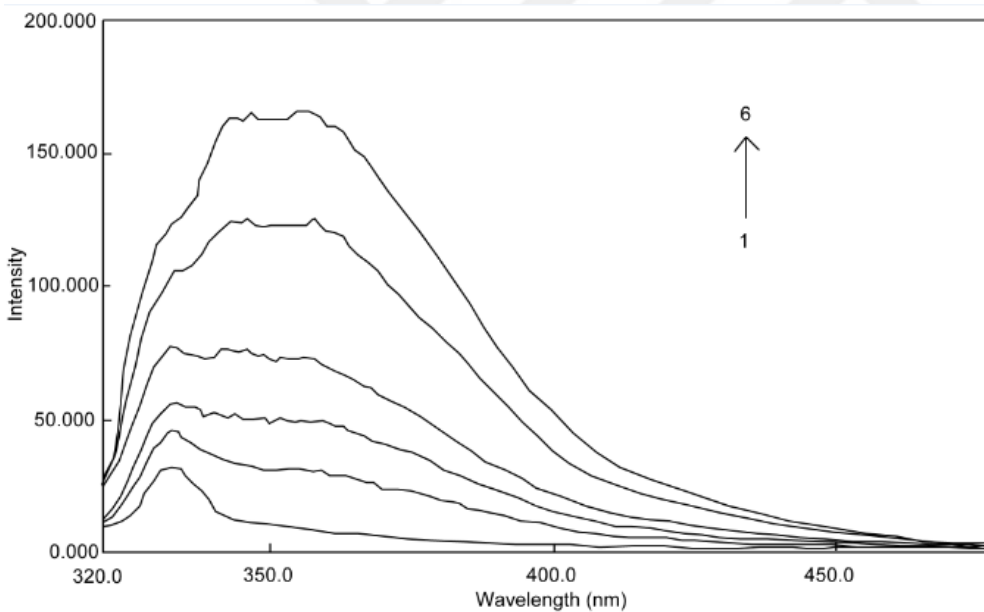


Figure 3.2. Fluorescence spectrum of 1-naphthol in methanol (1; blank, 2; 0.01 mg/L, 3; 0.02 mg/L, 4; 0.03 mg/L, 5; 0.05 mg/L, 6; 0.075 mg/L and slit width: 5nm).

3.2 Calibration graphs for 1-naphthol

Figures 3.3 and 3.4 illustrate the calibration graphs of 1-naphthol in water and methanol, respectively. The limit of detection (LOD) and the limit of quantification (LOQ) values of the method in each media were calculated on the basis of;

$$LOD = \frac{\sigma}{S} \times 3 \quad (1)$$

$LOQ = \frac{\sigma}{S} \times 10$ (2) where as σ is the standard deviation of the responses of blank solution and S is the slope of the calibration curve.

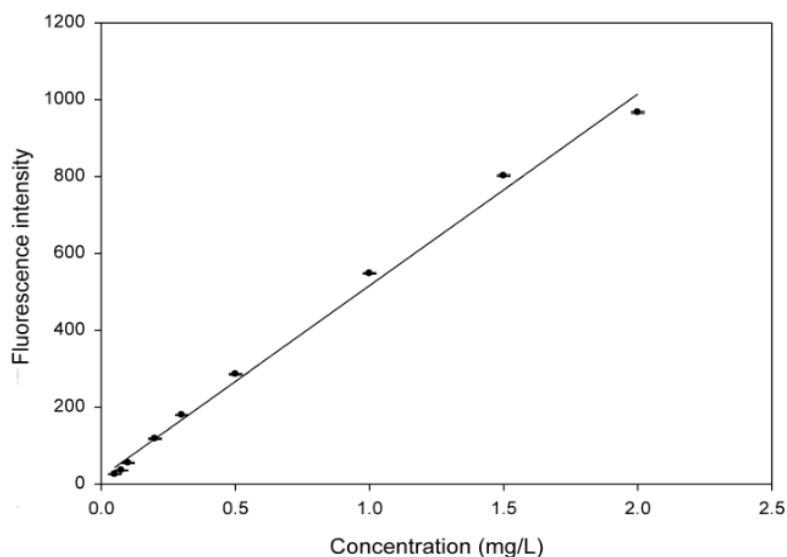


Figure 3.3. Calibration graph of 1-naphthol in water.

Calibration graph of 1-naphthol in water was linear between 0.050-2.000 mg/L with a regression coefficient (R^2) of 0.9940 and an equation with ($y = 498.9x + 19.424$). LOD and LOQ values for water medium were found to be 0.0054 and 0.018 mg/L, respectively.

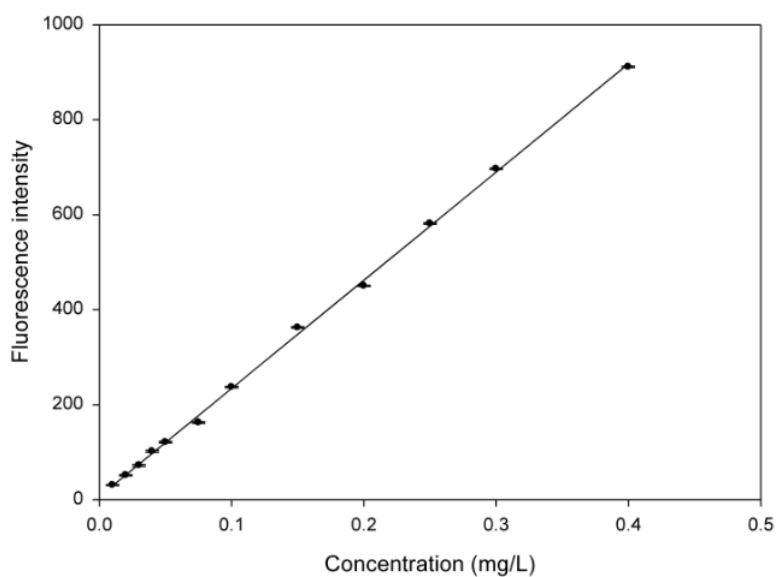


Figure 3.4. Calibration graph of 1-naphthol in methanol.

The calibration graph of 1-naphthol in methanol was linear between 0.010-0.400 mg/L with a R^2 of 0.9992 and an equation with ($y = 2279.2x + 7.3548$). LOD and LOQ values for methanol medium were found to be 0.0012 and 0.0040 mg/L, respectively.

3.3 The effect of monomer on 1-naphthol imprinting

In order to choose the polymer with the best imprinting factor for 1-naphthol, MIPs were synthesized by using four different functional monomers. The structures of functional monomers used in synthesis are shown in Figure 3.5. As stated in the literature, methacrylic acid is acidic, acrylamide is neutral and 2-(dimethylamino)ethyl methacrylate and 4-vinylpyridine are basic monomers (Ren et al. 2014). As shown in Figure 1.1, 1-naphthol has a functional group that has an ability to make Hydrogen bonds with the monomers.

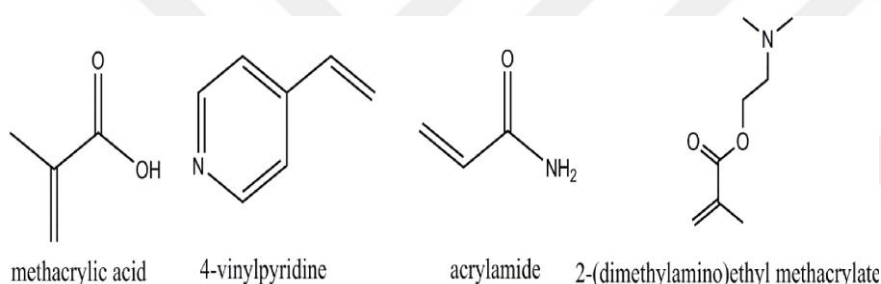


Figure 3.5. Structures of functional monomer used in MIP synthesis.

The imprinting factor (IF) can be stated as the ratio of the capacity of the imprinted polymer to capacity of the non-imprinted polymer. By evaluating the results of the batch re-binding studies, the effect of the functional monomer onto the imprinting of the template can easily be seen. The effect of the monomers were investigated by using the experimental batch adsorption capacities of the MIP and NIP. The imprinting factors of the polymers can be seen in Table 3.3.

Table 3.3. Imprinting factors of the synthesized polymers.

Polymer	Imprinting Factor (IF)
Methacrylic acid; MIP / NIP	1.13
2-(dimethylamino)ethyl methacrylate; MIP / NIP	1.19
Acrylamide; MIP / NIP	1.26
4-vinylpyridine; MIP / NIP	1.60

According to Table 3.3, when compared with its NIP, the MIP that prepared by using 4-vinylpyridine as functional monomer showed distinct difference in the adsorption capacities. Although both MIP and NIP showed a tendency on sorption of 1-naphthol, MIP adsorbed much more 1-naphthol than NIP. This was because the imprinted cavities of the MIP may cause the higher adsorption of the template compared with the NIP which has no imprinted sites.

NIP adsorptions for all the polymers used may be due to weak van der Waals forces or hydrogen bonds between functional monomers and 1-naphthol, or the interactions between cross-linker and 1-naphthol.

For other polymers synthesized with methacrylic acid, 2-(dimethylamino)ethyl methacrylate and acrylamide, there are less differences between the adsorbed amount of template in imprinted and non-imprinted polymers and it is thought to be imprinting is not effective in these polymers.

Since 4-vinylpyridine generate the best imprinting factor in 1-naphthol sorption, MIP prepared by 4-vinylpyridine was used for further sorption studies.

3.4 FTIR analysis of the polymers

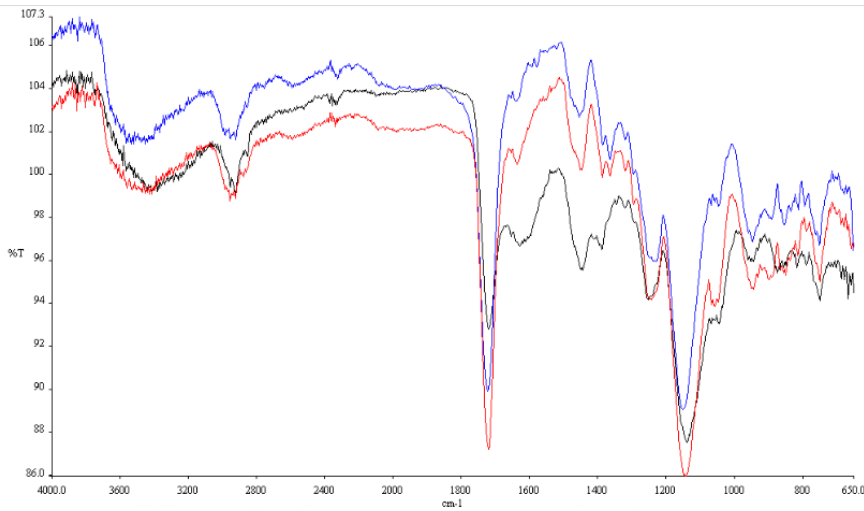


Figure 3.6. FTIR spectra of MIP, NIP and non-extracted MIP synthesized by methacrylic acid.

Figure 3.6 shows FTIR spectra of polymers synthesized by using methacrylic acid as functional monomer. As shown in Figure 3.6, FTIR spectra of all polymers are similar to each other. In FTIR spectra, peak at 3400-3500 cm^{-1} corresponds to -OH bond of methacrylic acid, peak at 2923-2957 cm^{-1} corresponds to C-H stretching. Peak at 1720 cm^{-1} corresponds to C=O bond and peak at 1150 cm^{-1} corresponds to ester group of the cross-linker, ethylene glycol dimethacrylate.

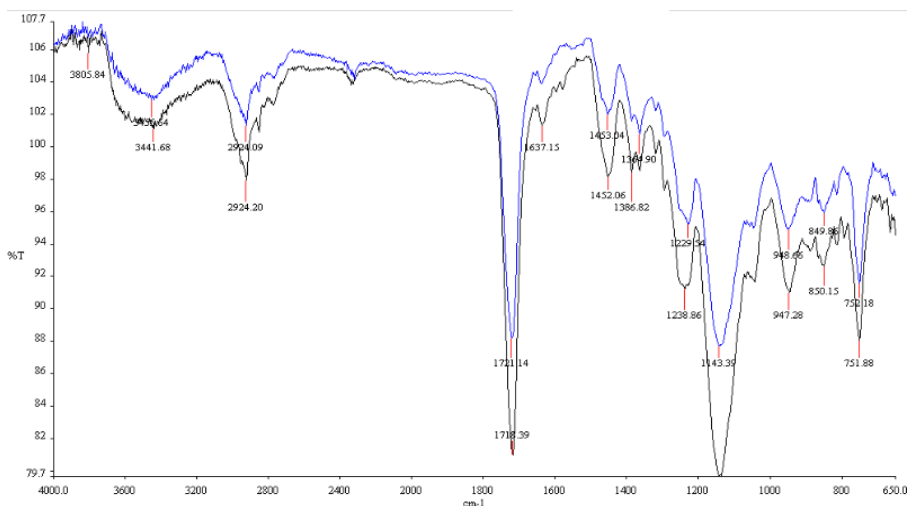


Figure 3.7. FTIR spectra of MIP and NIP synthesized by using 2-(dimethylamino)ethyl methacrylate.

As shown in Figure 3.7, there is no difference between the FTIR spectra of

polymers synthesized by using 2-(dimethylamino)ethyl methacrylate as functional monomer. Peaks at $2923\text{-}2957\text{ cm}^{-1}$ corresponds to C-H stretching, peaks at $1718\text{-}1721\text{ cm}^{-1}$ corresponds to C=O bond and peak at 1143 cm^{-1} corresponds to ester group of the cross-linker.

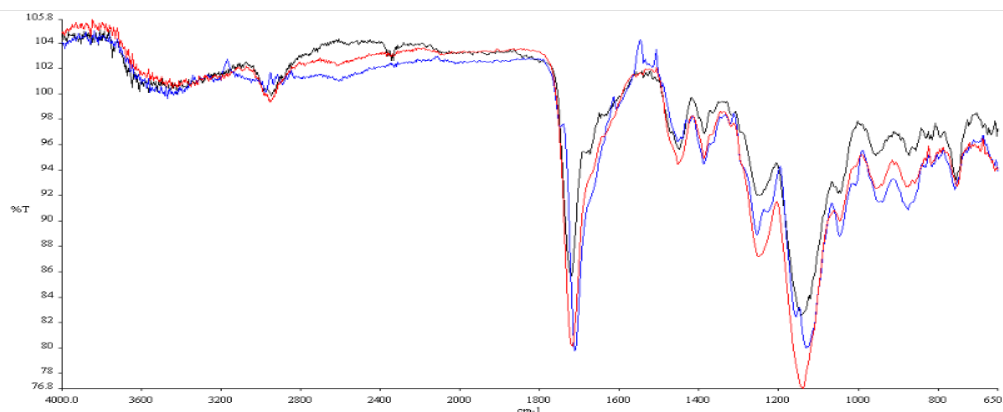


Figure 3.8. FTIR spectra of MIP, NIP and non-extracted MIP synthesized by using acrylamide.

As shown in Figure 3.8, similar to the other polymers, the FTIR spectra of NIP and MIP synthesized by using acrylamide are similar to each other. Spectra also contain the peaks at $2923\text{-}2957\text{ cm}^{-1}$ corresponds to C-H stretching, peaks at $1712\text{-}1721\text{ cm}^{-1}$ corresponds to C=O bond and peak at 1143 cm^{-1} corresponds to ester group of the cross-linker. Peaks at $3424\text{-}3471\text{ cm}^{-1}$ corresponds to the N-H bond of acrylamide.

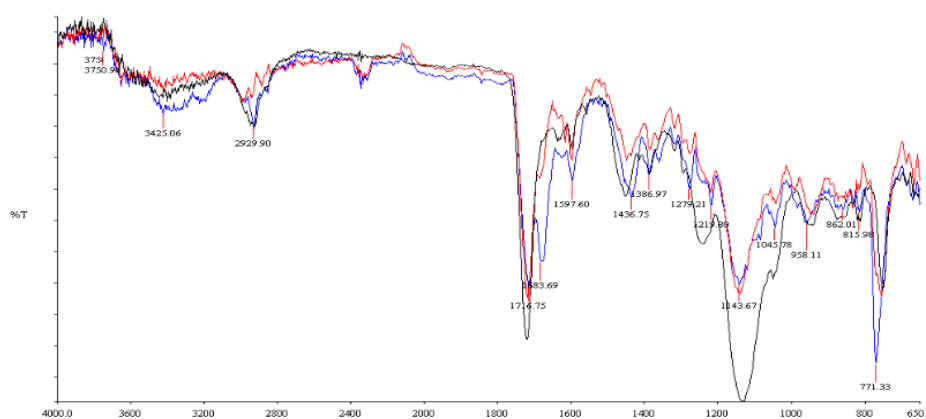


Figure 3.9. FTIR spectra of MIP, NIP and extracted MIP synthesized by using 4-vinylpyridine.

Figure 3.9 is the original spectra of polymers synthesized by using 4-vinylpyridine as functional monomer without making any graphical modification

for publication of this study. In this figure, the weak N–H stretch peak can be shown easily at 3425 cm^{-1} when compared to Figure 3.10 (B) spectrum.

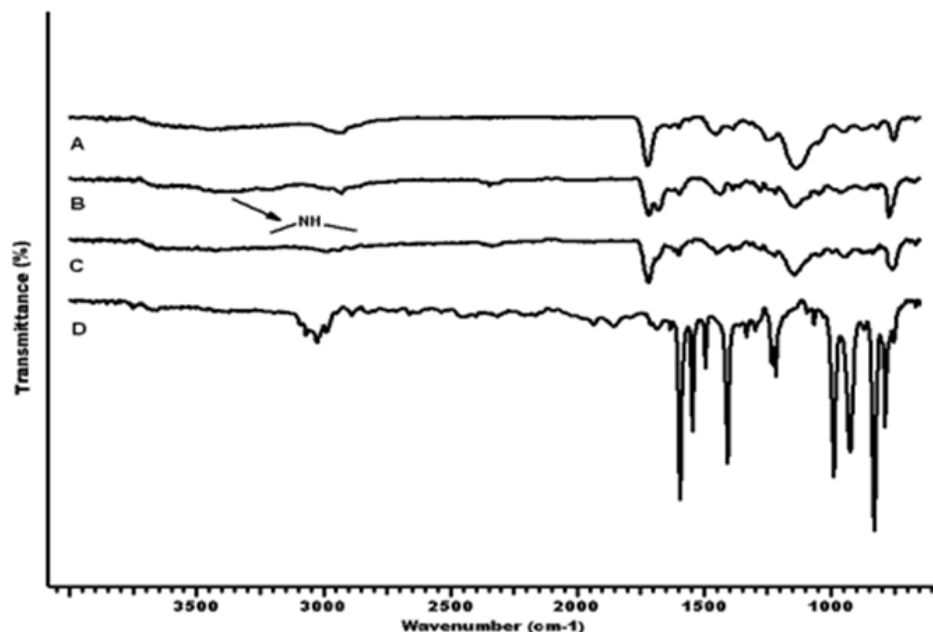


Figure 3.10. FTIR spectra of a) NIP b) non-extracted MIP c) MIP and d) 4-vinylpyridine

Figure 3.10 shows the FTIR spectra of 4-vinylpyridine, 1-naphthol imprinted polymer, non-imprinted polymer and non-extracted 1-naphthol imprinted polymer.

In Figure 3.10, weak N–H stretch can be observed at 3425 cm^{-1} for non-extracted MIP (spectrum B). This peak shows that H-bond occurs between 1-naphthol and the functional monomer 4-vinylpyridine. This peak is absent both in 4-vinylpyridine spectrum (spectrum D) since it has no N–H bond and in NIP spectrum (spectrum A) since it does not contain template and no N–H bond occurs.

In non-extracted MIP (spectrum B) the –OH bond of 1-naphthol does not exist in FTIR spectrum since it forms H-bond with 4-vinylpyridine. When 1-naphthol extracted from MIP (spectrum C), N–H bonds broken and the intensity of the N–H stretch decreases. Peak around at $2900\text{--}3000\text{ cm}^{-1}$ in all spectra responds to C–H stretching.

The presence of two peaks in all spectra around 1716 cm^{-1} and 1143 cm^{-1} correspond to C=O stretching and C–O stretching, respectively, exist in the ethylene

glycol dimethacrylate structure in the polymer matrix and these peaks are the evidence to a successful polymerization process.

3.5 Re-binding studies for 1-naphthol

Re-binding of 1-naphthol was studied in different solvents. In each experiment, the free template in the supernatant solution was measured by spectrofluorimetry.

Generally, in molecularly imprinting technology, water is not accepted as an ideal solvent since it has the ability to form hydrogen bonds between the analyte and the polymer structure but in this study, 1-naphthol can re-bind to the cavities of the polymer only in water.

As shown in Table 3.4, the re-binding efficiency of 1-naphthol in water was $88.3 \pm 1.2\%$ and in different organic solvents such as tetrahydrofuran, dichloromethane, ethanol, methanol and acetonitrile, 1-naphthol could not re-bind significantly onto MIP cavities. Thus, only water can be used as re-binding medium. This phenomenon is an important advantage for the determination of 1-naphthol in real water samples whereas any other extraction procedures are not necessary.

Table 3.4. Re-binding efficiency of 1-naphthol.

Solvent	Re-binding efficiency (%)
Tetrahydrofuran	Not significant
Dichloromethane	Not significant
Ethanol	Not significant
Methanol	Not significant
Acetonitrile	Not significant
Water	88.3±1.2 (n=3)

3.6 The effect of initial pH on 1-naphthol re-binding

In order to determine the effect of initial pH on re-binding efficiency of 1-naphthol, the initial pH of 1-naphthol solution was adjusted to desired pH value in the range of 3.0 to 10.0 by using HCl and NaOH solutions. As shown in Figure 3.11, the pH do not have a significant effect on re-binding efficiency of 1-naphthol. For all pH values the re-binding efficiency was higher than 80% and shows a slight increase as pH increases. pH 9.0 was selected as the optimum pH for the sorption studies.

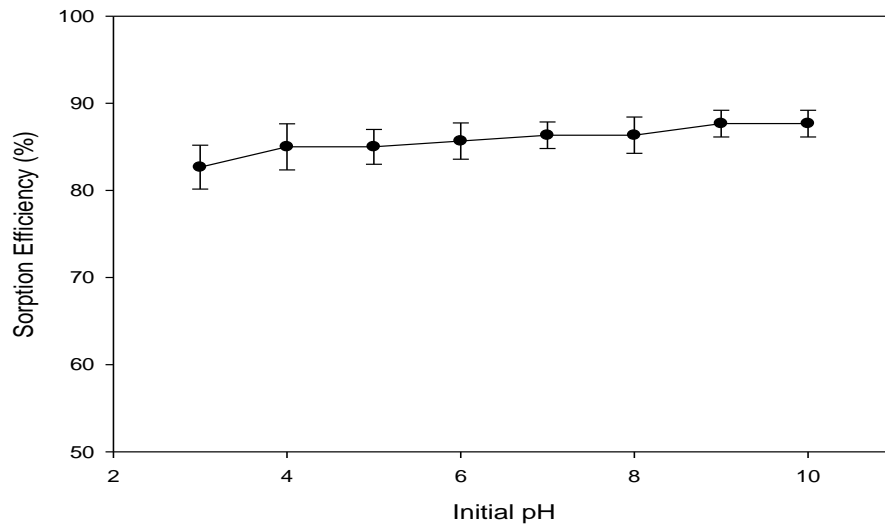


Figure 3.11. The effect of initial pH on re-binding efficiency of 1-naphthol (initial concentration: 1 mg/L, MIP amount: 20 mg, sample volume: 25 mL, contact time: 30minutes).

3.7 Effect of re-binding time

In order to find the optimum re-binding time, 2 mg/L 1-naphthol (pH~9) solutions were shaken for 5, 10, 15, 20, 30, 45 and 60 minutes with 30 mg of sorbent with the sample volume was 25 mL. The graph is shown in Figure 3.12.

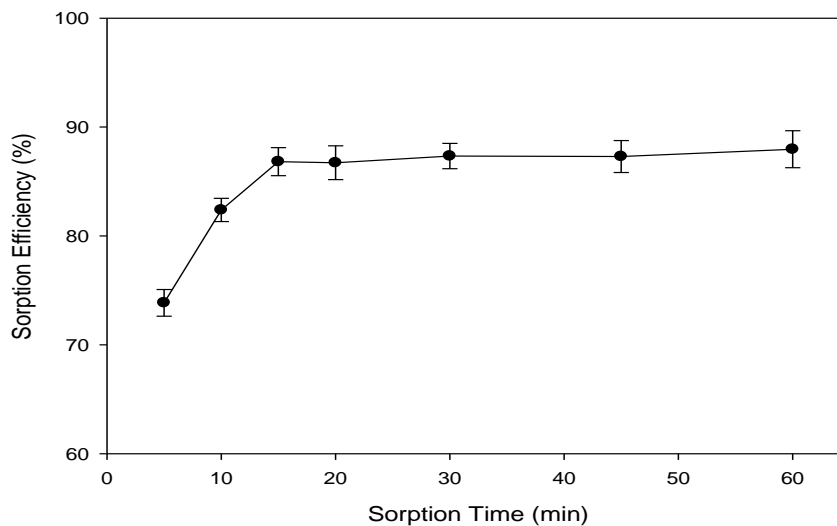


Figure 3.12. The effect of contact time on 1-naphthol sorption efficiency (MIP amount: 30 mg, initial concentration: 2 mg/L (in water, pH~9), sample volume: 25mL).

As shown in Figure 3.12, quantitative re-binding of 1-naphthol onto MIP is rapid and take place within 30 minutes. Thus, optimum re-binding time was selected as 30 minutes.

3.8 Recovery studies of 1-naphthol

Different solvents were used to recover adsorbed 1-naphthol from MIP. As shown in Table 3.5, recovery efficiencies for methanol, ethanol and tetrahydrofuran were found to be quantitative.

Table 3.5. Recovery of 1-naphthol with different solvents.

Solvent	Recovery(%) (n=3)
Methanol	96.79±0.81
Ethanol	95.62±1.24
Tetrahydrofuran	93.33±1.12
Dichloromethane	85.95±2.21
Acetonitrile	75.09±3.79
Water	Not significant

Although all these solvents can be used as recovery agent, methanol was chosen as the recovery solvent in the further studies.

3.9 Effect of recovery time

To find out the effect of time on recovery of 1-naphthol, MIPs were shaken with methanol for 5, 10, 15, 20, 30, 45 and 60 minutes. After ultra-centrifuge, recovered 1-naphthol was determined. The graph is shown in Figure 3.13.

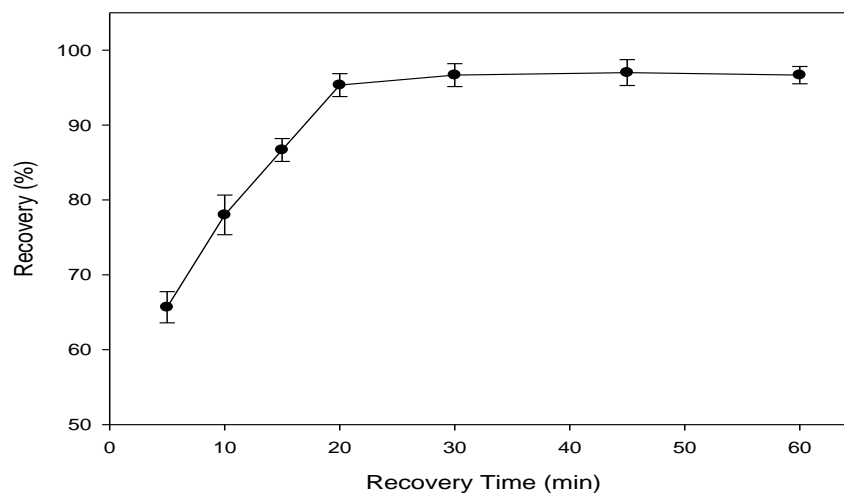


Figure 3.13. Effect of time on recovery (MIP amount: 30 mg, initial concentration: 0.1 mg/L (in water, pH ~9), solvent volume: 25mL).

As shown in Figure 3.13, release of 1-naphthol from MIP is rapid and take place within 20 minutes. Thus, 20 minutes was chosen as optimum recovery time.

3.10 Effect of adsorbent dose

Various amounts of sorbent were weighed and 25 mL of 2 mg/L 1-naphthol solutions were added onto the MIPs and shaken for 30 minutes. The effect of the adsorbent dose on 1-naphthol sorption is shown in Figure 3.14.

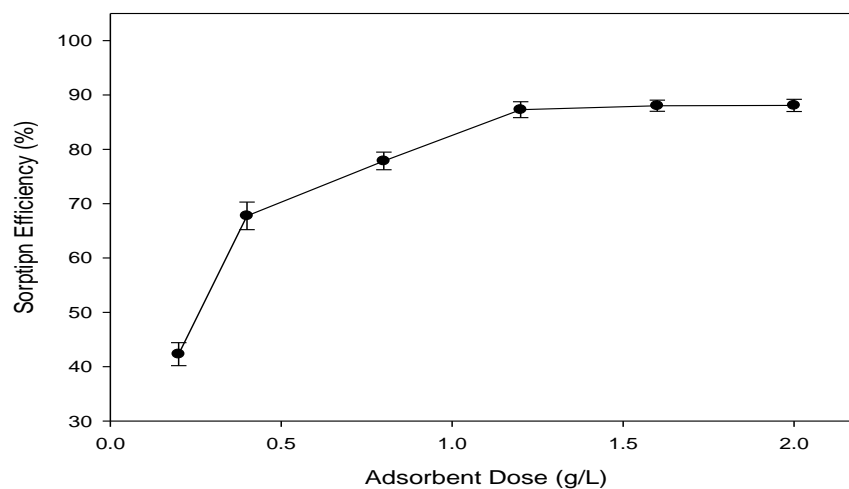


Figure 3.14. Adsorbent dose for the imprinted polymer (initial 1-naphthol concentration:

2.000 mg/L, sample volume: 25 mL, sorption time: 30 minutes, MIP amount: 5-50 mg).

As shown in Figure 3.14, for quantitative sorption of 1-naphthol minimum 1.2 g/L MIP should be used in batch system. Under this adsorbent dose, the amount of polymer was insufficient for quantitative sorption and sorption efficiency decreased. Beyond this adsorbent dose, the polymer reached its maximum capacity and the sorption efficiency remains constant at 90%.

3.11 Capacities of MIP and NIP

For determining the capacities of the polymers, two methods were used. First one is the experimental method where 30 mg MIP and NIP were shaken with 25 mL of 100 mg/L 1-naphthol (pH ~9) for 24 hours. 1-naphthol remained in the solutions was measured. The adsorption capacity of the polymer for 1-naphthol (Q , mg/g) was calculated by using the following equation:

$$Q = \frac{(C_i - C_e) \times V}{W} \quad (3)$$

where C_i is the initial concentration ($\mu\text{g/mL}$) and C_e is the equilibrium concentration of 1-naphthol ($\mu\text{g/mL}$), V is the volume of the solution (mL) and W is the mass of the polymer used (mg).

Second method was based on the scatchard analysis model. The scatchard equation is;

$$\frac{Q}{C} = \frac{Q_{\max} - Q}{K_d} \quad (4)$$

where Q is the amount of 1-naphthol adsorbed by polymer ($\mu\text{mol/g}$), C is the equilibrium concentration ($\mu\text{mol/L}$), Q_{\max} is the maximum binding capacity ($\mu\text{mol/g}$) and K_d is the equilibrium dissociation constant ($\mu\text{mol/L}$). 15 mg NIP and MIP were shaken with 25 mL of various initial concentration of 1-naphthol solution (1-50 mg/L) in water (pH ~9) for 2 hours for employing the scatchard analysis. The number of the linear regions in the scatchard graph presents the binding sites in the adsorbent used in the sorption studies as stated in the literatures; Yin et al. (2011) and Wang et al. (2007).

In the experimental method, capacities of NIP and MIP were found to be 44.36 ± 4.91 mg/g and 70.86 ± 7.22 mg/g ($n=3$), respectively.

When scatchard analysis applied to NIP, as illustrated in Figure 3.15, there is only one linear region in the equation and it can be concluded that there is only one type of binding responsible for 1-naphthol sorption. The linear region has an

equation of ($y = -0.0053x + 1.9008$) and with a R^2 of 0.8951.

Figure 3.16 represents the scatchard plots of MIP. As shown in Figure 3.16, for MIP, the equation has two different linear region and we can conclude that there is a heterogeneous distribution of binding sites on the imprinted polymer. Thus, there were two different types of binding sites responsible for the sorption of 1-naphthol. Linear regions have two equations with ($y = -0.0595x + 5.6445$) and ($y = -0.0045x + 2.4864$) two regression coefficients with 0.9011 and 0.9448, respectively. From the slopes and intercepts of the Scatchard equations, the dissociation constants (K_d) and the maximum binding capacities (Q_{max}) of the MIP and NIP were calculated and shown in Table 3.6.

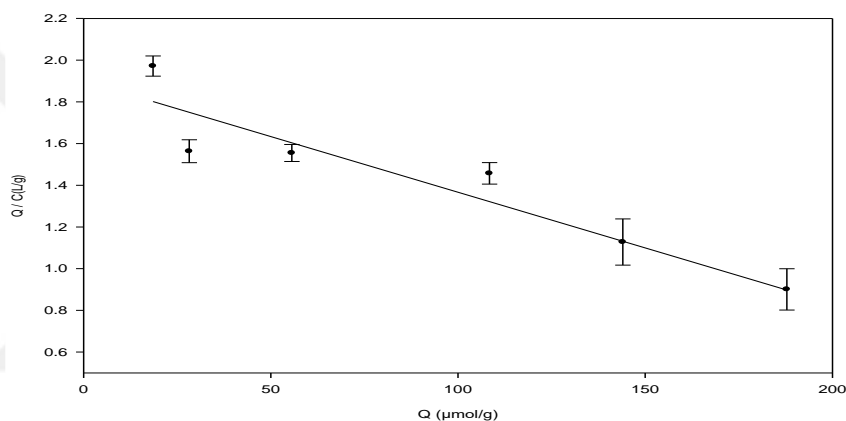


Figure 3.15. Scatchard plots of NIP (NIP amount: 15 mg, sample volume: 25 mL, initial concentration of 1-naphthol: 1-50 mg/L in water (pH ~9), contact time: 2 hours).

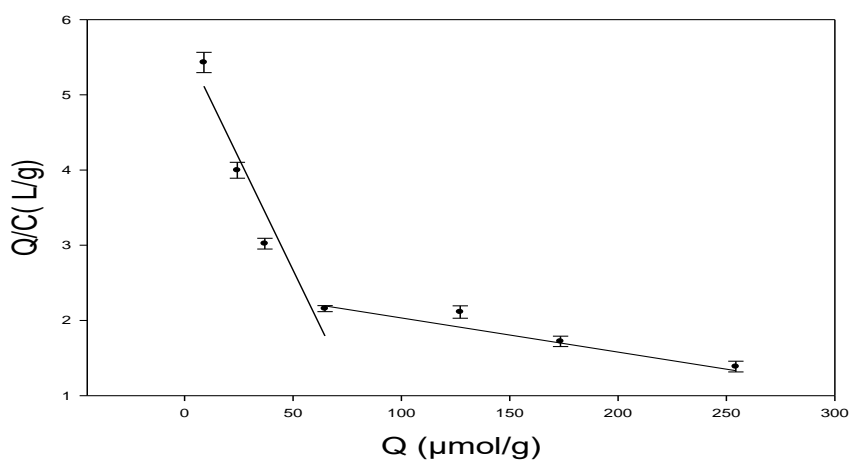


Figure 3.16. Scatchard plots of MIP (MIP amount: 15 mg, sample volume: 25 mL, initial concentration of 1-naphthol: 1-50 mg/L in water (pH ~9), contact time: 2 hours).

Table 3.6. Q_{\max} and K_d values calculated from the Scatchard plot.

	$Q_{\max 2}$ ($\mu\text{mol/g}$)	$Q_{\max 2}$ (mg/g)	$Q_{\max 1}$ ($\mu\text{mol/g}$)	$Q_{\max 1}$ (mg/g)	K_{d2} ($\mu\text{mol/L}$)	K_{d1} ($\mu\text{mol/L}$)
MIP	94.87	13.68	552.53	79.66	16.81	222.22
NIP	-	-	358.64	51.71	-	188.68

When the adsorption capacities calculated from the scatchard analysis and experimental method compared, the capacity values were found to be in good agreement; 79.66 and 70.86 ± 7.22 mg/g for MIP and 51.71 and 44.36 ± 4.91 mg/g ($n=3$) for NIP, respectively.

3.12 Reusability of imprinted polymer

25 mL of 1.0 mg/L 1-naphthol solution was shaken with 30 mg MIP for 30 minutes. After sorption, MIP was regenerated with 10 mL methanol.

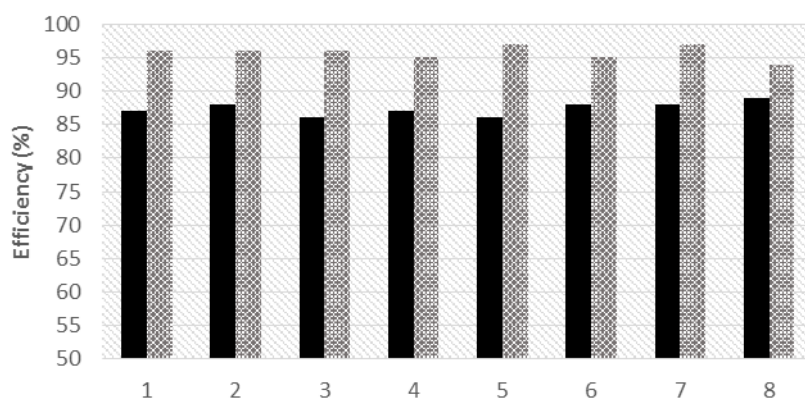


Figure 3.17. Reusability of the polymer.

Figure 3.17 shows that, MIP can be used at least eight consecutive adsorption-regeneration cycles without a obvious decrease both in sorption and recovery efficiencies. The efficiency of eight measurements for sorption and recovery were found to be 87.38 ± 0.99 and 95.75 ± 0.97 ($n=8$), respectively.

Therefore, MIP can be used repeatedly for 1-naphthol determination in water samples without any capacity loss.

3.13 Interference effects on determination of 1-naphthol

The interference effects of naphthalene, carbaryl, carbendazim and carbofuran were investigated on determination of 1-naphthol. A diverse substance, that causes a change in the fluorescence signal by more than $\pm 5\%$, was accepted as an interfering agent. Tolerable concentration of interferent can be defined as the maximum concentration of a substance that does not cause any interference effects on the determination of the analyte. In order to investigate the interference effect, 25 mL of 0.100 mg/L 1-naphthol solution with different amounts of possible interferent was shaken with 30 mg MIP for 30 minutes and after sorption, 1-naphthol was recovered with 10 mL methanol. The concentrations of interferents can be seen in Table 3.7.

Table 3.7. Interference effects on the determination of 1-naphthol (1-naphthol = 0.1 mg/L).

Interferent	Tolerable Concentration of Interferents (mg/L)
Naphthalene	3.0
Carbaryl	1.0
Carbendazim	5.0
Carbofuran	25.0

3.14 Analytical application

As the practical application of the method developed, water samples collected from the pet bottle, carboy water and the tap water from laboratory were filtered to remove any precipitate. 40 mL water sample was adjusted to pH ~ 9.0 and shaken with 50 mg MIP for 2 hours for 1-naphthol determination. After sorption, phases were separated by centrifuge and 1-naphthol remained in the solutions was

measured by spectrofluorimetry. It was found that 1-naphthol was not detected in the water samples and therefore, spike addition method was employed. Three parallel analyses were done for each sample. The results of the real water sample applications are shown in Table 3.8. The average recoveries of all water samples were in the range from 91-96%.

Table 3.8. Determination of 1-naphthol in real water samples.

Water sample	Found ($\mu\text{g/L}$)	Added ($\mu\text{g/L}$)	Average Found ($\mu\text{g/L}$)	Enrichment Factor	Total Recovery of Added 1-Naphthol (%)
Carboy water	<LOD*	25.0	23.3	4	93.8 \pm 1.7
Pet bottle	<LOD*	25.0	24.0	4	96.3 \pm 1.4
Tap water	<LOD*	25.0	22.8	4	91.1 \pm 1.2

*LOD = Limit of Detection (n=3)

As stated in the literature, 1-naphthol is being produced as the major product after photooxidation of aqueous solution of naphthalene. (McConkey et al., 2002). The same group also state that the same chemicals were formed in the presence of H_2O_2 . It was emphasized that the half-life of photolysis of naphthalene in surface waters is 71 hours (Agency for Toxic Substances and Disease Registry, 1995). Thus, the proposed method was applied for the determination of 1-naphthol after the photooxidation of naphthalene. For this experiment, 100 mg/L stock naphthalene solution was prepared by dissolving the appropriate amount of solid in the minimum amount of methanol and diluted to 100 mL with distilled water. 10 mg/L naphthalene solution was prepared by diluting the stock solution with distilled water.

The photooxidation of naphthalene was investigated in two different ways; in the first one, 10 mg/L 100mL naphthalene solution was exposed to direct sunlight (1), whereas in the second process, 1% H₂O₂ + 10 mg/L naphthalene solution (100mL) was exposed to direct sunlight (2).

After 5 days, produced 1-naphthol in the solutions was measured. For this purpose, the pH of the solution was adjusted to ~9 and added onto 120mg MMIP and shaken for 30 minutes. After sorption, phases were separated by centrifuge and 10mL methanol was added onto MIP and shaken for 30 minutes for recovering the adsorbed 1-naphthol. After 30 minutes, 1-naphthol was measured by spectrofluorimetry. Enrichment factor in this study was 10. The results of the analytical application are shown in Table 3.9.

Table 3.9. Determination of 1-naphthol after photooxidation of naphthalene.

Sample	Measured 1-naphthol (mg/L)	Enrichment Factor	1-naphthol concentration in the original sample (mg/L)
(1) 10 ppm Naphthalene + sunlight	0.06	10	0.006 (Interference effect of naphthalene)
(2) 10 ppm Naphthalene + 1% H ₂ O ₂ + sunlight	1.12	10	0.112

Remained naphthalene concentrations in the solutions were also measured and found to be as 4.8 ppm and 3.1 ppm, for (1) and (2), respectively. As shown in Table 3.9, after direct photolysis of naphthalene (1), the interference effect of naphthalene was observed because the remained naphthalene concentration in the solution was higher than the tolerable concentration. However, when H₂O₂ was added to the solution (2), the remained naphthalene in the solution was 3.1 ppm and it was under the tolerable concentration of naphthalene and no interference effect was observed in the determination of 1-naphthol.

4. Conclusion

In this study, a molecularly imprinted polymer based optical sensor is successfully developed for the determination of 1-naphthol. Sensitive, selective and rapid preconcentration and fluorimetric determination of 1-naphthol could be achieved by using the proposed method. The developed MIP can be suggested for the selective separation and preconcentration of 1-naphthol before its chromatographic determination.

In molecular imprinting technology, one of the most important parameters is the imprinting factor. Thus, in the synthesis of molecularly imprinted polymers, four different functional monomers were used and the imprinted polymer with the highest imprinting factor was selected for determination and preconcentration of 1-naphthol. The results show that the highest imprinting factor was obtained as 1.60 when 4-vinylpyridine was used as functional monomer. Characterization of the synthesized polymer and the optimization of performance parameters are performed successfully.

The re-binding and recovery studies reveal that the proposed method is rapid and the processes can be completed within an hour. The quantitative re-binding and recovery values are obtained as $87.38 \pm 0.99 \%$ and $95.75 \pm 0.97 \%$ ($n=8$), respectively.

The re-binding studies are performed in water and this is an important advantage of the proposed method since the method can be directly applied to determine the trace levels of 1-naphthol in real water samples without any pretreatment or extraction procedures.

Capacity studies show that the imprinted polymer act as an high-capacity adsorbent in the determination of 1-naphthol. Scatchard analysis and experimental method were employed and compared for determining the capacities of the synthesized polymers. The results of the Scatchard analysis and the experimental measurements are in good agreement: 79.66 and 70.86 ± 7.22 mg/g for the MIP capacity and 51.71 and 44.36 ± 4.91 mg/g for the NIP capacity, respectively.

Synthesized MIP could be used repeatedly for eight times without capacity loss and this lead to a more cheaper and economical detection system.

Scatchard plots of the MIP, demonstrating the two linear regions, indicates a heterogeneous distribution of binding sites on the polymer and two types of binding sites responsible for the sorption of 1-naphthol. However, for NIP, there is only one linear region which indicates that homogeneous distribution of binding sites are responsible for sorption of 1-naphthol.

In the proposed method, the calibration graphs of 1-naphthol in methanol and water were linear between 0.010 and 0.400 mg/L and 0.050 and 2.000 mg/L, respectively. The limits of detection (LOD) in methanol and water were satisfactory and 0.0012 and 0.0054 mg/L, while the limits of quantification (LOQ) were 0.0040 and 0.018 mg/L, respectively.

The proposed method is applied to real water samples and quantitative recoveries (91 % - 96 %) are obtained.



CHAPTER TWO - SELECTIVE AND SENSITIVE FLUORIMETRIC DETERMINATION OF CARBENDAZIM IN APPLE AND ORANGE AFTER PRECONCENTRATION WITH MAGNETITE-MOLECULARLY IMPRINTED POLYMER

1. Introduction

1.1 Carbendazim

Carbendazim, methylbenzimidazole-2-ylcarbamate (MBC) or 2-(Methoxycarbonylamino)-benzimidazole with its IUPAC names is an odourless organic compound with the molecular weight of 191.19 g/mol and the chemical formula of $C_9H_9N_3O_2$. Melting point of carbendazim is 302-307°C and vapour pressure is 9×10^{-5} Pa at 20°C. Carbendazim decomposes before boiling. It has density of 1.45 g/cm³ at 20°C, water solubility of 8 mg/L at 24°C (pH 7), and acid dissociation constant (pKa) of 4.2.

Carbendazim is crystalline white powder in room temperature and it is stable in acidic solutions but slowly decomposes in alkaline solutions and it is not flammable.

Carbendazim is soluble in different organic solvents but solubility of carbendazim in dimethylformamide is higher than other solvents. Figure 1.1 shows the structure of carbendazim.

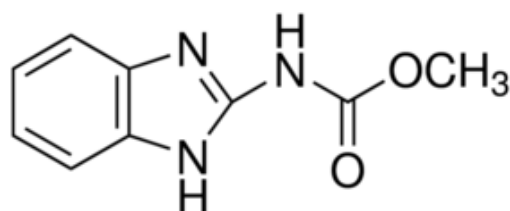


Figure 1.1. Structure of carbendazim.

1.2 Uses of carbendazim

Carbendazim is a benzimidazole fungicide which is widely used all over the world. Carbendazim is also metabolite of two other pesticides; benomyl and thiophanate-methyl. Among these pesticides, usage of benomyl was banned in 2001 but carbendazim and thiophanate-methyl still continued to be used as pesticides.

As well as other fungicides, carbendazim is also used to control fungi, which cause plant diseases. *Ascomycetes*, *Fungi Imperfecti* and *Basidiomycetes* are some examples of fungi which can lead to important problems in plants. Main plant diseases can be expressed as leaf spot, fruit spot, tuber decay and root rot. Carbendazim is mainly used on cereals, tobacco, vegetables, mushrooms, fruits, cotton to prevent these diseases (WHO, 1993).

Carbendazim, as a bactericide, kills bacteria, which cause plant diseases, by preventing the formation of pathogen (Chen et al., 2015). According to Patel et al. (2015), carbendazim is used to control worm in turf used in sports such as golf and tennis. General uses of carbendazim are listed in Table 1.1.

Table 1.1. General uses of carbendazim (APVMA, 2007).

Crops	Pest
Strawberries	Grey mould
Apples	Powdery mildew
Grapes	Grey mould
Bananas	Crown rot
Citrus	Blue and green moulds
Sugar cane	Pineapple disease
Pears	Black spot

Maximum Residue Levels (MRLs) of carbendazim in different types of crops in Turkey are stated by T.C. Gıda Tarım ve Hayvancılık Bakanlığı. Table 1.2 shows the MRL values of carbendazim in different crops.

Table 1.2. Maximum Residue Levels of carbendazim in different types of crops in Turkey (T.C. Gıda Tarım ve Hayvancılık Bakanlığı, 2009).

Crops	Maximum Residue Level (mg/kg)
Tomato	0.5
Orange	0.5
Lemon	0.7
Peach	0.2
Pepper	0.1
Plum	0.5
Lentil	0.1
Sugar beet	0.1
Wheat	0.1

1.3 Occurrence

In the environment, carbendazim is used as a fungicide and it is also the main degradation product of the pesticides benomyl and thiophanate-methyl (Li et al., 2015). Microbial activities are the main processes responsible for degradation of carbendazim in soil. Carbendazim can be degraded slowly by chemical and physical processes (Wang et al., 2010).

Benomyl, which is the main source of carbendazim, rapidly degrades to carbendazim in environment with a half-life of a few hours. Half-life of carbendazim is longer than benomyl in environment and it depends on the conditions of the environmental medium and varies from days up to a few months. The residual half-life of carbendazim also depends on the application type of the pesticide. Half-lives are given as 7.0 for pre-harvest usage of carbendazim and 6.5 days for post-harvest usage (Zhou et al., 2015).

Water Framework Directive - United Kingdom Technical Advisory Group (WFD-UKTAG) (2009) states that carbendazim shows slow partition from water into sediment and volatilisation is not accepted as one of the important environmental fate processes for carbendazim due to its low Henry's Law constant. The group also state that carbendazim may not be classified as readily biodegradable.

Carbendazim has hydrolysis half-life of 25 weeks. Half-lives of carbendazim on soil and turf are 6-12 months and 3-6 months, respectively. Under anaerobic conditions, 98% of carbendazim spread out sediment in seven days with a half-life of nearly 2 years. Under aerobic conditions, the half-life in non-sterile sediment was 1 month. Anaerobic degradation of carbendazim in soil and water is slower than aerobic degradation (WHO, 1993).

The half-life of carbendazim in soil is found to be 40 days under aerobic conditions. Under sterile conditions, effect of pH on carbendazim degradation was investigated and it can be seen that carbendazim was stable at acidic and neutral pH but it can be degraded at basic pH values. Carbendazim can be degraded with an half-life on approximately 50 days. The studies indicate that rate of degradation of carbendazim increases with increasing the temperature (JMPR, 1998). Degradation of carbendazim is shown in Table 1.3.

Table 1.3. Degradation half-lives of carbendazim in different conditions (JMPR, 1998).

Initial Concentration (mg/L)	Conditions	Half-life (days)
Hydrolytic degradation		
2,16	pH 9, 22°C	124
8	pH 5, 22°C	457
4	pH 5, 50°C	108
Photochemical degradation		
4,75	pH 5, 25°C	>35
Biological degradation		
27	aerobic, 20°C, oxygen uptake	>21
27	aerobic, 20°C, Zahn-Wallens test	<0,125

Carbendazim has a decomposition half-life of 2 months under aerobic conditions and a half-life of 25 months under anaerobic conditions in the water sediment systems (Li et al., 2015).

Half-lives of carbendazim in a water sample are 21 days under sunlight and 61 days in dark at pH~8 (Mallat et al., 1997).

Phototransformation of carbendazim in aqueous solution was investigated by Mazellier et al. (2002) and they declare that the protonated form of carbendazim is

stable towards UV whereas the neutral form can easily be photolyzed and the rate of the photolysis increased when the oxygen concentration increased.

The kinetic of photodecomposition of carbendazim was also investigated by Panades et al. (2000) at different pHs and different concentrations of dissolved oxygen. They show that the process has a first-order kinetic and rate of the degradation increases with pH and dissolved oxygen concentration.

Saien and Khezrianjoo (2008) show that TiO₂ particles can be used as catalyst for degradation of carbendazim in aqueous solutions. The results showed that UV/TiO₂ process shows better results than UV irradiation. Optimal conditions for quantitative degradation of fungicide was stated as; 70 mg/L of catalyst, pH of 6.73 and temperature of 25 °C with an irradiation of 75 minutes.

Escalada et al. (2006) investigate the photodegradation of carbendazim by using xanthene dye Rose Bengal or the natural pigment riboflavin.

1.4 Toxicity of carbendazim

Carbendazim has been used as pesticide since 1970. Upon its extensive usage, various studies have been developed to investigate the toxicity of carbendazim to human and animal health.

Since carbendazim has been widely used as fungicide in all over the world, its toxicity on different types of animal was also investigated.

Singhal et al. (2003) showed that carbendazim caused decrease in immunoglobulin levels in chicken.

Several studies have been carried out to show that carbendazim is toxic for marine life. Janakidevi et al. (2013) investigate the toxicity of carbendazim on aquatic organisms and they propose that the pesticide gives serious damages to the DNA of marine invertebrate *Donax faba*. In an other study, Silva et al. (2015) propose that DNA damage was observed when the water flea *Daphnia magna* was exposed to carbendazim. The serious effects of carbendazim on different types of water organisms were stated by Cuppen et al. (2000).

Jiang et al. (2014) studied the immunotoxic effect of carbendazim on zebra fish, *Danio rerio*. In the paper, it was suggested that the pesticide altered the mRNA levels in zebrafish. Another investigation of toxic effect of carbendazim over zebra fish was carried out by Andrade et al. (2016). The research group proposed that the

fungicide causes anomalies in zebrafish embryos. Jiang et al. (2015) emphasized that the pesticide causes endocrine disruption in zebrafish.

In soil, as a highly persistent pesticide, carbendazim residues may remain up to 2 years (Ellis et al., 2007). Thus, carbendazim shows negative effects on soil life. Various number of studies have been proceeded for the investigation of toxicity of carbendazim on different types of organisms that live in soil.

Especially, the studies were focused on the investigation of toxic effects of carbendazim on earthworms. Liu et al. (2012) investigate the median lethal concentrations of carbendazim in different types of soil. Authors state that the acidity of the soil affects the toxicity of the carbendazim on earthworms. Förster et al. (2006) examine the effect of various parameters on toxicity of carbendazim on earthworms. It was also stated in the literature that carbendazim was harmful and had negative effects on the reproduction of earthworms (Yasmin and D'Souza, 2007). The toxicity of the fungicide on earthworms was investigated by Lofs-Holmin (1981) in various types of soil.

Toxic effects of carbendazim on soil microbial activities were also evaluated by various scientists. Wang et al. (2009) demonstrate the effect of carbendazim on microbial activities in soil. The study mentioned that the negative effects of carbendazim may vary due to some parameters such as type of soil, temperature and the concentration of the pesticide. In an other study, it was emphasized that carbendazim over 100 ppm shows toxic effects to soil life (Wang et al., 2016).

European Food Safety Authority (EFSA) declare that carbendazim is not severely toxic via dermal, oral and inhalation exposures and pesticide is not also irritant to skin and eye. The report also indicates that carbendazim shows negative effects on male mammalian reproductive system (EFSA, 2010).

A plenty of studies have been carried out in order to determine the toxic effects of carbendazim on mammalian systems. For this purpose, the experiments were applied to mice, rats and human. Carbendazim especially shows serious effects on male mammalian reproductive system.

Yu et al. (2009) have reported that carbendazim causes negative effects on cells that take place in spermatogenic process in rats. It was also mentioned in the literature that carbendazim led to death in mice fetuses (Farag et al., 2011). In the same study, it was stated that malformations were observed on the skeletons of mice.

There are several studies focused on the toxicity of carbendazim on human cells. Zhou et al. (2015) proposed that the pesticide has negative influences on

protease systems and it may also show substantial effects on the human reproductive system. It was revealed in the literature that carbendazim causes changes in the levels of various hormones, shows negative effects on male reproductive system and shows vital effects on androgenic receptors (Rama et al., 2014). In a further study, Chang et al. (2010) studied the effect of carbendazim on human endometrial cells. The scientists showed that the pesticide altered the growth of endometrial cells.

It was stated that carbendazim at high dosages (>10000 ppm) causes changes in rats body weight and alters the proper functionality of liver and kidneys. It was also mentioned that the cell functions in dogs were also affected by carbendazim (Pfeil and Dellarco, 2005).

1.5 Analytical methods used for determination of carbendazim

Determination of pesticides in the environmental samples is very important since these chemicals can be hazardous. Trace levels of pesticides can be toxic or carcinogenic. Thus, especially over the last decade, many analytical methods have been developed for the determination of trace levels of pesticides in different samples. Sensitivity, selectivity, rapidness and cheapness are the most important parameters for the developed methods.

Mostly used method for determination of carbendazim is high-pressure liquid chromatography (HPLC). There are many studies carried out by using HPLC for preconcentration, separation or determination of carbendazim.

Generally, extraction techniques have been used for separation of organic compounds in a complex matrix before their determination. Wu et al. (2009) used dispersive liquid-liquid microextraction combined with high performance liquid chromatography equipped with fluorescence detection for the determination of carbendazim and thiabendazole in water and soil samples.

In an other study, Singh et al. (2007) used microwave-assisted extraction (MAE) for determination of thiophanate methyl and carbendazim residues in vegetable samples by HPLC.

Thomas et al. (1996) proposed a method for the determination of carbendazim in water that combines high-performance immunoaffinity chromatography and reversed phase-HPLC with a detection system which is consist of by either UV-Vis diode array detector (DAD) or mass spectrometry (MS).

Bernal et al. (1997) developed a method for determination of benomyl and carbendazim in different samples such as honey, bees wax, larvae, bees and pollen by reversed-phase-HPLC with fluorescence detection.

In a different study, a method for determination of carbendazim and thiabendazole in fruits and vegetables by using suitable cartridge and a HPLC-UV system has been proposed by Di Muccio et al (1999).

A chromatographic system has been also used by Singh et al. (2004) for simultaneous determination of thiamethoxam, imidacloprid and carbendazim in different vegetable samples.

Chen et al. (2015) has been used ultra-high performance liquid chromatography for determination of thiophanate-methyl and carbendazim in rapeseed.

Additionally to HPLC, other chromatographic techniques such as liquid and ion chromatography are widely used techniques for determination of carbendazim.

A method has been described by Blasco et al. (2002) for simultaneous determination of imidacloprid, carbendazim, methiocarb and hexythiazox in peaches and nectarines by using liquid chromatography–mass spectrometry. Subhani et al. (2013) described a new method for simultaneous determination of imidacloprid and carbendazim using ion chromatography with a fluorescence detector. Bean and Henion (1997) developed a method which employs the application of automated on-line immunoaffinity extraction coupled with tandem mass spectrometric detection for the ultra-trace determination of carbendazim in soil and lake water.

Supercritical fluid extraction combined with HPLC-DAD or gas chromatography-mass spectroscopy has been used for analysis of carbendazim, benomyl, thiophanate methyl and 2,4-dichlorophenoxyacetic acid in fruits and vegetables by Anastassiades and Schwack (1998).

Thiophanate-methyl and carbendazim residues in tomato were determined by ultra-performance liquid chromatography coupled with tandem mass spectrometry by Liu et al. (2014).

Various spectroscopic methods can be used for determination of carbendazim. A new method has been presented for determination of carbendazim with the aid of spectrophotometry by Pourreza et al (2015).

Ma et al. (2015) used surface-enhanced Raman scattering technique to determine carbendazim in tea leaves. This study suggested as a fast method for determination of carbendazim in tea since it does not consist any sample preparation procedures.

Since carbendazim shows native fluorescence, different methods depend on fluorescence measurements have been proposed by research groups. Xu et al. (2014) studied on developing a spectrofluorimetric method which depends on the formation of complex between 3,3'-benzidine/ β -cyclodextrin derivative and carbendazim. By measuring the fluorescence signal of the complex, a rapid and highly sensitive determination of the carbendazim could be achieved in water, vegetables and fruit samples. Another fluorimetric study for carbendazim determination was investigated by del Pozo et al. (2010) which depends on the inclusion-complex formation of the pesticide with cucurbit[7]uril. The proposed method was applied to orange samples. In an other fluorimetric study, simultaneous determination of carbendazim and benomyl has been proposed by Reyes et al. (2003) which is based on the measuring of native fluorescence of the pesticides. Carbendazim in rapeseed oil and peanut oil was determined by Chen et al. (2015) with high accuracy.

Rodriguez-Cuesta et al. (2003) described a method for determination of carbendazim, fuberidazole and thiabendazole by using three-dimensional excitation–emission matrix fluorescence and parallel factor analysis.

Martinez-Galera et al. (2003) develop a method depends on fluorimetry and use multivariate calibration techniques in order to determine carbendazim in water samples.

Electrochemical methods can also be used for determination of carbendazim. Different types of electrodes with different methods of electrochemistry can be used for electrochemical determination of carbendazim. In some circumstances, electrochemistry is less expensive when compared with other methods.

Doubly modified glassy carbon electrode has been used by Khare et al. (2015) for determination of carbendazim by using adsorptive stripping differential pulse voltammetry. Another voltammetric determination of carbendazim has been proposed by Luo et al. (2013) by using glassy carbon electrode modified with a hybrid nanomaterial.

Ribeiro et al. (2011) develop a method for preconcentration and determination of carbendazim which consist of multiwalled carbon nanotubes modified electrode and square wave adsorptive stripping voltammetry.

Yao et al. (2014) used carboxylic group functionalized poly(3,4-ethylenedioxythiophene) film electrode for voltammetric determination of carbendazim by using differential pulse anodic stripping voltammetry. Li and Chi (2009) determine carbendazim electrochemically by using multiwalled carbon nanotubes-polymeric methyl red film modified electrode.

A new voltammetric method has been proposed by del Pozo et al. (2011) which depends on the complex formation between carbendazim and cucurbit[7]uril. The proposed method was used to determine carbendazim in the apple samples by using differential pulse voltammetry.

Molecularly imprinted-solid phase extraction (MISPE) system has been used with HPLC-DAD for the preconcentration and separation of carbendazim, benomyl and thiabendazole by Zamora et al. (2009). Another chromatographic system combined with imprinted polymer has been used by Cacho et al. (2009) to preconcentrate, separate and determine benzimidazole fungicides.

1.6 Magnetite-Molecularly Imprinted Polymers

As mentioned in the first chapter of the thesis, molecularly imprinted polymers (MIPs) have been widely used for separation and determination of organic compounds. Over the last decade, magnetite (Fe_3O_4) particles coated with molecularly imprinted polymers, which can also be called as magnetite-molecularly imprinted polymers or magnetic-molecularly imprinted polymers (MMIPs), have received great attention in separation and determination of organic and inorganic compounds.

Mostly used methods for synthesis of MMIPs particles can be classified as; the incorporation of solid magnetite or ferrofluids in suspension polymerization or the post-magnetization of polymer particles by the precipitation of iron oxide (Ansell and Mosbach, 1998). After the precipitation of magnetite particles generated, surface of the particles were modified or functionalized. Then, the magnetite particles form a core-shell structure through polymerization with organic or inorganic materials (Zeng et al., 2012).

Kwasniewska et al. (2015) also state that preparation of magnetite-molecularly imprinted polymer particles can be categorized in four steps. According to the research group, magnetite particles are precipitated by adding NaOH or ammonia solution into mixture of iron(II) and iron(III) solution at 80-100°C, in the first step. Second step consist of the surface modification of the magnetite particles however some researchers may prefer to skip this step. In the third step, polymerization reaction proceeded and in the last step template was

removed from the polymer structure. Preparation of magnetite-molecularly imprinted polymer is shown in Figure 1.2.

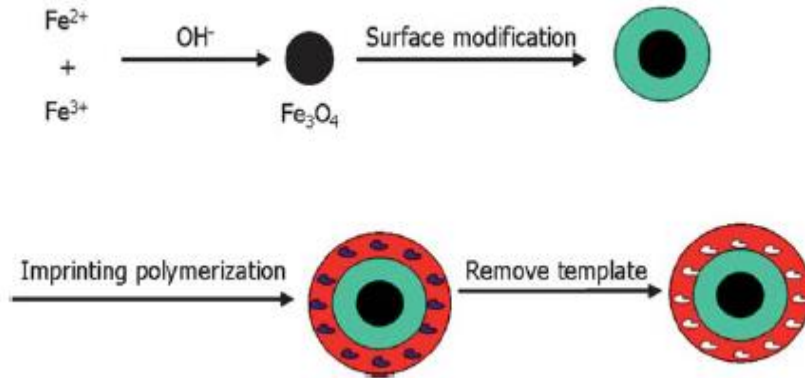


Figure 1.2. Preparation of MMIP particles (Chen and Li, 2012).

Surface molecular imprinting technique has some important advantages such as; improved mass transfer and effective binding ability, over traditional molecular imprinting technology (Guan et al., 2013). MMIPs were prepared by coating MIPs over magnetite (Fe₃O₄) particles. Thus, synthesized MMIPs can easily be separated from the sample by using a permanent magnet without applying any centrifugation or using filtration system and this brings effective and rapid separation (Zhang et al., 2014).

Su et al. (2015) state that adsorbents that have magnetic characteristics have important properties such as good dispersion, fast and effective binding. They also emphasize that these adsorbents can be isolated from different types of samples and the combination of magnetic separation and molecular imprinting technology reveal a method which is simple, sensitive, selective. Illustration of the experimental procedure is shown in Figure 1.3.

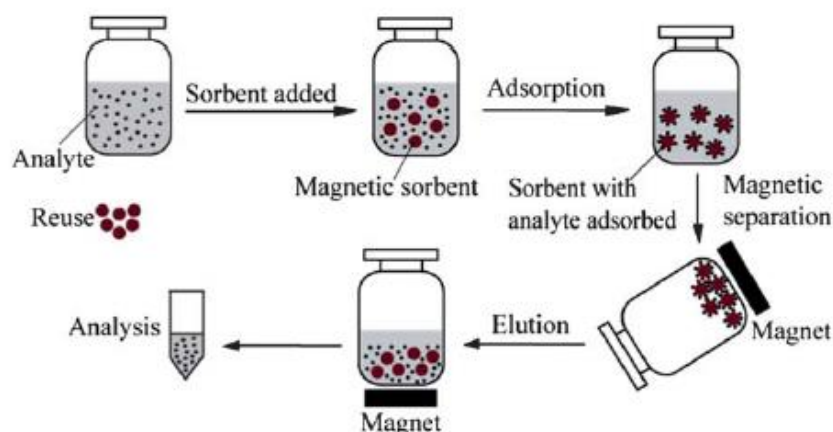


Figure 1.3. Schematic experimental procedure for MMIP (Chen and Li, 2012).

1.7 Applications of MMIPs

Molecularly imprinted polymer coated magnetite particles have been used in many areas for separation and determination of organic and inorganic substances. With the aid of magnetic property of the polymer, MMIPs can be used repeatedly without any efficiency loss.

Especially, over the last decade, number of the studies carried out by using MMIPs have been significantly increased since MMIPs provide cost-effective and rapid operation.

Usage of magnetite particles and modified magnetite particles in literature have been investigated in details by Kaur et al. (2014). The authors state that the particles have been used for the determination, preconcentration or separation of trace levels of various organic and inorganic compounds such as pesticides, dyes, and metal ions.

It was mentioned in the literature that magnetite based adsorbents also have been used for the separation of enzymes and proteins (Giakisikli and Anthemidis, 2013). In the determination of organic compounds, in order to improve the selectivity of the adsorbent, generally, magnetite particles have been coated with molecularly imprinted polymers.

Piao and Chen (2012) proposed a method for separation of Sudan dyes by using MMIPs as adsorbent in HPLC analysis. Xie et al. (2015) have also proposed a method based on MMIPs for detection of Sudan dyes by HPLC-UV system. Malachite green was detected by using electrochemiluminescence as detector and

MMIPs as solid support for adsorption in an other study proposed by Huang et al. (2015).

Spectrophotometric preconcentration and detection of Rhodamine B was proposed by Su et al. (2015) by using surface modified magnetite molecularly imprinted polymers. Luo et al. (2011) developed a new magnetite-molecularly imprinted polymer for detection of five different dyes in aqueous samples.

Determination and separation of phenolic compounds with MMIPs have been widely proposed in literature.

Chen et al. (2013) synthesized imprinted polymer by using acrylamide as monomer and ethylene glycol dimethacrylate as cross-linker and they coated magnetite particles with this polymer and used this MMIP for extraction of resveratrol from wine. Cao et al. (2014) developed a method consisted of MMIP as adsorbent and chemiluminescence as detector for determination of bisphenol A.

MMIPs, synthesized by using N-isopropylacrylamide as functional monomer, have been used as adsorbent for separation of 2,4,5-trichlorophenol in aqueous solutions (Wang et al., 2015). MMIPs coated on carbon nanotubes for detection of 4-nonylphenol with HPLC in river, rain and tap waters with the capacity of 54.4 mg/g was proposed by Rao et al. (2014).

MMIPs can also be used for the determination of trace levels of pharmaceutical active ingredients and antibacterial drugs.

Chen et al. (2009) developed a method based on MMIPs for determination of four antibiotics tetracycline, oxytetracycline, metacycline and chlortetracycline. The research group proposed that they separate and analyse these antibiotics from egg and tissue samples by using MMIP based tandem MS system. In a further study, Kong et al. (2012) proposed a method for the detection of sulfamethazine antibiotic in animal feed. They emphasized that the proposed adsorbent has an imprinting factor of 9.5 and adsorption capacity of 344.8 $\mu\text{g/g}$. Ahmadi et al. (2014) suggested an optical method based on MMIPs for determination of mefenamic acid with a detection limit of 50.0 ng/L. HPLC-DAD system has been used for the determination of carbamazepine after preconcentrated with MMIPs (Zhang et al. 2013). MMIPs have also been used for removing an antibiotic erythromycin in water samples (Ou et al., 2015).

Separation and determination of biochemical and biomedical compounds by using MMIPs have been also examined by various scientists.

Wang et al. (2009) suggested a method based on magnetite molecularly imprinted polymer for separation of estrone hormone which can be used in biomedical applications. Qiu et al. (2012) proposed a method which brings the combination of the selectivity of MMIP and the sensitivity of chemiluminescence for the epinephrine detection. A new method based on the magnetic imprinted polymer was proposed by Gao et al. (2014) for the extraction of bovine hemoglobin in blood samples.

Determination of pesticide residues in various environmental samples have been widely proceeded by using magnetite molecularly imprinted polymers.

Ma and Chen (2014) proposed a method based on MMIP-HPLC-UV for the detection of four different insecticides in fruits. In a further study, Shaikh et al. (2014) extracted two organochlorine pesticides from water with the aid of MMIPs. MMIPs have been used for the determination of triazine herbicides in vegetables and fruits by Hu et al. (2009).

1.8 The aim of study

Carbendazim is a widely used systemic fungicide and trace levels of carbendazim give serious damages to endocrine system and show mutagenic and teratogenic effects on animals. Carbendazim is embriotoxic and phytotoxic and it also shows negative effects on the male mammalian reproductive system. Therefore, quantitative determination of trace levels of carbendazim is very important. The aim of this chapter is to develop a MMIP-based fluorimetric method for the quantitative determination of carbendazim.

2. Experimental

2.1 Reagents

All reagents and chemicals were analytical grade. Glassware was cleaned by soaking them in dilute nitric acid (10%) and rinsed with distilled water prior to use.

Methacrylic acid (99%), ethylene glycol dimethacrylate (97%), N,N-dimethylformamide (>99%), chloroform (>99.5%), ethanol (>99.5%), methanol (>99.5%), acetonitrile (>99.5%), dichloromethane (>99.5%), 2,2'-azobis(isobutyronitrile) (98%), tetrahydrofuran (>99.5%), sodium hydroxide (98%), hydrochloric acid (37%), naphthalene (98%), thiabendazole (98%), methylisobutylketone (98.5%), polyvinylalcohol (99%), iron(II) chloride tetrahydrate ($\text{FeCl}_2 \cdot 4\text{H}_2\text{O}$) (99%) and iron(III) chloride hexahydrate ($\text{FeCl}_3 \cdot 6\text{H}_2\text{O}$) (99%) were purchased from Merck. Thifensulfuron methyl (97%), tebuconazole (98%) and chlorothalonil (98%) were purchased from TCI. Carbendazim (97%) and carbofuran (98%) were purchased from Aldrich. Carbaryl pestanal (>99.5) was purchased from Fluka. Oleic acid (65-88%) was purchased from Applichem. Thiram (97%) and 1-naphthol (99%) was purchased from Alfa Aesar.

Stock carbendazim solutions (100 mg/L) were prepared by dissolving appropriate amount of pesticide in methanol and diluting it to 100 mL with methanol.

Stock carbendazim solutions (50 mg/L) were prepared by dissolving solid in the appropriate amount of the methanol and diluting it with distilled water and stored at 4°C in the dark. Working standard solutions were prepared by diluting the stock solutions daily by distilled water.

Thiram, chlorothalonil, thifensulfuron methyl, tebuconazole, 1-naphthol, carbaryl, naphthalene, carbofuran and carbendazim solutions in distilled water were prepared by dissolving the appropriate amount of pesticide in a minimum amount of methanol and diluting it by distilled water.

2.2 Apparatus and operating conditions

The spectrofluorometric measurements were carried out using a Shimadzu RF- 5301 PC spectrofluorophotometer. The cuvettes of quartz glass (1-1 cm) were used.

Fourier transform infrared spectra (FTIR) were recorded on a Perkin-Elmer FTIR One B spectrometer.

Nüve BM 302 water bath shaker and Biosan Orbital OS-10 shaker were used.

The pH measurements were performed by using a Orion 4 Star pH meter. pH meter was calibrated before every measurement.

Tacussel électronique model magnetic stirrer used for stirring during pH studies.

For centrifugation, Nüve NF 800 was used at 3000 rpm.

Chilvert model hot-plate was used.

Biosan MM-1000 type overhead stirrer was used.

All weight measurements were performed using a Precisa XB220A (readability: 0.0001 g).

The morphologies of magnetite and magnetite-molecularly imprinted polymers were analyzed by scanning electron microscopy (SEM) (JEOL, Tokyo, Japan). Magnetic measurements were carried out using a vibrating sample magnetometer (Cryogenic Limited PPMS).

2.3 Synthesis of Magnetite Particles

Magnetite (Fe_3O_4) particles were prepared by the coprecipitation method, as stated in the literatures by Chen and Li (2013) and Liu et al. (2014).

0.01 mol $\text{FeCl}_2 \cdot 4\text{H}_2\text{O}$ and 0.02 mol $\text{FeCl}_3 \cdot 6\text{H}_2\text{O}$ were dissolved in 100 mL distilled water. The mixture was stirred vigorously and purged with nitrogen gas at 80°C . 50 mL of 2M NaOH was added into the solution and formation of black precipitate was observed. After one hour, the magnetite particles were isolated from the solvent by ultra centrifuge. Then, the isolated particles were washed with distilled water for three times. After washing step, magnetite particles were separated by an external magnet. Prepared magnetite particles were finally dried in water bath at 80°C for an hour under nitrogen atmosphere.

2.4 Synthesis of Magnetite-Molecular Imprinted Polymer (MMIP) for Carbendazim

Magnetite particles were coated with imprinted polymer by using suspension polymerization stated by He et al. (2014).

Magnetite-molecular imprinted polymer (MMIP) was synthesized in several steps, as follows:

1 mmol carbendazim was dissolved in 20 mL N,N-dimethylformamide under gentle heating. 4 mmol methacrylic acid was added and the solution was stirred for one hour for the preparation of pre-assembly solution. After one hour, 20 mmol ethylene glycol dimethacrylate, the cross-linker, was added to pre-assembly solution. Meanwhile, 1 g magnetite was stirred with 3 mL oleic acid for 10 minutes. These two solutions were mixed and the mixture was named as pre-polymerization mixture.

1.8 g polyvinyl alcohol (PVA) was dissolved in 60 mL distilled water under gentle heating to obtain its saturated solution. Saturated PVA solution was purged with N₂ gas and transferred in to two-necked-flat-bottomed flask. Pre-polymerization mixture was mixed with saturated PVA solution and the mixture was purged with N₂ gas again and 0.1 g 2,2'-azobis(isobutyronitrile), the initiator, was added to the mixture. The polymerization reaction was allowed to be proceed under 60°C under N₂ atmosphere for 5 hours.

Synthesized MMIPs were separated by an external magnet and washed with methanol/acetic acid (9:1, v/v) mixture and methanol for three times, respectively. MMIPs were dried at 50°C in oven before using in extraction studies. Magnetic-non imprinted polymers (MNIPs) were synthesized with similar process without using the carbendazim.

2.5 Extraction of carbendazim from MMIPs

Batch extraction was applied for the extraction of carbendazim from synthesized MMIPs and methanol was used as the extractant.

0.5 g of synthesized MMIPs were weighed and transferred in to 50mL-falcon tube and extracted with an appropriate amount of methanol. The fresh aliquot of methanol was changed with the existed one after 2 hours of contact time. To prevent the leakage of the template in re-binding studies, the extraction was repeated until the signal of template was not observed in spectrofluorimeter at λ_{max} : 309 nm. Similar extraction procedure was applied to MNIPs. After the extraction, MMIPs and MNIPs were dried in oven before using in re-binding studies.

2.6 Re-binding studies of carbendazim to MMIPs

MIPs obtained from the batch extraction were used to investigate the re-binding studies of carbendazim.

Re-binding procedure was performed as follow: 80 milligrams of polymer was added to a 50-mL falcon tube containing 15 mL 0.2 mg/L carbendazim solution. After being shaken for 30 minutes at room temperature, polymers were separated from the solution with an external magnet. The free carbendazim concentration in the supernatant solution was detected by spectrofluorimetry and concentration of carbendazim was calculated by using a calibration curve. The re-binding of carbendazim on to MNIP was also measured in a similar manner.



3 Results and Discussion

3.1 Fluorescence properties

Fluorescence properties of carbendazim in different solvents were investigated. Excitation (λ_{ex}) and emission wavelengths (λ_{em}) are shown in Table 3.1. As shown in Table 3.1, carbendazim has fluorescence signal in water and organic solvents except acetone.

Table 3.1. Excitation (λ_{ex}) and emission wavelengths (λ_{em}) of carbendazim in different solvents.

Solvent	Excitation wavelength (λ_{ex}) (nm)	Emission wavelength (λ_{em}) (nm)
Tetrahydrofuran	290	312
Ethanol	285	310
Methanol	280	306
Dichloromethane	285	311
Acetonitrile	285	309
Water	280	308
Chloroform	280	309
N,N-dimethylformamide	285	314
Acetone	-	-

Fluorescence spectra of carbendazim in water and methanol are shown in Figures 3.1 and 3.2, respectively. The spectra of carbendazim in these solvents were given since carbendazim can be re-bound to the imprinted polymer in water and re-bound carbendazim can be recovered in methanol.

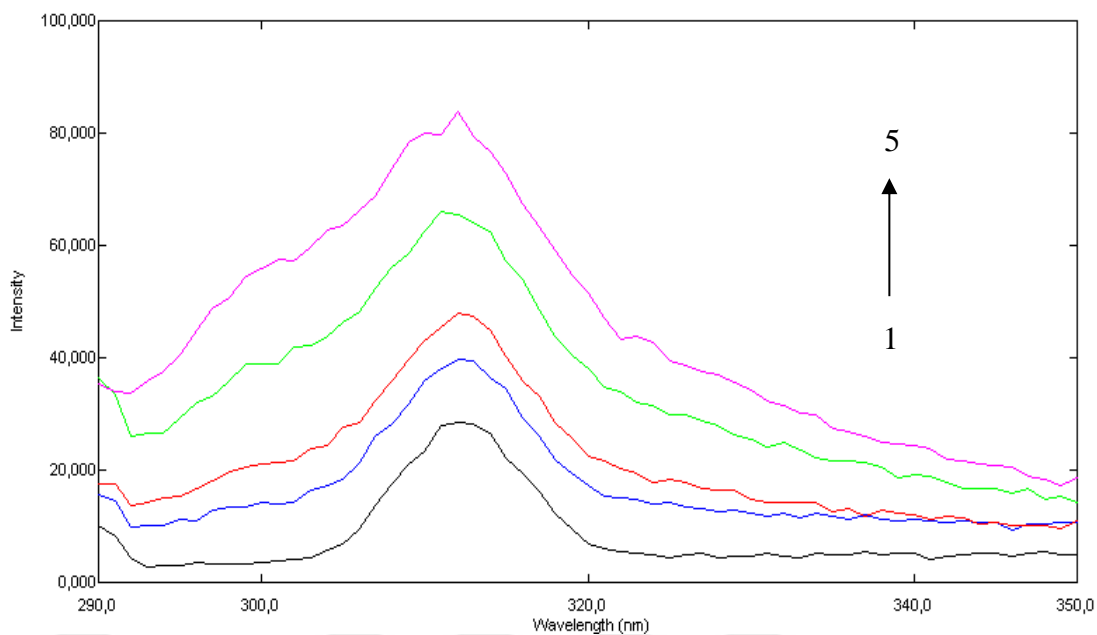


Figure 3.1. The fluorescence spectrum of carbendazim in water (1; blank, 2; 0.05 mg/L, 3; 0.1 mg/L, 4; 0.2 mg/L, 5; 0.3 mg/L and slit width: 5nm).

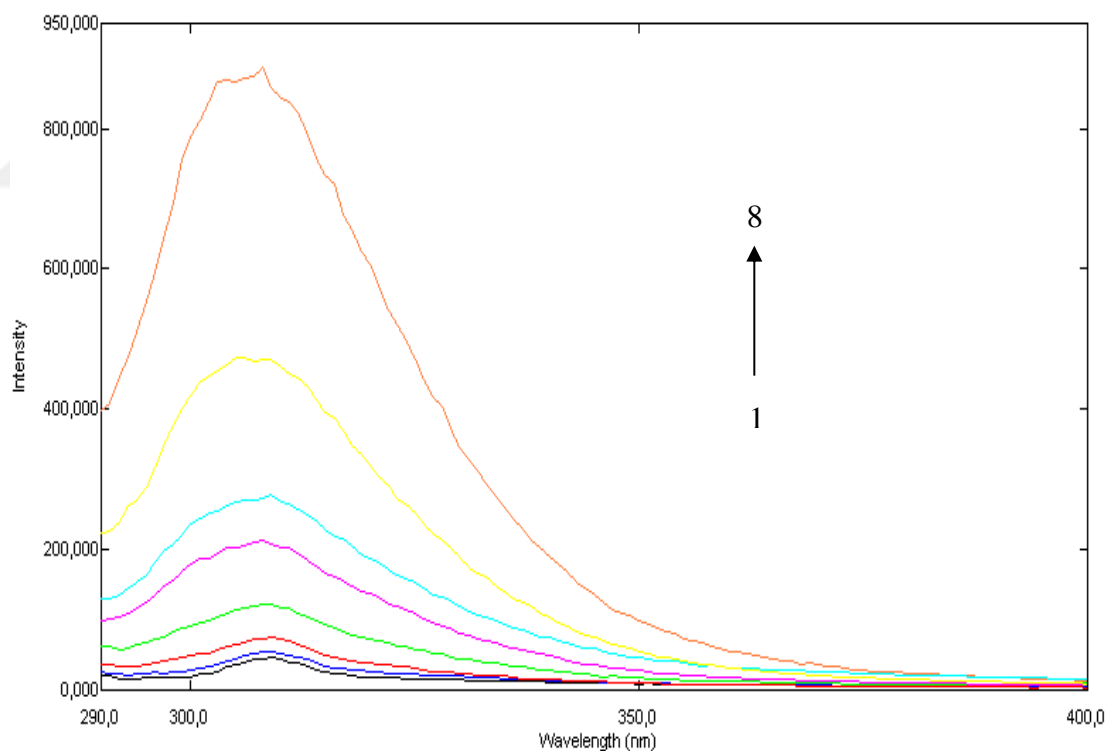


Figure 3.2. The fluorescence spectrum of carbendazim in methanol (1; blank, 2; 0.01 mg/L, 3; 0.025 mg/L, 4; 0.05 mg/L, 5; 0.1 mg/L, 6; 0.2 mg/L, 7; 0.3 mg/L, 8; 0.5 mg/L and slit width: 5nm).

3.2 Calibration graphs for carbendazim

Figures 3.3 and 3.4 illustrate the calibration graphs of carbendazim in water and methanol, respectively. The limit of detection (LOD) and the limit of quantification (LOQ) values of the method in each media were calculated on the basis of;

$$LOD = \frac{\sigma}{S} \times 3 \quad (1)$$

$LOQ = \frac{\sigma}{S} \times 10$ (2) where as σ is the standard deviation of the responses of blank solution and S is the slope of the calibration curve.

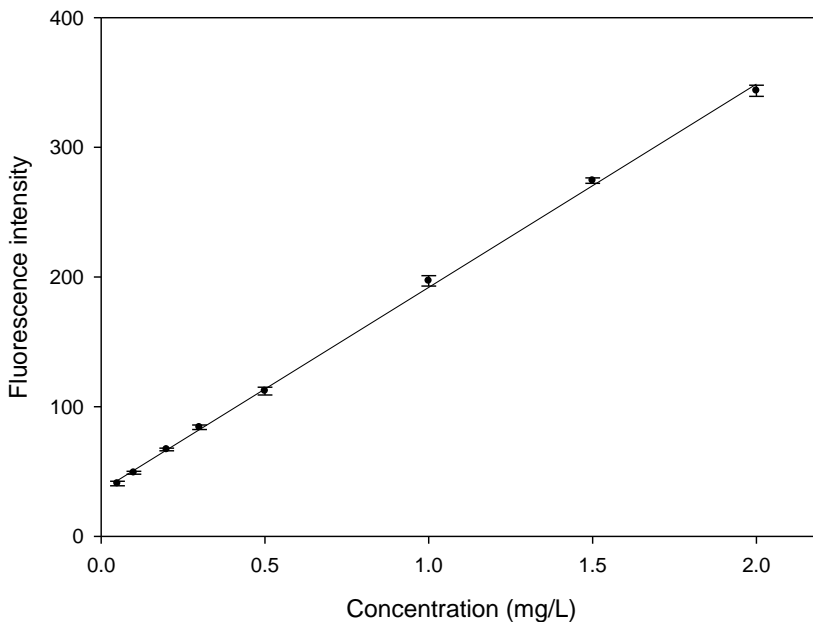


Figure 3.3. Calibration graph of carbendazim in water.

Calibration graph of carbendazim in water was linear between 0.050-2.000 mg/L with a regression coefficient (R^2) of 0.9987 and an equation with ($y=156.75x + 35.272$). LOD and LOQ values for water medium were found to be 0.010 and 0.034 mg/L, respectively.

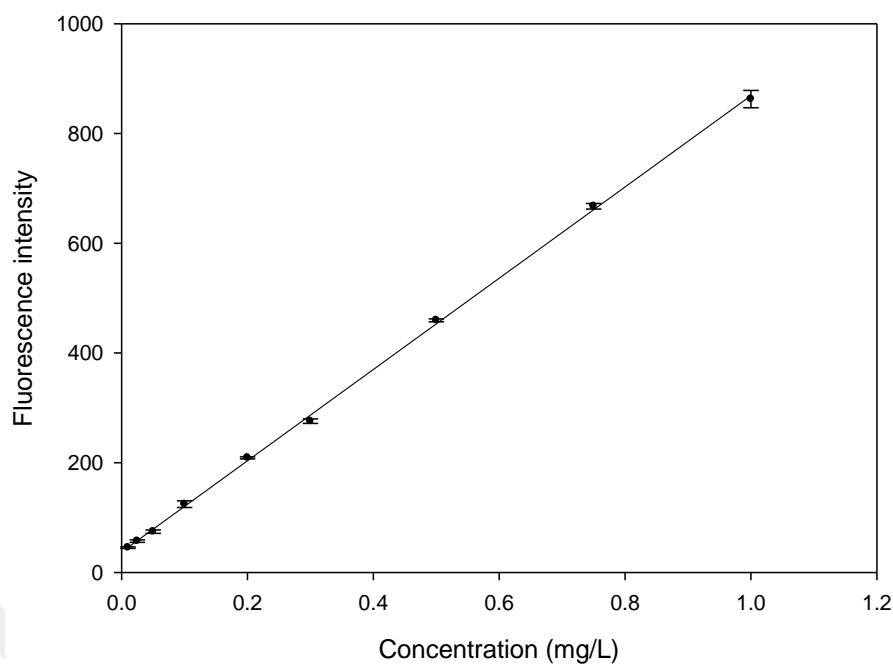


Figure 3.4. Calibration graph of carbendazim in methanol.

Calibration graph of carbendazim in methanol was linear between 0.010-1.000 mg/L with a regression coefficient (R^2) of 0.9992 and an equation with ($y=831.58x + 37.207$). LOD and LOQ values for water medium were found to be 0.0023 and 0.0078 mg/L, respectively.

3.3 FTIR analysis of synthesized polymers

FTIR spectra of synthesized MMIP, extracted MMIP, MNIP and magnetite particles were investigated. FTIR spectra show the differences between synthesized polymers.

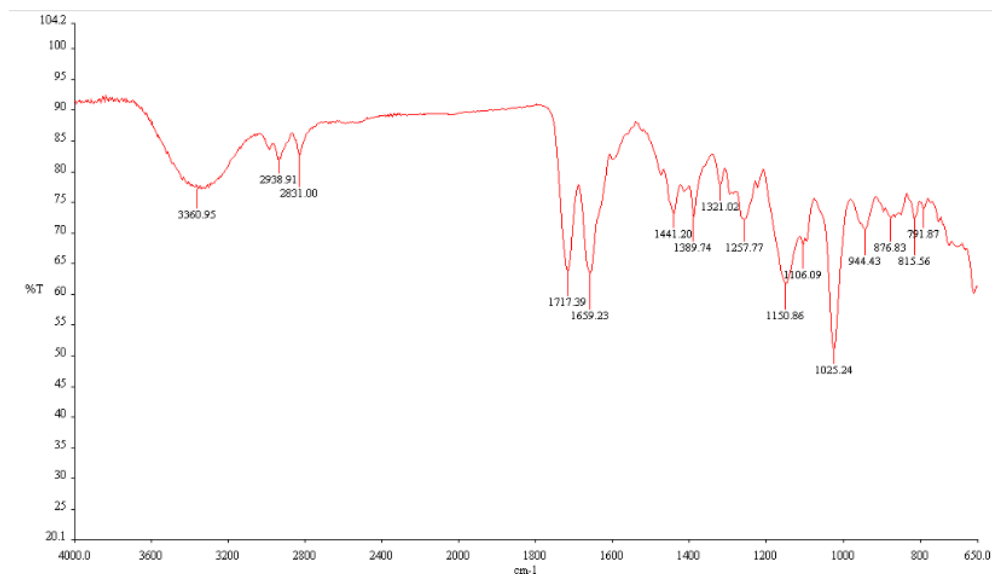


Figure 3.5. FTIR spectrum of synthesized MMIP.

Figure 3.5 shows the FTIR spectrum of synthesized MMIP which consists of carbendazim, methacrylic acid, ethylene glycol dimethacrylate and magnetite.

Peaks in the spectrum at 1717 cm^{-1} , 1150 cm^{-1} and 1025 cm^{-1} correspond to C=O stretching, C-O stretching and ester group respectively, exist in the ethylene glycol dimethacrylate structure in the polymer matrix. These peaks are the evidence to a successful polymerization process.

Presence of OH-bond peak at 3360 cm^{-1} corresponds to methanol which is used to wash polymer at the end of the synthesis procedure stated before. Peaks at 2938 cm^{-1} and 2831 cm^{-1} in MMIP spectrum respond to asymmetrical and symmetrical C-H stretching, respectively.

The peak at 1659 cm^{-1} in FTIR spectrum corresponds to carbendazim in MMIP. This is thought to be due to the shift occurred in C=C stretching of benzimidazole ring of carbendazim as reported by 1640 cm^{-1} by Laurella et al. (2015) is thought to be existed by shifting of this peak.

Differences in spectra of MMIP and magnetite is the presence of the coating of magnetite with the imprinted polymer. Figure 3.6 shows the difference of FTIR spectra between MMIP and magnetite particles. Figure 3.6 is the evidence of coating of magnetite particles with the molecularly imprinted polymer.

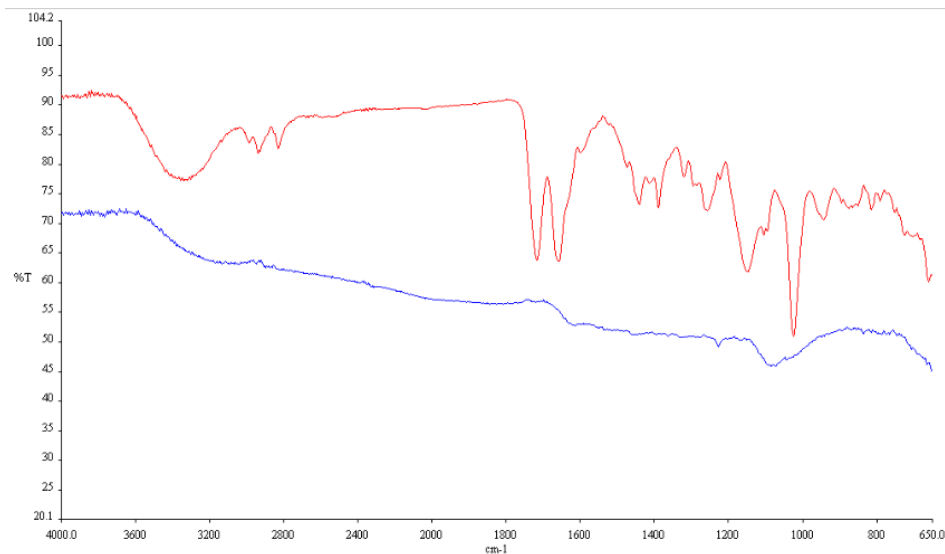


Figure 3.6. FTIR spectra of MMIP (red line) and magnetite particles (blue line).

When the carbendazim has been extracted out of the MMIP with methanol, some changes has been occurred in FTIR of the MMIP.

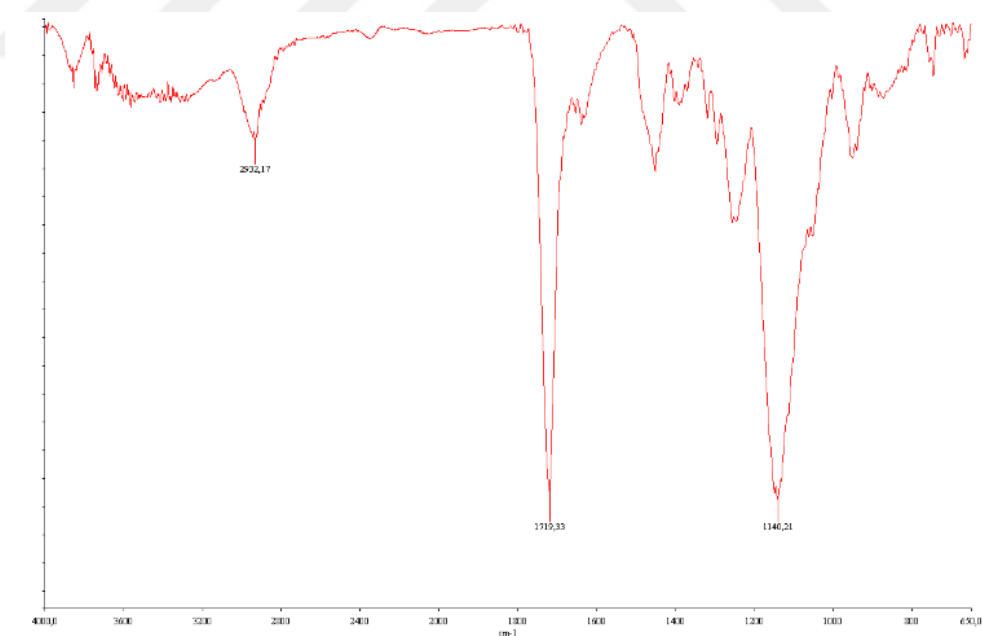


Figure 3.7. FTIR spectrum of extracted MMIP.

Figure 3.7 shows the FTIR spectrum of the extracted MMIP. As compared with Figure 3.5, it can be seen that some peaks are disappeared in Figure 3.7.

OH-bond peak at 3360 cm^{-1} was disappeared in FTIR spectrum of MMIP because methanol has been removed from the polymer after the extracted MMIP has been dried in oven.

Peak at 1659 cm^{-1} , which was thought to be related to aromatic C=C stretching of carbendazim, was also disappeared in the spectrum since carbendazim was extracted out of the polymer structure with methanol.

Peaks in the spectrum at 1719 cm^{-1} and 1150 cm^{-1} correspond to C=O stretching and C-O stretching respectively, exist in the ethylene glycol dimethacrylate.

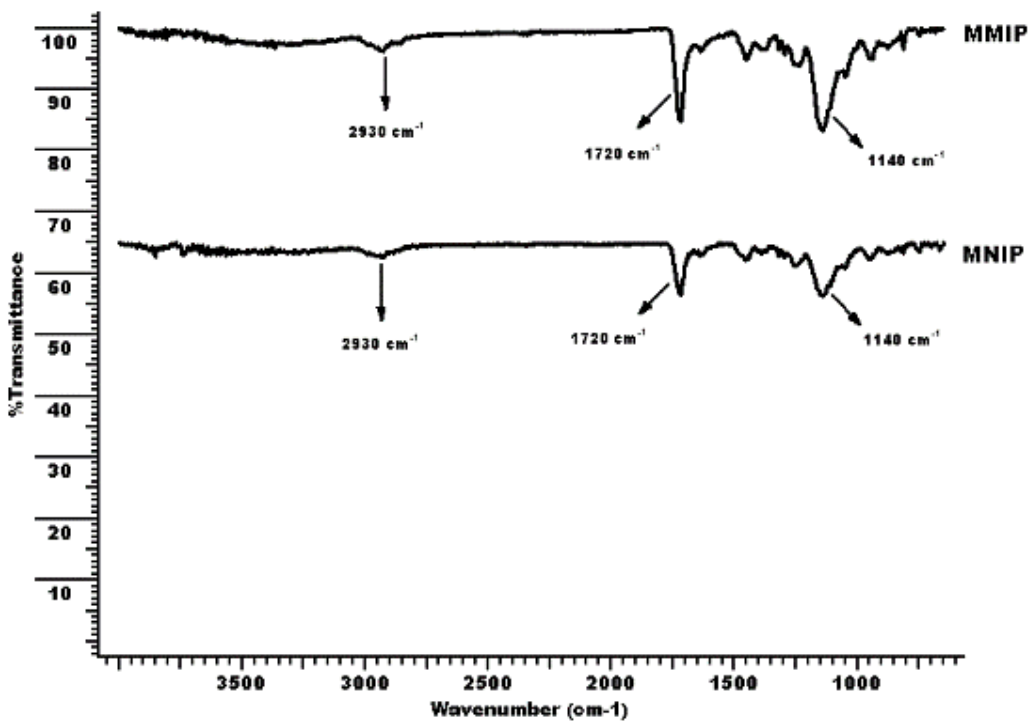


Figure 3.8. FTIR spectra of extracted MMIP and MNIP.

Figure 3.8 illustrates the FTIR spectra of extracted MMIP and MNIP. As expected, spectra are similar to each other. Since carbendazim is extracted out of the polymer structure, extracted MMIP and also MNIP are both consist of magnetite particles coated with the polymer structure made up of methacrylic acid and ethylene glycol dimethacrylate with the aid of the initiator 2,2'-azobis(isobutyronitrile).

Both polymer involve the same FTIR peaks around at 1719 cm^{-1} and 1140

cm^{-1} which correspond to C=O stretching and C-O stretching respectively, exist in the ethylene glycol dimethacrylate.

3.4 Re-binding studies for carbendazim

Re-binding of carbendazim was investigated in different solvents. In each experiment, the unadsorbed template in the supernatant solution was measured by spectrofluorimetry.

As expressed in details in the first chapter of thesis, water is not accepted as an ideal solvent in molecular imprinting technology but carbendazim can re-bind to the cavities of the MMIP only in water.

Table 3.2 shows the re-binding efficiencies of carbendazim in different solvents. Carbendazim can re-bind to cavities on the surface of the MMIP only in water. In optimum conditions, re-binding efficiency of carbendazim was found to be $99.69 \pm 3.23\%$ ($n=3$).

In different organic solvents, carbendazim could not re-bind significantly onto cavities. Thus, only water can be used as re-binding medium. This is an important advantage of the method for the determination of carbendazim in real water samples whereas any other extraction procedures are not necessary.

Table 3.2. Re-binding efficiencies of carbendazim in different solvents.

Solvent	Re-binding efficiency (%)
Tetrahydrofuran	Not significant
Dichloromethane	Not significant
Ethanol	Not significant
Methanol	Not significant
Acetonitrile	Not significant
Water	99.69±3.23 (n=3)
Acetone	Not significant
Chloroform	Not significant
N,N-dimethylformamide	Not significant

3.5 The effect of initial pH on re-binding of carbendazim

In order to determine the effect of initial pH on re-binding efficiency of carbendazim, the initial pH of carbendazim solution was adjusted to desired pH value in the range of 3.0 to 10.0 by using HCl and NaOH solutions. Carbendazim solutions with an initial concentration of 0.2 mg/L and sample volume of 10 mL were shaken with 80 mg MMIP for 30 minutes. After sorption, the free carbendazim in the solution was measured. As shown in Figure 3.9, pH and re-binding efficiency remains constant nearly at 100% over pH 5. All pH values over 5 can be used for

quantitative re-binding of carbendazim. pH 8.0 was selected as the optimum pH for the sorption studies.

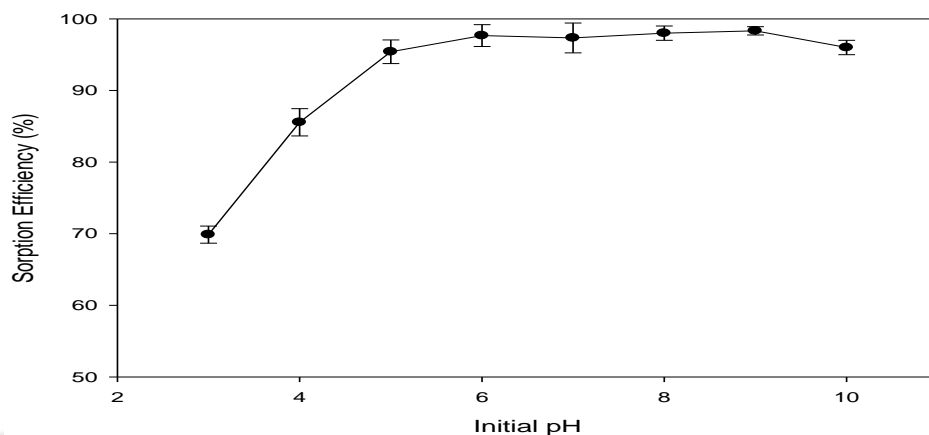


Figure 3.9. The effect of initial pH on re-binding efficiency of carbendazim (initial concentration: 0.2 mg/L, MMIP amount: 80 mg, sample volume: 10 mL, contact time: 30minutes).

3.6 Effect of re-binding time

Optimum re-binding time for carbendazim sorption was investigated. 0.05 mg/L carbendazim (pH~8) solutions were shaken for 1, 5, 10, 20, 30, 50 and 60 minutes with 100 mg of sorbent with the sample volume was 15 mL. As shown in Figure 3.10, quantitative re-binding of carbendazim onto MMIP is rapid and take place within 30 minutes. Thus, optimum re-binding time was selected as 30 minutes.

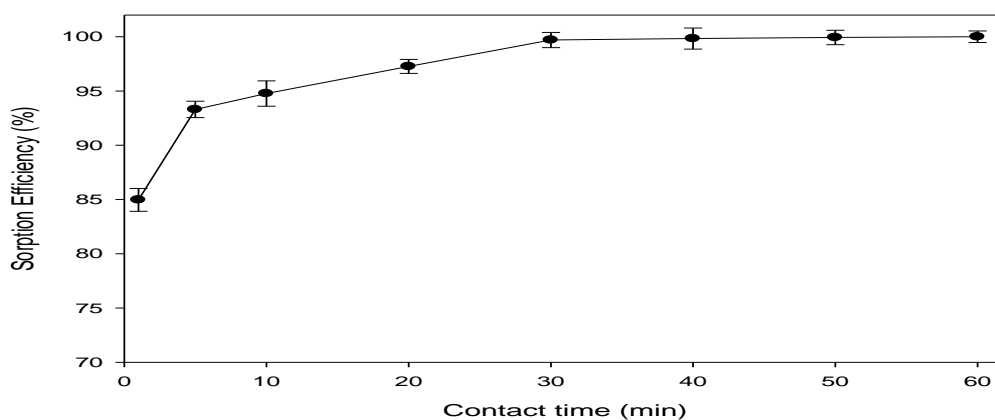


Figure 3.10. Effect of re-binding time (initial concentration: 0.05 mg/L (pH~8), sample volume: 15 mL, MMIP amount: 100 mg).

3.7 Recovery studies of carbendazim

Different solvents were used to recover adsorbed carbendazim from MMIP. As shown in Table 3.3, methanol should be used for quantitative recovery of carbendazim.

Table 3.3. Recovery of carbendazim with different solvents.

Solvent	Recovery (%) (n=3)
Methanol	96.76±3.97
Ethanol	81.44±4.24
Acetonitrile	83.39±3.89
N,N-dimethylformamide	36.61±5.03

3.8 Effect of recovery time

To find out the effect of time on the recovery of carbendazim, MMIPs were shaken with methanol for 1, 5, 10, 20, 30, 40, 50 and 60 minutes. The graph is shown in Figure 3.11.

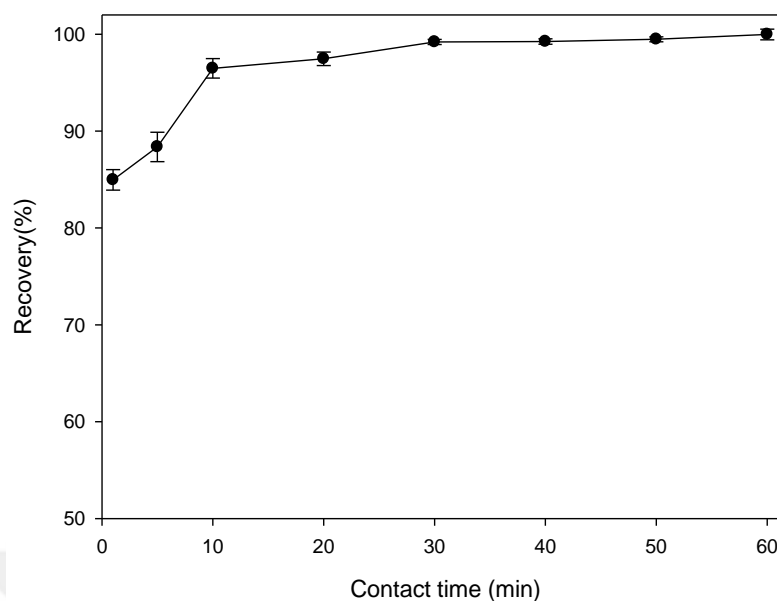


Figure 3.11. Effect of time on recovery of carbendazim (MMIP amount: 100 mg, initial carbendazim concentration: 0.05 mg/L (in water, pH ~8), sample volume: 10 mL, solvent volume: 10 mL).

As shown in Figure 3.11, quantitative recovery of carbendazim take place within 30 minutes. Thus, 30 minutes was chosen as optimum recovery time.

3.9 Effect of adsorbent dose

To determine the optimum adsorbent dose for the quantitative sorption of carbendazim in different sample volumes, various amounts of MMIP were weighed and 15 mL of 0.1 mg/L carbendazim solutions in water at pH~8 were added onto the MMIPs and shaken for 60 minutes. The effect of the adsorbent dose on carbendazim sorption is shown in Figure 3.12.

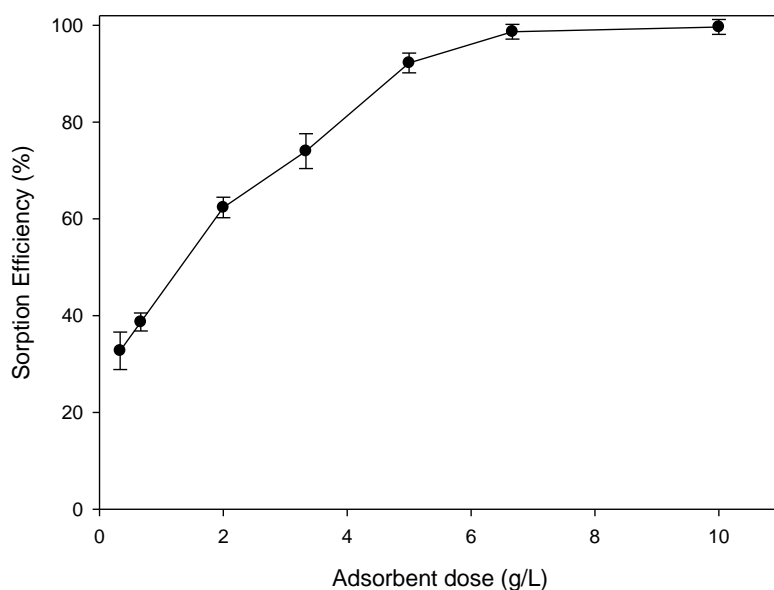


Figure 3.12. Adsorbent dose for quantitative sorption of carbendazim (initial carbendazim concentration: 0.1 mg/L (in water pH~8), sample volume: 15 mL, sorption time: 60 minutes, MMIP amount: 5-150 mg).

As shown in Figure 3.12, for quantitative sorption of carbendazim, minimum 6.5 g/L MMIP should be used. Under this adsorbent dose, the amount of MMIP was insufficient for quantitative sorption and sorption efficiency decreased. Beyond this adsorbent dose, the polymer reached its maximum capacity and the sorption efficiency remains constant at ~100%.

3.10 Capacities of MMIP and MNIP

To determine the capacities of the synthesized polymers used in the sorption studies, two methods were used.

First one is the experimental method where 50 mg MMIP and MNIP were shaken with 25 mL 20 mg/L carbendazim (pH ~8) for 24 hours. Carbendazim remained in the solutions was measured directly by spectrofluorometer. The adsorption capacity of the polymer for carbendazim (Q , mg/g) was calculated by using the following equation:

$$Q = \frac{(C_i - C_e) \times V}{W} \quad (3)$$

where C_i is the initial concentration ($\mu\text{g/mL}$) and C_e is the equilibrium concentration of carbendazim ($\mu\text{g/mL}$), V is the volume of the solution (mL) and W is the mass of the polymer used (mg).

Second method was based on the scatchard analysis model. The scatchard equation is;

$$\frac{Q}{C} = \frac{Q_{max}-Q}{K_d}$$
 (4) where Q is the amount of carbendazim adsorbed by polymer ($\mu\text{mol/g}$), C is the equilibrium concentration ($\mu\text{mol/L}$), Q_{max} is the maximum binding capacity ($\mu\text{mol/g}$) and K_d is the equilibrium dissociation constant ($\mu\text{mol/L}$). 30 mg MNIP and MMIP were shaken with 15 mL of various initial concentration of carbendazim solution (0.15-5 mg/L) in water (pH ~8) for 4 hours for employing the scatchard analysis.

Figure 3.13 shows the scatchard plots of MNIP. As illustrated in Figure 3.13, there is one linear region in the equation and it can be concluded that there is only one type of binding responsible for carbendazim sorption. The linear region has an equation of ($y = -0.2588x + 0.4654$) and with a regression coefficient (R^2) of 0.9851.

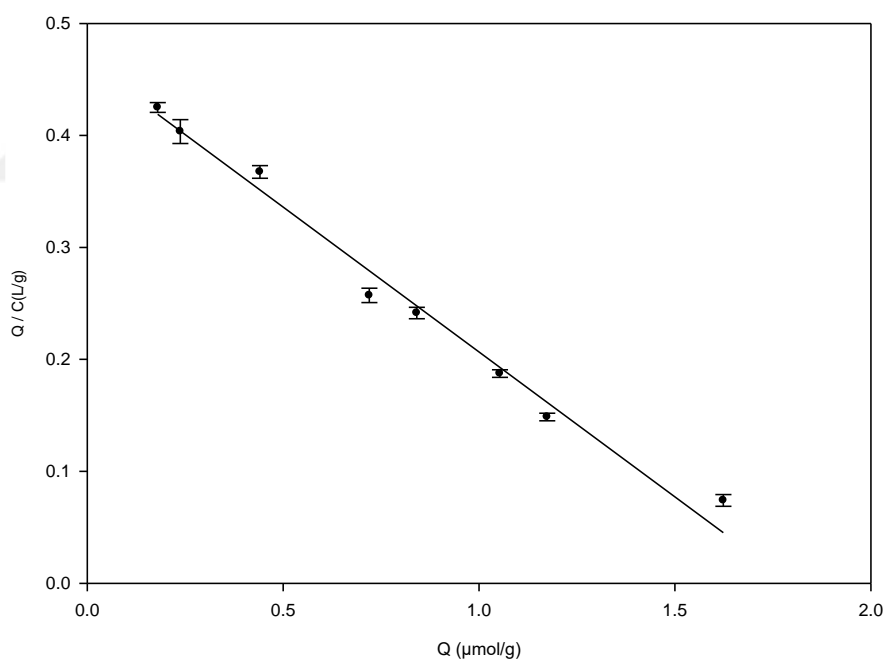


Figure 3.13. Scatchard plots of MNIP (MNIP amount: 30 mg, sample volume: 15 mL, initial concentration of carbendazim: 0.15-5 mg/L in water (pH ~8) contact time:4 hours).

Figure 3.14 represents the scatchard plots of MMIP. As shown in Figure 3.14, for MMIP, the equation has two different linear regions and we can conclude that there is a heterogeneous distribution of binding sites on the imprinted polymer. Thus, there were two different types of binding sites responsible for the sorption of

carbendazim. Linear regions have two equations with ($y = -0.8122x + 1.0392$) and ($y = -0.0315x + 0.3698$) two regression coefficients with 0.9879 and 0.9770, respectively.

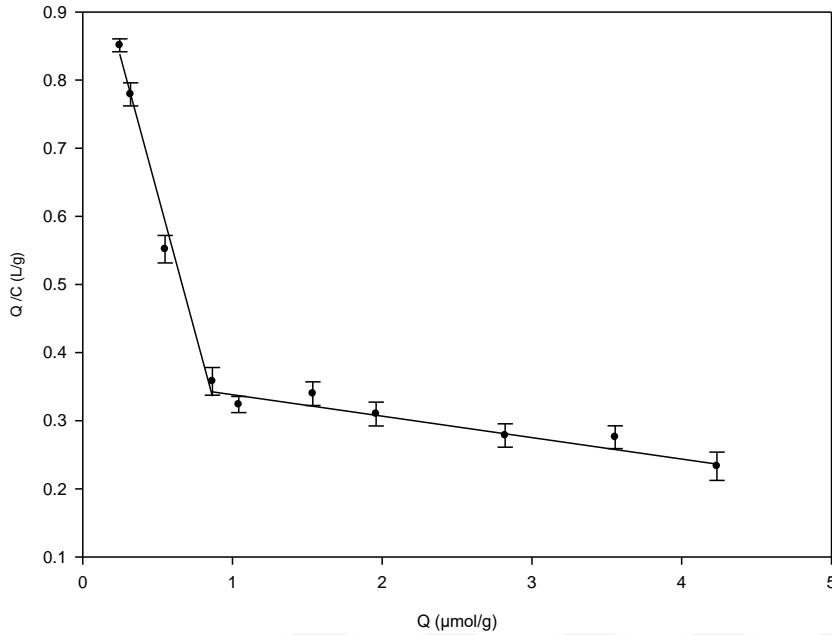


Figure 3.14. Scatchard plots of MMIP (MMIP amount: 30 mg, sample volume: 15 mL, initial concentration of carbendazim: 0.15-5 mg/L in water (pH ~8) contact time:4 hours).

From the slopes and intercepts of the Scatchard equations, the dissociation constants (K_d) and the maximum binding capacities (Q_{max}) of the MMIP and MNIP were calculated and shown in Table 3.4.

Table 3.4. Q_{max} and K_d values calculated from the Scatchard plot.

	Q_{max2} (μmol/g)	Q_{max2} (mg/g)	Q_{max1} (μmol/g)	Q_{max1} (mg/g)	K_{d2} (μmol/L)	K_{d1} (μmol/L)
MMIP	1.28	0.25	11.74	2.25	1.23	31.75
MNIP	-	-	1.80	0.34	-	3.86

In the experimental method, capacities of MNIP and MMIP were found to be 0.56 ± 0.08 mg/g and 2.31 ± 0.63 mg/g ($n=3$), respectively. When the adsorption capacities calculated from the scatchard analysis and experimental method

compared, the capacity values were found to be in good agreement.

3.11 Reusability of imprinted polymer

10 mL of 0.050 mg/L carbendazim solution was shaken with 100 mg MMIP for 30 minutes. After sorption, MMIP was separated from the solution with an external magnet and regenerated with 10 mL methanol.

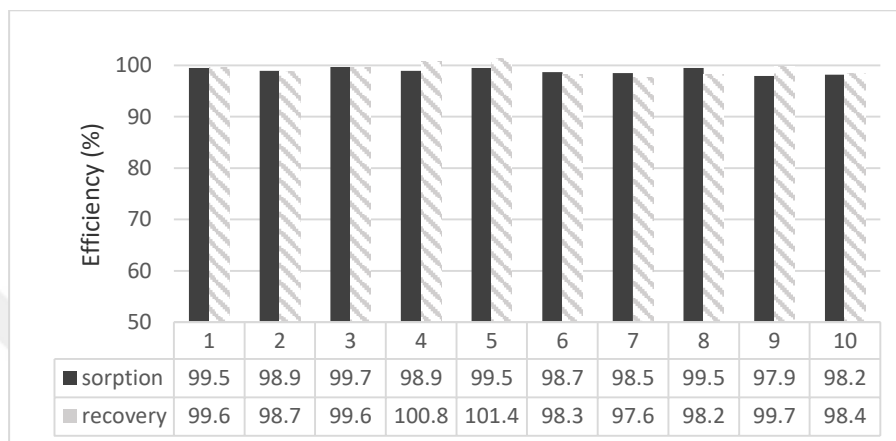


Figure 3.15. Reusability of the polymer.

As shown in Figure 3.15, MMIP can be used at least ten consecutive adsorption-regeneration cycles without a obvious decrease both in sorption and recovery efficiencies. The efficiencies of ten measurements for sorption and recovery were found to be 98.93 ± 0.61 and 99.23 ± 1.21 , respectively. Therefore, MMIP can be used repeatedly for carbendazim determination in water samples without any capacity loss. Reusability of the polymer makes the system more economical.

3.12 Interference effects on determination of carbendazim

The interference effects of thiabendazole, carbofuran, carbaryl, 1-naphthol, tebuconazole, thifensulfuron methyl, chlorothalonil and thiram were investigated on determination of carbendazim. A diverse substance, that causes a change in the fluorescence signal by more than $\pm 5\%$, was accepted as an interfering agent. Tolerable ratio of a substance can be defined as the ratio of the maximum concentration of a substance to the concentration of an analyte without showing any interfering effects. In agricultural applications, carbendazim can be used in the form of agrochemical fungicide mixture together with tebuconazole, thifensulfuron

methyl, chlorothalonil and tetramethylthiuram disulfide pesticides for controlling various plant diseases. Thus, in the presence of these pesticides, it is very important to determine trace carbendazim accurately.

In order to investigate the interference effect, 15 mL of 0.050 mg/L carbendazim solution with different amounts of possible interferent was shaken with 100 mg MMIP for 30 minutes and after sorption, carbendazim was recovered with 15 mL methanol. The tolerance ratio of interferents can be seen in Table 3.5.

Table 3.5. Interference effects on the determination of carbendazim (carbendazim = 0.050 mg/L).

Interferent	Tolerance Ratio of Interferents
Carbofuran	5
Carbaryl	7.5
Thifensulfuron methyl	25
Tebuconazole	25
1-Naphthol	50
Chlorothalonil	75
Thiram	75

3.13 SEM images and VSM analysis of the synthesized particles

Figure 16a and Figure 16b shows the SEM images of magnetite and MMIP particles, respectively. It is obvious that there is an increase in the diameter of the particles and these results clearly confirmed the successful coating of magnetite particles.

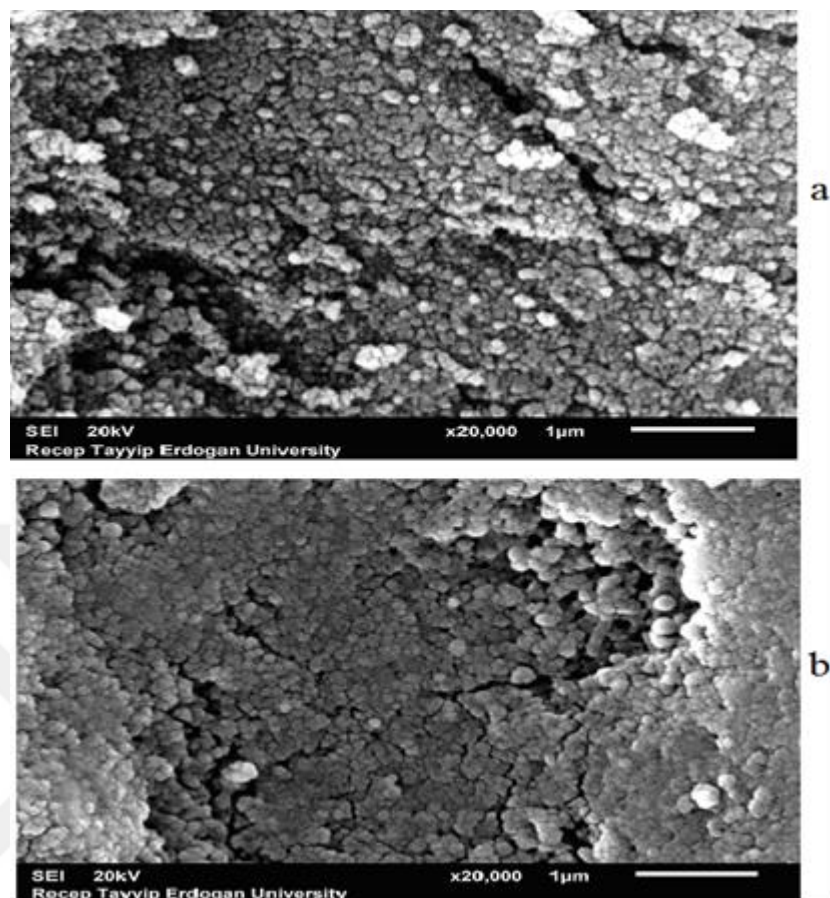


Figure 3.16. SEM images of a) magnetite b) MMIP.

As stated in the literature, VSM analysis has been widely used for the evidence of successful coating of magnetite particles and the preparation of magnetite-molecularly imprinted particles (Chen et al. 2009; Qi et al., 2016). The magnetic properties of magnetite and MMIP were investigated by VSM at room temperature. Figure 3.17 shows the magnetic hysteresis loops of the magnetite and MMIP particles. Magnetite achieved a saturation magnetization value (M_s) of 52.65 emu g^{-1} while the M_s value of MMIP significantly reduced to 7.31 emu g^{-1} . This result is the evidence of effective coating of magnetite with the imprinted polymer.

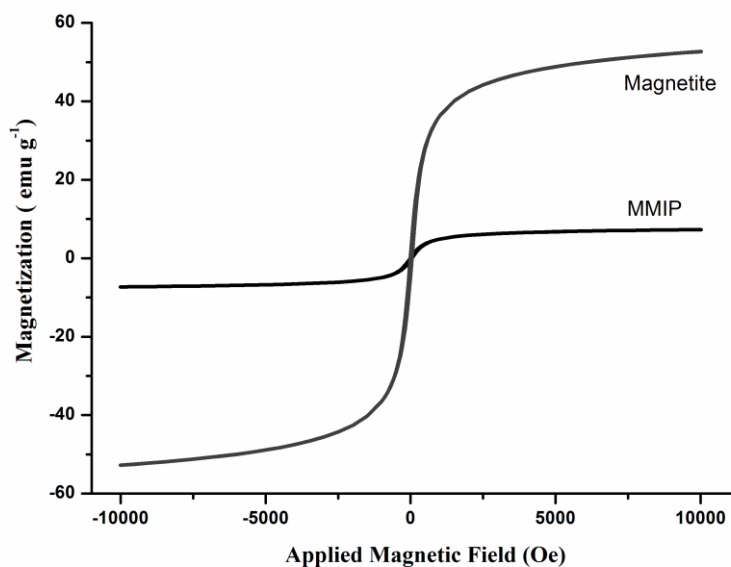


Figure 3.17. The magnetization curves of magnetite and MMIP.

3.14 Analytical application

Carbendazim is being used in different types of vegetables. Thus, analytical application was evaluated and the proposed method has been used for the determination of carbendazim in apple and orange.

Analytical applications were carried out in two different ways. Fruit samples were prepared according to the procedure proposed by Sanagi et al. (2013).

In the first method, according to the procedure; 50 grams of fruit samples (apple and orange) were chopped and homogenized by using blender. 10 g of sample was placed in a 100 mL-beaker. 10 mL of methanol and 10 mL of water was added onto sample and the suspension was sonicated for 30 minutes in an ultrasonic bath. The suspension was filtered through black ribbon filter paper and the solution was diluted to 100 mL with distilled water after adjusting its pH to 8.

100 mL (pH~8) solution was shaken with 250 mg MMIP for two hours for determination of carbendazim. Then, MMIP was separated from the solution with a permanent magnet. 25 mL methanol was added and shaken with MMIP for 30 minutes to recover the adsorbed carbendazim. Carbendazim was not detected in the fruit samples and, therefore, spike addition method was employed. Three parallel

analyses were done for each fruit sample. The results of the sample application are shown in Table 3.6. The recoveries of samples for orange and apple were found to be 95.67 ± 2.08 and 103.33 ± 1.53 , respectively.

Table 3.6. Determination of carbendazim in apple and orange.

Sample	Added ($\mu\text{g L}^{-1}$)*	Found ($\mu\text{g L}^{-1}$)*	Enrichment Factor	Total Recovery of Added Carbendazim (%)
Orange	-	<LOD**	-	-
	25	23.9 ± 0.5	4	95.7 ± 2.1
	50	48.3 ± 0.5	4	96.6 ± 1.1
	75	75.6 ± 0.4	4	100.8 ± 0.5
Apple	-	<LOD**	-	-
	25	25.8 ± 0.4	4	103.3 ± 1.5
	50	48.4 ± 1.3	4	96.8 ± 2.7
	75	76.1 ± 0.3	4	101.5 ± 0.4

*(n=3)

**LOD = Limit of Detection

In the second way, same procedure was followed as mentioned above with an only difference that, this time the spike addition was directly applied to the fruits. 5 mL, 2 mg/L carbendazim was injected to (110g) orange and (85g) apple and the fruits were chopped and homogenized by using blender.

10 mL of methanol and 10 mL of water was added onto chopped sample and the suspension sonicated for 30 minutes in an ultrasonic bath. The suspension was filtered through black ribbon filter paper and the solution was diluted to 100 mL with distilled water after adjusting its pH to 8.

100 mL (pH~8) solution was shaken with 250mg MMIP for 2 hours for

determination of carbendazim. After sorption, 25mL methanol was added onto MMIPs and shaken for 30 minutes for recovering the adsorbed carbendazim. Three parallel analyses were done for each sample. The results of the sample application are shown in Table 3.7.

Table 3.7. Analytical application of the proposed method.

Sample	Expected Concentration of Carbendazim (mg/L)	Average Found (mg/L)	Enrichment Factor	Total Recovery of Added Carbendazim (%)*
Orange	0.100	0.092	4	92.09±3.01
Apple	0.100	0.097	4	97.33±4.50

*(n=3)

4. Conclusion

A novel method is developed in this study for the determination of carbendazim. Magnetic-molecularly imprinted polymer (MMIP) has been used for the first time in the literature for the sensitive and selective determination and preconcentration of carbendazim.

MMIP can be separated from the solution easily and rapidly with the aid of its magnetic property. One of the main advantages of the method is that MMIP can be used repeatedly at least ten times for quantitative determination of carbendazim without any efficiency loss since the loss of adsorbent during separation is negligible.

The re-binding and recovery studies reveal that the proposed method is rapid and the processes can be completed within an hour. The quantitative re-binding and recovery values are found to be as 98.93 ± 0.61 and 99.23 ± 1.21 % (n=10), respectively.

Scatchard analysis and experimental method were employed and compared for determining the capacities of the synthesized polymers. When the results of the capacities calculated from the scatchard analysis and experimental method compared, the capacity values were found to be in good agreement; 2.25 and 2.31 ± 0.63 mg/g for MMIP and 0.34 and 0.56 ± 0.08 mg/g for MNIP, respectively. From the Scatchard plots of the MMIP, it can be concluded that there is a heterogeneous distribution of binding sites on the polymer and two types of binding sites responsible for the sorption of carbendazim. However, for MNIP, there is only one linear region which indicates that homogeneous distribution of binding sites are responsible for sorption of the pesticide.

The limits of detection (LOD) in methanol and water were satisfactory and 2.3 $\mu\text{g/L}$ and 10 $\mu\text{g/L}$, while the limits of quantification (LOQ) were 7.8 and 34 $\mu\text{g/L}$, respectively. The calibration graphs of carbendazim in methanol and water were linear between 10 - 1000 $\mu\text{g/L}$ and 50 - 2000 $\mu\text{g/L}$, respectively.

The proposed method has an important advantage that high-tolerable-ratio values are obtained for the pesticides; tebuconazole, thifensulfuron methyl, chlorothalonil and tetramethylthiuram disulfide which can be used together with carbendazim as agrochemical fungicide mixtures in agricultural applications.

Thus, trace levels of carbendazim can be determined accurately in the presence of these pesticides by using the proposed method.

The proposed method is an ideal method which can be used for the determination of carbendazim in real samples. The proposed method is applied to apple and orange and quantitative recoveries (92% - 103%) are obtained. Since the re-binding studies are performed in water, the proposed method may also be used for the direct preconcentration of carbendazim in real water samples.



REFERENCES

- Agency for Toxic Substances and Disease Registry**, 1995, Toxicological profile for naphthalene, 1-methylnaphthalene, and 2-methylnaphthalene, Atlanta, Department of Health and Human Services, 181p
- Ahmadi, M., Madrakian, T. and Afkhami, A.**, 2014, Molecularly imprinted polymer coated magnetite nanoparticles as an efficient mefenamic acid resonance light scattering nanosensor, *Analytica Chimica Acta*, 852: 250–256 pp
- Alvarez-Diaz, A., Costa, J.M., Pereiro, R. and Sanz-Medel, A.**, 2009, Halogenated molecularly imprinted polymers for selective determination of carbaryl by phosphorescence measurements, *Analytical and Bioanalytical Chemistry*, 394:1569–1576 pp
- Anastassiades, M. and Schwack, W.**, 1998, Analysis of carbendazim, benomyl, thiophanate methyl and 2,4-dichlorophenoxyacetic acid in fruits and vegetables after supercritical fluid extraction, *Journal of Chromatography A*, 825: 45–54 pp
- Anderson, R.A., Ariffin, M.M., Cormack, P.A.G. and Miller, E.I.**, 2008, Comparison of molecularly imprinted solid-phase extraction (MISPE) with classical solid-phase extraction (SPE) for the detection of benzodiazepines in post-mortem hair samples, *Forensic Science International*, 174: 40–46 pp
- Andrade, T.S., Henriques, J.F., Almeida, A.R., Machado, A.L., Koba, O., Giang, P.T., Soares, A.M.V.M. and Domingues, I.**, 2016, Carbendazim exposure induces developmental, biochemical and behavioural disturbance in zebrafish embryos, *Aquatic Toxicology*, 170: 390-399 pp
- Ansell, R.J. and Mosbach, K.**, 1998, Magnetic molecularly imprinted polymer beads for drug radioligand binding assay, *Analyst*, 123: 1611–1616 pp
- Armbrust, K.L. and Crosby, D.G.**, 1991, Fate of carbaryl, 1-naphthol, and atrazine in seawater, *Pacific Science*, 45: 314-320 pp
- Asensio-Ramos, M., Hernandez-Borges, J., Gonzalez-Hernandez, G. and Rodriguez-Delgado, M.A.**, 2012, Hollow-fiber liquid-phase microextraction for the determination of pesticides and metabolites in soils and water samples using HPLC and fluorescence detection, *Electrophoresis*, 33: 2184–2191 pp
- Ashraf, H. and Husain, Q.**, 2010, Use of DEAE cellulose adsorbed and crosslinked white radish (*Raphanus sativus*) peroxidase for the removal of α -

REFERENCES (Continue)

naphthol in batch and continuous process, *International Biodeterioration & Biodegradation*, 64: 27–31 pp

Atkinson, R., Arey, J., Zielinska, B. and Aschmann, S.M., 1987, Kinetics and products of the gas-phase reactions of OH radicals and N₂O₅ with naphthalene and biphenyl, *Environmental Science & Technology*, 21: 1014-1022 pp

Australian Pesticides and Veterinary Medicines Authority, 2007, The reconsideration of registrations of products containing carbendazim or thiophanate-methyl and their associated approved labels, Kingston, Australia, 27p

Baggiani, C., Anfossi, L. and Giovannoli, C., 2007, Solid phase extraction of food contaminants using molecular imprinted polymers, *Analytica Chimica Acta*, 591: 29–39 pp

Baker, J.R., 1947, The histochemical recognition of certain guanidine derivatives, *Quarterly Journal of Microscopical Science*, 88: 115-121 pp

Bamoniri, A., Pourali, A.R. and Nazifi, S.M.R., 2013, Facile synthesis of 1-naphthol azo dyes with nano SiO₂/HIO₄ under solvent-free conditions, *Bulletin of the Chemical Society of Ethiopia*, 27: 439-445 pp

Bayer, 2003, 1-naphthol test plan justification, Bayer CropScience LP, Bayer Corporation, Pittsburgh, USA, 56p

Bean, K.A. and Henion, J.D., 1997, Determination of carbendazim in soil and lake water by immunoaffinity extraction and coupled-column liquid chromatography–tandem mass spectrometry, *Journal of Chromatography A*, 791: 119–126 pp

Beltran, A., Borrull, F., Cormack, P.A.G. and Marce, R.M., 2010, Molecularly-imprinted polymers: useful sorbents for selective extractions, *Trends in Analytical Chemistry*, 29: 1363–1375 pp

Bernal, J.L., del Nozal, M.J., Toribio, L., Jimenez, J.J. and Atienza, J., 1997, High-performance liquid chromatographic determination of benomyl and carbendazim residues in apiarian samples, *Journal of Chromatography A*, 787: 129-136 pp

Blasco, C., Fernández, M., Picó, Y., Font, G. and Mañes, J., 2002, Simultaneous determination of imidacloprid, carbendazim, methiocarb and hexythiazox in peaches and nectarines by liquid chromatography–mass spectrometry, *Analytica Chimica Acta*, 461: 109–116 pp

REFERENCES (Continue)

- Booth, G.**, 2000, Naphthalene Derivatives-Ullmann's Encyclopedia of Industrial Chemistry, *Wiley-VCH Verlag GmbH & Co. KGaA*, Oldham, United Kingdom, 671-722 pp
- Bourne, J.R., Kut, O.M., Lenzner, J. and Maire, H.**, 1990, Kinetics of the diazo coupling between 1-naphthol and diazotized sulfanilic acid, *Industrial & Engineering Chemistry Research*, 29: 1761-1765 pp
- Branger, C., Meouche, W. and Margailan, A.**, 2013, Recent advances on ion-imprinted polymers, *Reactive & Functional Polymers*, 73: 859–875 pp
- Bruner, K.A. and Fisher, S.W.**, 1993, The effects of temperature, pH, and sediment on the fate and toxicity of 1-naphthol to the midge larvae *Chironomus riparius*, *Journal of Environmental Science and Health. Part A: Environmental Science and Engineering and Toxicology*, 28: 1341-1360 pp
- Brüggemann, O.**, 2003, Molecularly Imprinted Polymers: A New Dimension in Analytical Bioseparation, In: Freitag, R. (ed) *Synthetic Polymers for Biotechnology and Medicine*, *Landes Bioscience*, Georgetown, 134- 161 pp
- Byun, H.S., Youn, Y.N., Yun, Y.H. and Yoon, S.D.**, 2010, Selective separation of aspirin using molecularly imprinted polymers, *Separation and Purification Technology*, 74: 144–153 pp
- Cacho, C., Turiel, E. and Pérez-Conde, C.**, 2009, Molecularly imprinted polymers: An analytical tool for the determination of benzimidazole compounds in water samples, *Talanta*, 78: 1029–1035 pp
- Cao, W., Chao, Y., Liu, L., Liu, Q. and Pei, M.**, 2014, Flow injection chemiluminescence sensor based on magnetic oil-based surface molecularly imprinted nanoparticles for determination of bisphenol A, *Sensors and Actuators B*, 204: 704–709 pp
- Cerniglia, C.E., Gibson, D.T. and Van Baalen, C.**, 1980, Oxidation of naphthalene by cyanobacteria and microalgae, *Journal of General Microbiology*, 116: 495-500 pp
- Chang, C.C., Hsieh, Y.Y., Hsu, K.H., Tsai, H.D., Lin, W.H. and Lin, C.S.**, 2010, Deleterious effects of arsenic, benomyl and carbendazim on human endometrial cell proliferation in vitro, *Taiwanese Journal of Obstetrics & Gynecology*, 49: 449-454 pp

REFERENCES (Continue)

- Chen, F.F., Xie, X.Y. and Shi, Y.P.**, 2013, Preparation of magnetic molecularly imprinted polymer for selective recognition of resveratrol in wine, *Journal of Chromatography A*, 1300: 112–118 pp
- Chen, H., Zhang, W., Yang, Z., Tang, M., Zhang, J., Zhu, H., Lu, P., Hu, D. and Zhang, K.**, 2015, Determination of thiophanate-methyl and carbendazim in rapeseed by solid-phase extraction and ultra-high performance chromatography with photodiode array detection, *Instrumentation Science and Technology*, 43: 511–523 pp
- Chen, L. and Li, B.**, 2012, Application of magnetic molecularly imprinted polymers in analytical chemistry, *Analytical Methods*, 4: 2613–2621 pp
- Chen, L. and Li, B.**, 2013, Magnetic molecularly imprinted polymer extraction of chloramphenicol from honey, *Food Chemistry*, 141: 23–28 pp
- Chen, L., Liu, J., Zeng, Q., Wang, H., Yu, A., Zhang, H. and Ding, L.**, 2009, Preparation of magnetic molecularly imprinted polymer for the separation of tetracycline antibiotics from egg and tissue samples, *Journal of Chromatography A*, 1216: 3710–3719 pp
- Chen, L., Xu, S. and Li, J.**, 2011, Recent advances in molecular imprinting technology: current status, challenges and highlighted applications, *Chemical Society Reviews*, 40: 2922–2942 pp
- Chen, M., Zhao, Z., Lan, X., Chen, Y., Zhang, L., Ji, R. and Wang, L.**, 2015, Determination of carbendazim and metiram pesticides residues in rapeseed and peanut oils by fluorescence spectrophotometry, *Measurement*, 73: 313–317 pp
- Chen, S., Jiang, L. and Dan, Y.**, 2012, Synthesis of core-shell latex particles through one-step emulsion polymerization, *Journal of Macromolecular Science, Part B: Physics*, 51: 605–618, 2012 pp
- Chen, Y.C., Brazier, J.F., Yan, M., Bargo, P.R. and Prahl, S.A.**, 2004, Fluorescence-based optical sensor design for molecularly imprinted polymers, *Sensors and Actuators B*, 102: 107–116 pp
- Cormack, P.A.G. and Elorza, A.Z.**, 2004, Molecularly imprinted polymers: synthesis and characterisation, *Journal of Chromatography B*, 804: 173–182 pp.

REFERENCES (Continue)

- Courtois, J., Fischer, G., Schauff, S., Albert, K. and Irgum, K.,** 2006, Interactions of bupivacaine with a molecularly imprinted polymer in a monolithic format studied by NMR, *Analytical Chemistry*, 78: 580-584 pp
- Cuppen, J.G.M., Van den Brink, P.J., Camps, E., Uil, K.F. and Brock, T.C.M.,** 2000, Impact of the fungicide carbendazim in freshwater microcosms. I. Water quality, breakdown of particulate organic matter and responses of macroinvertebrates, *Aquatic Toxicology*, 48: 233–250 pp
- da Silva, M.R., Vão, E.R., Temtem, M., Mafra, L., Caldeira, J., Aguiar-Ricardo, A. and Casimiro, T.,** 2010, Clean synthesis of molecular recognition polymeric materials with chiral sensing capability using supercritical fluid technology. Application as HPLC stationary phases, *Biosensors and Bioelectronics*, 25: 1742–1747 pp
- da Silva, M.S. and Casimiro, T.,** 2012, High affinity polymers by molecular imprinting for drug delivery, Polymerization, Dr. Ailton De Souza Gomes (Ed.), *InTech*, Croatia, 145-162 pp
- Daghbouche, Y., Garrigues, G. and de la Guardia, M.,** 1995, Solid phase preconcentration-Fourier transform infrared spectrometric determination of carbaryl and 1-naphthol, *Analytica Chimica Acta*, 314: 203-212 pp
- del Pozo, M., Alonso, M., Hernandez, L. and Quintana, C.,** 2011, An electrochemical approach for the cucurbit[7]uril/ carbendazim supramolecular inclusion complex. application to carbendazim determination in apples, *Electroanalysis*, 23: 189 – 195 pp
- del Pozo, M., Hernández, L. and Quintana, C.,** 2010, A selective spectrofluorimetric method for carbendazim determination in oranges involving inclusion-complex formation with cucurbit[7]uril, *Talanta*, 81: 1542–1546 pp
- Di Muccio, A., Girolimetti, S., Barbini, D.A., Pelosi, P., Generali, T., Vergori, L., De Merulis, G., Leonelli, A. and Stefanelli, P.,** 1999, Selective clean-up applicable to aqueous acetone extracts for the determination of carbendazim and thiabendazole in fruits and vegetables by high-performance liquid chromatography with UV detection, *Journal of Chromatography A*, 833: 61–65 pp

REFERENCES (Continue)

- Ebrahimzadeh, H., Asgharinezhad, A.A., Moazzen, E., Amini, M.M. and Sadeghi, O.,** 2015, A magnetic ion-imprinted polymer for lead(II) determination: A study on the adsorption of lead(II) by beverages, *Journal of Food Composition and Analysis*, 41: 74–80 pp
- Ellis, S.R., Hodson, M.E. and Wege, P.,** 2007, The influence of different artificial soil types on the acute toxicity of carbendazim to the earthworm *Eisenia fetida* in laboratory toxicity tests, *European Journal of Soil Biology*, 43: 239-245 pp
- Escalada, J.P., Pajares, A., Gianotti, J., Massad, W.A., Bertolotti, S., Amat-Guerri, F. and Garcia, N.A.,** 2006, Dye-sensitized photodegradation of the fungicide carbendazim and related benzimidazoles, *Chemosphere*, 65: 237–244 pp
- European Food Safety Authority,** 2010, Conclusion on the peer review of the pesticide risk assessment of the active substance carbendazim, *EFSA Journal*, Parma, Italy, 8(5) 1598, 76p
- Farag, A., Ebrahim, H., ElMazoudy, R. and Kadous, E.,** 2011, Developmental toxicity of fungicide carbendazim in female mice, *Birth Defects Research (Part B)*, 92: 122–130 pp
- Foulger, J.H.,** 1931, The use of the molisch (α -naphthol) reactions in the study of sugars in biological fluids, *The Journal of Biological Chemistry*, 92: 345-353 pp
- Förster, B., Garcia, M., Francimari, O. and Römbke, J.,** 2006, Effects of carbendazim and lambda-cyhalothrin on soil invertebrates and leaf litter decomposition in semi-field and field tests under tropical conditions (Amazônia, Brazil), *European Journal of Soil Biology*, 42: 171-179 pp
- Gambino, G.L., Pagano, P., Scordino, M., Sabatino, L., Scollo, E., Traulo, P. and Gagliano, G.,** 2008, Determination of plant hormones in fertilizers by high-performance liquid chromatography with photodiode array detection: Method development and single-laboratory validation, *Journal of AOAC International*, 91: 1245–1256 pp
- Gao, R., Mu, X., Hao, Y., Zhang, L., Zhang, J. and Tang, Y.,** 2014, Combination of surface imprinting and immobilized template techniques for preparation of core–shell molecularly imprinted polymers based on directly amino-modified

REFERENCES (Continue)

- Fe₃O₄ nanoparticles for specific recognition of bovine hemoglobin, *Journal of Materials Chemistry B*, 2: 1733–1741 pp
- Garcia, R., Cabrita, M.J. and Freitas, A.M.C.**, 2011, Application of molecularly imprinted polymers for the analysis of pesticide residues in food—a highly selective and innovative approach, *American Journal of Analytical Chemistry*, 2: 16-25 pp
- Ge, S., Zhao, P., Yan, M., Zang, D. and Yu, J.**, 2012, Multi-branch chemiluminescence–molecular imprinting sensor for sequential determination of carbofuran and omethoate in foodstuff, *Analytical Methods*, 4: 3150–3156 pp
- Giakisikli, G. and Anthemidis, A.N.**, 2013, Magnetic materials as sorbents for metal/metalloid preconcentration and/or separation. A review, *Analytica Chimica Acta*, 789: 1– 16 pp
- Guan, W.S., Lei, J.R., Wang, X., Zhou, Y., Lu, C.C. and Sun, S.F.**, 2013, Selective recognition of beta-cypermethrin by molecularly imprinted polymers based on magnetite yeast composites, *Journal of Applied Polymer Science*, 129: 1952–1958 pp
- Guo, L.Q., Zeng, Y.B., Guan, A.H. and Chen, G.N.**, 2011, Preparation and characterization of molecularly imprinted silica particles for selective adsorption of naphthalene, *Reactive & Functional Polymers*, 71: 1172–1176 pp
- He, D., Zhang, X., Gao, B., Wang, L., Zhao, Q., Chen, H., Wang, H. and Zhao, C.**, 2014, Preparation of magnetic molecularly imprinted polymer for the extraction of melamine from milk followed by liquid chromatography-tandem mass spectrometry, *Food Control*, 36: 36-41 pp
- Hu, Y., Liu, R., Zhang, Y. and Li, G.**, 2009, Improvement of extraction capability of magnetic molecularly imprinted polymer beads in aqueous media via dual-phase solvent system, *Talanta*, 79: 576–582 pp
- Huang, B., Zhou, X., Chen, J., Wu, G. and Lu, X.**, 2015, Determination of malachite green in fish based on magnetic molecularly imprinted polymer extraction followed by electrochemiluminescence, *Talanta*, 142: 228–234 pp

REFERENCES (Continue)

- Huang, X., Zhao, G., Liu, M., Li, F., Qiao, J. and Zhao, J.,** 2012, Highly sensitive electrochemical determination of 1-naphthol based on high-index facet SnO₂ modified electrode, *Electrochimica Acta*, 83: 478–484 pp
- Janakidevi, V., Nagarani, N., Yokeshbabu, B., Kumaraguru, A.K. and Ramakritinan, C.M.,** 2013, A study of proteotoxicity and genotoxicity induced by the pesticide and fungicide on marine invertebrate (*Donax faba*), *Chemosphere*, 90: 1158–1166 pp
- Jia, G., Li, L., Qiu, J., Wang, X., Zhu, W., Sun, Y. and Zhou, Z.,** 2007, Determination of carbaryl and its metabolite 1-naphthol in water samples by fluorescence spectrophotometer after anionic surfactant micelle-mediated extraction with sodium dodecylsulfate, *Spectrochimica Acta Part A*, 67: 460–464 pp
- Jiang, H., Jiang, D., Shao, J. and Sun, X.,** 2016, Magnetic molecularly imprinted polymer nanoparticles based electrochemical sensor for the measurement of gram-negative bacterial quorum signaling molecules (N-acyl-homoserine-lactones), *Biosensors and Bioelectronics*, 75: 411–419 pp
- Jiang, J., Wu, S., Wang, Y., An, X., Cai, L., Zhao, X. and Wu, C.,** 2015, Carbendazim has the potential to induce oxidative stress, apoptosis, immunotoxicity and endocrine disruption during zebrafish larvae development, *Toxicology in Vitro*, 29: 1473–1481 pp
- Jiang, J., Wu, S., Wu, C., An, X., Cai, L. and Zhao, X.,** 2014, Embryonic exposure to carbendazim induces the transcription of genes related to apoptosis, immunotoxicity and endocrine disruption in zebrafish (*Danio rerio*), *Fish & Shellfish Immunology*, 41: 493-500 pp
- Jiang, X., Jiang, N., Zhang, H. and Liu, M.,** 2007, Small organic molecular imprinted materials: their preparation and application, *Analytical and Bioanalytical Chemistry*, 389: 355–368 pp
- Joint Meeting on Pesticides Residues,** 1998, Carbendazim (072), Joint FAO/WHO Meetings on Pesticide Residues Report, 76p
- Kanan, M.,** 2002, A study of the photodegradation of carbaryl: the influence of natural organic matter and the use of silver zeolite γ as a catalyst, MSc thesis, The University of Maine, 122p

REFERENCES (Continue)

- Kapuci, M., Ulker, Z., Gurkan, S. and Alpsy, L.,** 2014, Determination of cytotoxic and genotoxic effects of naphthalene, 1-naphthol and 2-naphthol on human lymphocyte culture, *Toxicology and Industrial Health*, 30: 82–89 pp
- Kaur, A. and Gupta, U.,** 2009, A review on applications of nanoparticles for the preconcentration of environmental pollutants, *Journal of Materials Chemistry*, 19: 8279–8289 pp
- Kaur, R., Hasan, A., Iqbal, N., Alam, S., Saini, M.L. and Raza, S.K.,** 2014, Synthesis and surface engineering of magnetic nanoparticles for environmental cleanup and pesticide residue analysis: A review, *Journal of Separation Science*, 37: 1805–1825 pp
- Khare, N.G., Dar, R.A. and Srivastava, A.K.,** 2015, Determination of carbendazim by adsorptive stripping differential pulse voltammetry employing glassy carbon paste electrode modified with graphene and amberlite XAD 2 resin, *Electroanalysis*, 27: 1915–1924 pp
- Komiyama, M., Takeuchi, T., Mukawa, T. and Asanuma, H.,** 2003, Molecular Imprinting: From Fundamentals to Applications, *Wiley-VCH Verlag GmbH & Co. KGaA*, Germany, 159p.
- Kong, X., Gao, R., He, X., Chen, L. and Zhang, Y.,** 2012, Synthesis and characterization of the core-shell magnetic molecularly imprinted polymers (Fe_3O_4 @MIPs) adsorbents for effective extraction and determination of sulfonamides in the poultry feed, *Journal of Chromatography A*, 1245: 8–16 pp
- Kwasniewska, K., Gadzala-Kopciuch, R. and Buszewski, B.,** 2015, Magnetic molecular imprinted polymers as a tool for isolation and purification of biological samples, *Open Chemistry Journal*, 13: 1228–1235 pp
- Larkin, M.J. and Day, M.J.,** 1986, The metabolism of carbaryl by three bacterial isolates, *Pseudomonas* spp. (NCIB 12042 & 12043) and *Rhodococcus* sp. (NCIB 12038) from garden soil, *Journal of Applied Microbiology*, 60: 233–42 pp
- Laurella, S.L., Diez, C.M.P., Lick, I.D., Allegretti, P.E. and Erben, M.F.,** 2015, Evaluation of silica as an adsorbent for carbendazim from aqueous solutions, *International Journal of Engineering and Technical Research*, 3: 96–101 pp

REFERENCES (Continue)

- Lee, L.L.**, 2006, Synthesis and application of molecularly imprinted solid-phase extraction for the determination of terbutaline in biological matrices, MSc thesis, Universiti Sains Malaysia, 184p
- Li, J. and Chi, Y.**, 2009, Determination of carbendazim with multiwalled carbon nanotubes-polymeric methyl red film modified electrode, *Pesticide Biochemistry and Physiology*, 93: 101–104 pp
- Li, L., Liu, E., Wang, X., Chen, J. and Zhang, X.**, 2015, Simultaneous determination of naphthol isomers at poly(3-methylthiophene)-nano-Au modified electrode with the enhancement of surfactant, *Materials Science and Engineering C*, 53: 36–42 pp
- Li, Y.F., Jin, J., Guo, Q., Ha, Y.M. and Li, Q.P.**, 2015, Complexation of synthetic CDM-AM copolymer with natamycin and carbendazim to improve solubility and fungicidal activity, *Carbohydrate Polymers*, 125: 288–300 pp
- Liang, G., Liu, X. and Li, X.**, 2013, Highly sensitive detection of α -naphthol based on G-DNA modified gold electrode by electrochemical impedance spectroscopy, *Biosensors and Bioelectronics*, 45: 46–51 pp
- Liu, J., Yin, D., Zhang, S., Liu, H. and Zhang, Q.**, 2015, Synthesis of polymeric core/shell microspheres with spherical virus-like surface morphology by Pickering emulsion, *Colloids and Surfaces A: Physicochemical and Engineering Aspects*, 466: 174–180 pp
- Liu, K., Pan, X., Han, Y., Tang, F. and Yu, Y.**, 2012, Estimating the toxicity of the weak base carbendazim to the earthworm (*Eisenia fetida*) using in situ pore water concentrations in different soils, *Science of the Total Environment*, 438: 26–32 pp
- Liu, N., Dong, F., Liu, X., Xu, J., Li, Y., Han, Y., Zhu, Y., Cheng, Y., Chen, Z., Tao, Y. and Zheng, Y.**, 2014, Effect of household canning on the distribution and reduction of thiophanate-methyl and its metabolite carbendazim residues in tomato, *Food Control*, 43: 115–120 pp
- Liu, X., Yu, D., Yu, Y. and Ji, S.**, 2014, Preparation of a magnetic molecularly imprinted polymer for selective recognition of rhodamine B, *Applied Surface Science*, 320: 138–145 pp

REFERENCES (Continue)

- Lofs-Holmin, A.**, 1981, Influence in field experiments of benomyl and carbendazim on earthworms (Lumbricidae) in relation to soil texture, *Swedish Journal of Agricultural Research*, 11: 141-147 pp
- Lok, C.M. and Son, R.**, 2009, Application of molecularly imprinted polymers in food sample analysis – a perspective, *International Food Research Journal*, 16: 127-140 pp
- Lopez, M.H., Gonzalez, M.A. and Molina, M.I.L.**, 1999, Synchronous-derivative phosphorimetric determination of 1- and 2-naphthol in irrigation water by employing β -cyclodextrin, *Talanta*, 49: 679–689 pp
- Luo, Q., Zhan, Y., Huang, Y., Yang, L., Tu, X. and Luo, S.**, 2011, Removal of water-soluble acid dyes from water environment using a novel magnetic molecularly imprinted polymer, *Journal of Hazardous Materials*, 187: 274–282 pp
- Luo, S., Wu, Y. and Gou, H.**, 2013, A voltammetric sensor based on GO–MWNTs hybrid nanomaterial-modified electrode for determination of carbendazim in soil and water samples, *Ionics*, 19: 673–680 pp
- Luo, Y., Liu, L., Li, L. and Deng, Q.**, 2006, Chromatographic separation of the enantiomers of a series of C2-asymmetric bi-naphthyl compounds by molecularly imprinted polymers, *Chromatographia*, 64: 393-397 pp
- Ma, C.H., Zhang, J., Hong, Y.C., Wang, Y.R. and Chen, X.**, 2015, Determination of carbendazim in tea using surface enhanced Raman spectroscopy, *Chinese Chemical Letters*, 26:1455–1459 pp
- Ma, G. and Chen, L.**, 2014, Development of magnetic molecularly imprinted polymers based on carbon nanotubes–Application for trace analysis of pyrethroids in fruit matrices, *Journal of Chromatography A*, 1329: 1– 9 pp
- Maggio, R.M., Damiani, P.C. and Olivieri, A.C.**, 2010, Four-way kinetic-excitation-emission fluorescence data processed by multi-way algorithms. Determination of carbaryl and 1-naphthol in water samples in the presence of fluorescent interferents, *Analytica Chimica Acta*, 677: 97–107 pp
- Mallat, E., Barcel, D. and Tauler, R.**, 1997, Degradation study of benomyl and carbendazim in water by liquid chromatography and multivariate curve resolution methods, *Chromatographia*, 46: 342-350 pp

REFERENCES (Continue)

- Martinez-Galera, M., Picon-Zamora, D., Martinez-Vidal, J.L., Garrido-Frenich, A., Espinosa-Mansilla, A., de la Pena, A.M. and Salinas-Lopez, F.**, 2003, Determination of carbendazim, thiabendazole and fuberidazole using a net analyte signal-based method, *Talanta*, 59: 1107-1116 pp
- Mathew, L., Reddy, M.L.P., Rao, T.P., Iyer, C.S.P. and Damodaran, A.D.**, 1995, Simple spectrophotometric method for the determination of carbaryl in soil and insecticide formulations, *Analyst*, 120: 1799-1801 pp
- Mayes, A.G. and Whitcombe, M.J.**, 2005, Synthetic strategies for the generation of molecularly imprinted organic polymers, *Advanced Drug Delivery Reviews*, 57: 1742– 1778 pp
- Mazellier, P., Leroy, E. and Legube, B.**, 2002, Photochemical behavior of the fungicide carbendazim in dilute aqueous solution, *Journal of Photochemistry and Photobiology A: Chemistry*, 153: 221–227 pp
- McConkey, B.J., Hewitt, L.M., Dixon, D.G. and Greenberg, B.M.**, 2002, Natural sunlight induced photooxidation of naphthalene in aqueous solution, *Water, Air, and Soil Pollution*, 136: 347–359 pp
- Meeker, J.D., Ryan, L., Barr, D.B. and Hauser, R.**, 2006, Exposure to nonpersistent insecticides and male reproductive hormones, *Epidemiology*, 17: 61–68 pp
- Meeker, J.D., Singh, N.P., Ryan, L., Duty, S.M., Barr, D.B., Herrick, R.F., Bennett, D.H. and Hauser, R.**, 2004, Urinary levels of insecticide metabolites and DNA damage in human sperm, *Human Reproduction*, 19: 2573–2580 pp
- Mohammed, D.H.**, 2010, Spectrophotometric determination of 1-naphthol via charge transfer complex formation, *National Journal of Chemistry*, 38: 201-210 pp
- Montgomery, J.H.**, 2007, Groundwater Chemicals Desk Reference, Fourth Edition, *CRC Press, Taylor & Francis Group*, Boca Raton, Florida, 1752p
- Morejon, L., Mendizabal, E., Delgado, J.A., Davidenko, N., Lopez-Dellamary, F., Manriquez, R., Ginebra, M.P., Gil, F.J. and Planell, J.A.**, 2005, Synthesis and characterization of poly (methyl methacrylate-styrene) copolymeric beads for bone cements, *Latin American Applied Research*, 35:175-182 pp

REFERENCES (Continue)

- Nasiri-Majd, M., Taher, M.A. and Fazelirad, H.**, 2015, Synthesis and application of nano-sized ionic imprinted polymer for the selective voltammetric determination of thallium, *Talanta*, 144: 204–209 pp
- Ou, H., Chen, Q., Pan, J., Zhang, Y., Huang, Y. and Qi, X.**, 2015, Selective removal of erythromycin by magnetic imprinted polymers synthesized from chitosan-stabilized Pickering emulsion, *Journal of Hazardous Materials*, 289: 28–37 pp
- Pakade, V.E.**, 2012, Development and application of imprinted polymers for selective adsorption of metal ions and flavonols in complex samples, PhD thesis, Faculty of Science, University of the Witwatersrand, 262p
- Panades, R., Ibarz, A. and Esplugas, S.**, 2000, Photodecomposition of carbendazim in aqueous solutions, *Water Research*, 34: 2951–2954 pp
- Patel, G.M., Rohit, J.V., Singhal, R.K. and Kailasa, S.K.**, 2015, Recognition of carbendazim fungicide in environmental samples by using 4-aminobenzenethiol functionalized silver nanoparticles as a colorimetric sensor, *Sensors and Actuators B*, 206: 684–691 pp
- Pearse Jr., G.A.**, 1963, Spectrophotometric determination of 1-naphthol, *Analytical Chemistry*, 35: 1954–1955 pp
- Pfeil, R. and Dellarco, V.**, 2005, Carbendazim (addendum), Joint FAO/WHO Meetings on Pesticide Residues, *Joint Meeting on Pesticide Residues*, 87–106 pp
- Piao, C. and Chen, L.**, 2012, Separation of Sudan dyes from chilli powder by magnetic molecularly imprinted polymer, *Journal of Chromatography A*, 1268: 185–190 pp
- Pichon, V. and Chapuis-Hugon, F.**, 2008, Role of molecularly imprinted polymers for selective determination of environmental pollutants-A review, *Analytica Chimica Acta*, 622: 48–61 pp
- Piletsky, S.A., Karim, K., Piletska, E.V., Day, C.J., Freebairn, K.W., Legge, C. and Turner, A.P.F.**, 2001, Recognition of ephedrine enantiomers by molecularly imprinted polymers designed using a computational approach, *Analyst*, 126: 1826–1830 pp
- Poma, A., Turner, A.P.F. and Piletsky, S.A.**, 2010, Advances in the manufacture of MIP nanoparticles, *Trends in Biotechnology*, 28: 629–637 pp

REFERENCES (Continue)

- Pourreza, N., Rastegarzadeh, S. and Larki, A.,** 2015, Determination of fungicide carbendazim in water and soil samples using dispersive liquid-liquid microextraction and microvolume UV–vis spectrophotometry, *Talanta*, 134: 24–29 pp
- Preuss, R., Angerer, J. and Drexler, H.,** 2003, Naphthalene-an environmental and occupational toxicant, *International Archives of Occupational and Environmental Health*, 76: 556-76 pp
- Preuss, R. and Angerer, J.,** 2004, Simultaneous determination of 1- and 2-naphthol in human urine using on-line clean-up column-switching liquid chromatography–fluorescence detection, *Journal of Chromatography B*, 801: 307–316 pp
- Qi, Y., Li, G., Wei, C., Zhao, L. and Gong, B.,** 2016, Preparation of magnetic molecularly imprinted polymer for melamine and its application in milk sample analysis by HPLC, *Journal of Biomedical Sciences*, 5: 1-10
- Qiu, H., Luo, C., Sun, M., Lu, F., Fan, L. and Li, X.,** 2012, A chemiluminescence sensor for determination of epinephrine using graphene oxide – magnetite-molecularly imprinted polymers, *Carbon*, 50: 4052-4060 pp
- Rajabi, H.R. and Razmpour, S.,** 2016, Synthesis, characterization and application of ion imprinted polymeric nanobeads for highly selective preconcentration and spectrophotometric determination of Ni²⁺ ion in water samples, *Spectrochimica Acta Part A: Molecular and Biomolecular Spectroscopy*, 153: 45–52 pp
- Rama, E.M., Bortolan, S., Vieira, M.L., Gerardin, D.C.C. and Moreira, E.G.,** 2014, Reproductive and possible hormonal effects of carbendazim, *Regulatory Toxicology and Pharmacology*, 69: 476–486 pp
- Rao, D.M., Murty, A.S. and Swarup, P.A.,** 1984, Relative toxicity of technical grade and formulated carbaryl and 1-naphthol to, and carbaryl-induced biochemical changes in, the fish *Cirrhinus mrigala*, *Environmental Pollution Series A, Ecological and Biological*, 34: 47-54 pp
- Rao, W., Cai, R., Yin, Y., Long, F. and Zhang, Z.,** 2014, Magnetic dummy molecularly imprinted polymers based on multi-walled carbon nanotubes for rapid selective solid-phase extraction of 4-nonylphenol in aqueous samples, *Talanta*, 128: 170–176 pp

REFERENCES (Continue)

- Ren, Z., Kong, D., Wang, K. and Zhang, W.,** 2014, Preparation and adsorption characteristics of an imprinted polymer for selective removal of Cr(VI) ions from aqueous solutions, *Journal of Materials Chemistry A*, 2: 17952–17961 pp
- Reyes, J.F.G., Barrales, P.O. and Diaz, A.M.,** 2003, Gel-surface enhanced fluorescence sensing system coupled to a continuous-flow assembly for simultaneous monitoring of benomyl and carbendazim, *Analytica Chimica Acta*, 493: 35–45 pp
- Ribeiro, W.F., Selva, T.M.G., Lopes, I.C., Coelho, E.C.S., Lemos, S.G., de Abreu, F.C., do Nascimento, V.B. and de Araujo, M.C.U.,** 2011, Electroanalytical determination of carbendazim by square wave adsorptive stripping voltammetry with a multiwalled carbon nanotubes modified electrode, *Analytical Methods*, 3: 1202–1206 pp
- Rodriguez-Cuesta, M.J., Boqué, R., Rius, F.X., Zamora, D.P., Martinez-Galera, M. and Frenich, A.G.,** 2003, Determination of carbendazim, fuberidazole and thiabendazole by three-dimensional excitation–emission matrix fluorescence and parallel factor analysis, *Analytica Chimica Acta*, 491: 47–56 pp
- Saien, J. and Khezrianjoo, S.,** 2008, Degradation of the fungicide carbendazim in aqueous solutions with UV/TiO₂ process: Optimization, kinetics and toxicity studies, *Journal of Hazardous Materials*, 157: 269–276 pp
- Sanagi, M.M., Salleh, S., Ibrahim, W.A.W., Naim, A.A., Hermawan, D., Miskam, M., Hussain, I. and Aboul-Enein, H.Y.,** 2013, Molecularly imprinted polymer solid-phase extraction for the analysis of organophosphorus pesticides in fruit samples, *Journal of Food Composition and Analysis*, 32: 155–161 pp
- Santa-Cruz, P. and Garcia-Reiriz, A.,** 2014, Application of third-order multivariate calibration algorithms to the determination of carbaryl, naphthol and propoxur by kinetic spectroscopic measurements, *Talanta*, 128: 450–459 pp
- Scientific Committee on Consumer Products,** 2008, Opinion on 1-naphthol, European Commission, Brussels, 26p

REFERENCES (Continue)

- Scorrano, S., Mergola, L., Del Sole, R. and Vasapollo, G.,** 2011, Synthesis of molecularly imprinted polymers for amino acid derivatives by using different functional monomers, *International Journal of Molecular Sciences*, 12: 1735-1743 pp
- Shaikh, H., Memon, N., Bhangar, M.I., Nizamani, S.M. and Denizli, A.,** 2014, Core-shell molecularly imprinted polymer-based solid-phase microextraction fiber for ultra trace analysis of endosulfan I and II in real aqueous matrix through gas chromatography-micro electron capture detector, *Journal of Chromatography A*, 1337: 179-187 pp
- Silva, A.R.R., Cardoso, D.N., Cruz, A., Lourenço, J., Mendo, S., Soares, A.M.V.M. and Loureiro, S.,** 2015, Ecotoxicity and genotoxicity of a binary combination of triclosan and carbendazim to *Daphnia magna*, *Ecotoxicology and Environmental Safety*, 115: 279-290 pp
- Singh, S.B., Foster, G.D. and Khan, S.U.,** 2004, Microwave-assisted extraction for the simultaneous determination of thiamethoxam, imidacloprid, and carbendazim residues in fresh and cooked vegetable samples, *Journal of Agricultural and Food Chemistry*, 52: 105-109 pp
- Singh, S.B., Foster, G.D. and Khan, S.U.,** 2007, Determination of thiophanate methyl and carbendazim residues in vegetable samples using microwave-assisted extraction, *Journal of Chromatography A*, 1148: 152-157 pp
- Singhal, L.K., Bagga, S., Kumar, R. and Chauhan, R.S.,** 2003, Down regulation of humoral immunity in chickens due to carbendazim, *Toxicology in Vitro*, 17: 687-692 pp
- Stewart, N.E., Millemann, R.E. and Breese, W.P.,** 1967, Acute toxicity of the insecticide sevin[®] and its hydrolytic product 1-naphthol to some marine organisms, *Transactions of the American Fisheries Society*, 96: 25-30 pp
- Su, X., Li, X., Li, J., Liu, M., Lei, F., Tan, X., Li, P. and Luo, W.,** 2015, Synthesis and characterization of core-shell magnetic molecularly imprinted polymers for solid-phase extraction and determination of Rhodamine B in food, *Food Chemistry*, 171: 292-297 pp
- Subhani, Q., Huang, Z., Zhu, Z. and Zhu, Y.,** 2013, Simultaneous determination of imidacloprid and carbendazim in water samples by ion chromatography

REFERENCES (Continue)

with fluorescence detector and post-column photochemical reactor, *Talanta*, 116: 127–132 pp

Sulekha, P.B., 2002, Synthesis, characterisation and uses of polymer bound antioxidants, PhD thesis, Department of Polymer Science and Rubber Technology, Cochin University Of Science And Technology, 178p

T.C. Gıda Tarım ve Hayvancılık Bakanlığı, 2009, Türk gıda kodeksi gıda maddelerinde bulunmasına izin verilen pestisitlerin maksimum kalıntı limitleri tebliği, 32p

Tan, X., Hu, Q., Wu, J., Li, X., Li, P., Yu, H., Li, X. and Lei, F., 2015, Electrochemical sensor based on molecularly imprinted polymer reduced graphene oxide and gold nanoparticles modified electrode for detection of carbofuran, *Sensors and Actuators B*, 220: 216–221 pp

Thomas, D.H., Lopez-Awla, V., Betowski, L.D. and Van Emon, J., 1996, Determination of carbendazim in water by high-performance immunoaffinity chromatography on-line with high-performance liquid chromatography with diode-array or mass spectrometric detection, *Journal of Chromatography A*, 724: 207-217 pp

Turkall, R.M., Skowronski, G.A., Kadry, A.M. and Abdel-Rahman, M.S., 1994, A comparative study of the kinetics and bioavailability of pure and soil-adsorbed naphthalene in dermally exposed male rats, *Archives of Environmental Contamination and Toxicology*, 26: 504-509 pp

Turkewitsch, P., Masse, R. and Powell, W.S., 2005, Molecular Imprinting, In: Lakowicz, J.R. and Geddes, C.D. (ed) Topics in Fluorescence Spectroscopy, Advanced Concepts in Fluorescence Sensing Part B: Macromolecular Sensing, *Springer Science+Business Media Inc.*, New York, 157-209 pp

Vasapallo, G., Del Sole, R., Mergola, L., Lazzoi, M.R., Scardino, A., Scorrano, S. and Mele, G., 2011, molecularly imprinted polymers: present and future prospective, *International Journal of Molecular Sciences*, 12: 5908-5945 pp

Walsh, R., 2010, Development and characterisation of molecularly imprinted suspension polymers, PhD thesis, Pharmaceutical and Molecular Biotechnology Research Centre Waterford Institute of Technology, 254p

REFERENCES (Continue)

- Wang, C., Wang, F., Zhang, Q. and Liang, W.,** 2016, Individual and combined effects of tebuconazole and carbendazim on soil microbial activity, *European Journal of Soil Biology*, 72: 6-13 pp
- Wang, F., Wang, F., Zhu, D. and Chen, W.,** 2015, Effects of sulfide reduction on adsorption affinities of colloidal graphene oxide nanoparticles for phenanthrene and 1-naphthol, *Environmental Pollution*, 196: 371-378 pp
- Wang, J., Pan, J., Yin, Y., Wu, R., Dai, X., Dai, J., Gao, L. and Ou, H.,** 2015, Thermo-responsive and magnetic molecularly imprinted Fe₃O₄@carbon nanospheres for selective adsorption and controlled release of 2,4,5-trichlorophenol, *Journal of Industrial and Engineering Chemistry*, 25: 321–32 pp
- Wang, X., Wang, L., He, X., Zhang, Y. and Chen, L.,** 2009, A molecularly imprinted polymer-coated nanocomposite of magnetic nanoparticles for estrone recognition, *Talanta*, 78: 327–332 pp
- Wang, X., Xu, Z., Bing, N. and Yang, Z.,** 2007, Preparation and aqueous recognition of metal complex imprinted polymer using N-vinyl-2-pyrrolidone as functional monomer, *Chinese Journal of Chemical Engineering*, 15: 595-599 pp
- Wang, Y.S., Huang, Y.J., Chen, W.C. and Yen, J.H.,** 2009, Effect of carbendazim and pencycuron on soil bacterial community, *Journal of Hazardous Materials*, 172: 84–91 pp
- Wang, Z., Wang, Y., Gong, F., Zhang, J., Hong, Q. and Li, S.,** 2010, Biodegradation of carbendazim by a novel actinobacterium *Rhodococcus jialingiae* djl-6-2, *Chemosphere*, 81: 639–644 pp
- Water Framework Directive - United Kingdom Technical Advisory Group,** 2009, Proposed EQS for water framework directive annex VIII substances: carbendazim (for consultation), Edinburgh, Scotland, 60p
- Widstrand, C., Larsson, F., Fiori, M., Civitareale, C., Mirante, S. and Brambilla, G.,** 2004, Evaluation of MISPE for the multi-residue extraction of β -agonists from calves urine, *Journal of Chromatography B*, 804: 85–91 pp

REFERENCES (Continue)

- Wilson, G.D., Doherty, M.D. and Cohen, G.M.,** 1985, Selective toxicity of 1-naphthol to human colorectal tumour tissue, *British Journal of Cancer*, 51: 853-863 pp
- World Health Organization,** 1993, International programme on chemical safety-environmental health criteria 149 - Carbendazim, Geneva, 132p
- Wu, Q., Li, Y., Wang, C., Liu, Z., Zang, X., Zhou, X. and Wang, Z.,** 2009, Dispersive liquid-liquid microextraction combined with high performance liquid chromatography-fluorescence detection for the determination of carbendazim and thiabendazole in environmental samples, *Analytica Chimica Acta*, 638: 139-145 pp
- Wu, W., Jiang, W., Xia, W., Yang, K. and Xing, B.,** 2012, Influence of pH and surface oxygen-containing groups on multiwalled carbon nanotubes on the transformation and adsorption of 1-naphthol, *Journal of Colloid and Interface Science*, 374: 226-231 pp
- Wu, Z.L., Yang, H., Jiao, F.P., Liu, Q., Chen, X.Q. and Yu, Y.G.,** 2015, Carbon nanoparticles pillared multi-walled carbon nanotubes for adsorption of 1-naphthol: Thermodynamics, kinetics and isotherms, *Colloids and Surfaces A: Physicochemical and Engineering Aspects*, 470: 149-160 pp
- Xiao, X., Yan, K., Xu, X. and Li, G.,** 2015, Rapid analysis of ractopamine in pig tissues by dummy-template imprinted solid-phase extraction coupling with surface-enhanced raman spectroscopy, *Talanta*, 138: 40-45 pp
- Xie, X., Chen, L., Pan, X. and Wang, S.,** 2015, Synthesis of magnetic molecularly imprinted polymers by reversible addition fragmentation chain transfer strategy and its application in the Sudan dyes residue analysis, *Journal of Chromatography A*, 1405: 32-39 pp
- Xu, J., Rong, X., Tian, T. and Qiu, F.,** 2014, Study on the determination of carbendazim in water and vegetable samples, *Advanced Materials Research*, 955-959: 1351-1354 pp
- Xu, S.,** 2000, Environmental fate of carbaryl, Environmental Monitoring & Pest Management Department of Pesticide Regulation, Sacramento, 18p
- Yan, H. and Row, K.H.,** 2006, Characteristic and synthetic approach of molecularly imprinted polymer, *International Journal of Molecular Sciences*, 7: 155-178 pp

REFERENCES (Continue)

- Yang, M., Koga, M., Katoh, T. and Kawamoto, T.,** 1999, A study for the proper application of urinary naphthols, new biomarkers for airborne polycyclic aromatic hydrocarbons, *Archives of Environmental Contamination and Toxicology*, 36: 9-108 pp
- Yang, S., Guo, Z., Sheng, G. and Wang, X.,** 2012, Investigation of the sequestration mechanisms of Cd(II) and 1-naphthol on discharged multi-walled carbon nanotubes in aqueous environment, *Science of the Total Environment*, 420: 214–221 pp
- Yao, Y., Wen, Y., Zhang, L., Wang, Z., Zhang, H. and Xu, J.,** 2014, Electrochemical recognition and trace-level detection of bactericide carbendazim using carboxylic group functionalized poly(3,4-ethylenedioxythiophene) mimic electrode, *Analytica Chimica Acta*, 831: 38–49 pp
- Yasmin, S. and D'souza, D.,** 2007, Effect of pesticides on the reproductive output of *eisenia fetida*, *Bulletin of Environmental Contamination and Toxicology*, 79: 529–532 pp
- Yin, X., Liu, Q., Jiang, Y. and Luo, Y.,** 2011, Development of andrographolide molecularly imprinted polymer for solid-phase extraction, *Spectrochimica Acta Part A*, 79: 191–196 pp
- Yu, D., Hu, X., Wei, S., Wang, Q., He, C. and Liu, S.,** 2015, Dummy molecularly imprinted mesoporous silica prepared by hybrid imprinting method for solid-phase extraction of bisphenol A, *Journal of Chromatography A*, 1396: 17–24 pp
- Yu, G., Liu, Y., Xie, L. and Wang, X.,** 2009, Involvement of Sertoli cells in spermatogenic failure induced by carbendazim, *Environmental Toxicology and Pharmacology*, 27: 287–292 pp
- Yuan, Y.K., Xiao, X.L., Wang, Y.S., Xue, J.H., Li, G.R., Kang, R.H., Zhang, J.Q. and Shi, L.F.,** 2010, Quartz crystal microbalance with β -cyclodextrin/TiO₂ composite films coupled with chemometrics for the simultaneous determination of urinary 1- and 2-naphthol, *Sensors and Actuators B*, 145: 348–354 pp

REFERENCES (Continue)

- Zamora, O., Paniagua, E.E., Cacho, C., Vera-Avila, L.E. and Perez-Conde, C.,** 2009, Determination of benzimidazole fungicides in water samples by on-line MISPE–HPLC, *Analytical and Bioanalytical Chemistry*, 393: 1745–1753 pp
- Zeng, H., Wang, Y., Nie, C., Kong, J. and Liu, X.,** 2012, Preparation of magnetic molecularly imprinted polymers for separating rutin from Chinese medicinal plants, *Analyst*, 2012, 137: 2503-2512 pp
- Zhang, W., Chen, J., Pan, B. and Zhang, Q.,** 2006, Cooperative adsorption behaviours of 1-naphthol and 1-naphthylamine onto nonpolar macroreticular adsorbents, *Reactive & Functional Polymers*, 66: 485–493 pp
- Zhang, W., Hong, C., Pan, B., Xu, Z., Zhang, Q. and Lv, L.,** 2008, Removal enhancement of 1-naphthol and 1-naphthylamine in single and binary aqueous phase by acid–basic interactions with polymer adsorbents, *Journal of Hazardous Materials*, 158: 293–299 pp
- Zhang, W., Hong, C., Pan, B., Zhang, Q., Jiang, P. and Jia, K.,** 2009, Sorption enhancement of 1-naphthol onto a hydrophilic hyper-cross-linked polymer resin, *Journal of Hazardous Materials*, 163: 53–57 pp
- Zhang, X., Wang, Y. and Yang, S.,** 2014, Simultaneous removal of Co(II) and 1-naphthol by core–shell structured Fe₃O₄@cyclodextrin magnetic nanoparticles, *Carbohydrate Polymers*, 114: 521–529 pp
- Zhang, Y. and Zhuang, H.,** 2009, Poly (acridine orange) film modified electrode for the determination 1-naphthol in the presence of 2-naphthol, *Electrochimica Acta*, 54: 7364–7369 pp
- Zhang, Y.L., Zhang, J., Dai, C.M., Zhou, X.F. and Liu, S.G.,** 2013, Sorption of carbamazepine from water by magnetic molecularly imprinted polymers based on chitosan-Fe₃O₄, *Carbohydrate Polymers*, 97: 809– 816 pp
- Zhang, Z., Chen, X., Rao, W., Chen, H. and Cai, R.,** 2014, Synthesis and properties of magnetic molecularly imprinted polymers based on multiwalled carbon nanotubes for magnetic extraction of bisphenol A from water, *Journal of Chromatography B*, 965: 190–196 pp
- Zhao, G., Li, J. and Wang, X.,** 2011, Kinetic and thermodynamic study of 1-naphthol adsorption from aqueous solution to sulfonated graphene nanosheets, *Chemical Engineering Journal*, 173: 185– 190 pp

REFERENCES (Continue)

- Zhong, S., Tan, S.N., Ge, L., Wang, W. and Chen, J.,** 2011, Determination of bisphenol A and naphthols in river water samples by capillary zone electrophoresis after cloud point extraction, *Talanta*, 85: 488–492 pp
- Zhou, J., Xiong, K., Yang, Y., Ye, X., Liu, J. and Li, F.,** 2015, Deleterious effects of benomyl and carbendazim on human placental trophoblast cells, *Reproductive Toxicology*, 51: 64–71 pp
- Zhou, Q., Wang, G. and Xie, G.,** 2014, Preconcentration and determination of bisphenol A, naphthol and dinitrophenol from environmental water samples by dispersive liquid-phase microextraction and HPLC, *Analytical Methods*, 6: 187-193 pp
- Zhu, G., Gai, P., Yang, Y., Zhang, X. and Chen, J.,** 2012, Electrochemical sensor for naphthols based on gold nanoparticles/hollow nitrogen-doped carbon microsphere hybrids functionalized with SH- β -cyclodextrin, *Analytica Chimica Acta*, 723: 33– 38 pp

CURRICULUM VITAE

Name : Raif İLKTAÇ
Citizenship : Turkish Republic Of Northern Cyprus
Date of Birth : 29.05.1988
Place of Birth : Lefkoşa/KKTC
E-mail address: raifilktac@gmail.com

Academic Status	Department/Branch	Universty	Period
B.Sc.	Chemistry	Ege	2005-2009
M.Sc.	Chemistry	Ege	2009-2011
PhD	Chemistry	Ege	2011-2017

Publications:

Henden, E., İşlek, Y., Kavas, M., Aksuner, N., Yayayürük, O., Çiftçi, T.D. and İlktaç, R., 2011, A study of mechanism of nickel interferences in hydride generation atomic absorption spectrometric determination of arsenic and antimony, *Spectrochimica Acta Part B: Atomic Spectroscopy*, 66: 793-798 pp

İlktaç, R., Aksuner, N. and Henden, E., 2016, Molecularly Imprinted Polymer Based Fluorimetric Sensor for the Preconcentration and Determination of 1-Naphthol, *Analytical Letters*, 49: 958-968 pp

İlktaç, R., Aksuner, N. and Henden, E., 2016, Preconcentration and highly sensitive fluorimetric determination of Tin(IV) by using a novel nickel/nickel boride nanosorbent, *Spectroscopy Letters*, 48: 375-381 pp

İlktaç, R., Aksuner, N. and Henden, E., 2017, Selective and sensitive fluorimetric determination of carbendazim in apple and orange after preconcentration with magnetite-molecularly imprinted polymer, *Spectrochimica Acta Part A: Molecular and Biomolecular Spectroscopy*, 174: 86-93 pp